ISSN 2701-939X

Communications in

Development and Assembling of Textile Products

CDATP

Year 2020, Volume 1, Issue 2

Communications in Development and Assembling of Textile Products (CDATP)

ISSN 2701-939X is an international, ***peer reviewed, pure open access journal.***

www.cdatp.org

https://journals.qucosa.de/cdatp

Publisher

Chair of Development and Assembly of Textile Products
Technische Universität Dresden
Faculty of Mechanical Science and Engineering
Institute of Textile Machinery and High Performance Material Technology (ITM)
01062 Dresden

Tel.: +49 (0) 351 463-39313
Fax: +49 (0) 351 463-39301
E-Mail: yordan.kyosev@tu-dresden.de
http://tu-dresden.de/mw/itm/mt
http://tu-dresden.de/mw/itm
http://www.facebook.com/ITM.TUDresden

Besucheradresse:
Hohe Straße 6, Zi. 141
01069 Dresden

Principal Contact

Prof. Dr.-Ing. habil. Yordan **Kyosev**

Head of the Chair of Development and Assembly of Textile Products
yordan.kyosev@tu-dresden.de

Support Contact

Dr. Lutz **Kowalke**

journals@qucosa.de

Editorial Team

About the Journal

Aim

The journal **“Communications in Development and Assembling of Textile Products”** (CDATP) **ISSN 2701-939X** is an international, ***peer reviewed, pure open access journal.***

It has the mission to offer a forum for scientific exchange in the interdisciplinary area of the ***engineering development of textile based products and the technology of their assembling***.

Scope

Topic of interests are **new, not published** research results and materials related to:

- development of products of textiles
- textile materials, their production and parameter identification
- 2D and 3D pattern design
- optimisation and body shape fitting
- 3D/4D scanning, data processing
- cutting and investigations on preparatory processes
- assembling technologies – sewing, welding, gluing, thermoforming, folding, packing
- textile logistics
- recycling of textile products
- numerical modelling of all these processes
- interaction between clothing and human body with all its aspect related to mechanical, thermal, moisture, processes and human body comfort
- biomechanics related to textile product development
- other related topics.

Article types

The journal publishes communications in two types/parts:

A) **peer reviewed journal articles** (research papers, review of state-of-the art papers)
B) *not reviewed* ***communications*** in form of reports, data sets, technique reviews, conference papers, abstracts, discussions.

Language

The language of the **peer reviewed articles** is only **English**.

The non-reviewed communications have to be preferably in English, but can be published in German or other languages, too, if the editorial team is able to check the formal level and the quality of the material on this language. In this case title and abstract in English language has to be provided.

Review process for the review articles

Each submission is reviewed from at least four persons.

1. After the submission two of the Editors-in-Chief, or Editor-in-Chief and one Member of the Editorial Board (in case the other Editor-in-Chief is co-author or related to the authors of the manuscript) check the manuscript and decide about its potential for publication.

2. If the novelty and content is suitable two independent reviewers are invited to review the material. In case that their opinion is very different, additional reviewers can be invited.

The review process is **open and transparent for author and reviewers:**

- the reviewers can see the authors of the material
- the author receives the complete feedback of the reviewers, *without their personal data* (**single blind review process**).

Discussions on previous published results are welcome and will be published without review in form of short communication with DOI, too.

The length of the reviewed papers is not limited, but only well structured materials will be considered for publication.

Publication form

The journal is a **purely online journal**, without print issues. All published papers are available as **open access papers** in PDF format under Creative Commons Attribution-NonCommercial-NoDerivatives 4.0 International License.

Formally, all published manuscripts are structured in **two issues per year**.

References

The references have to be formatted following the **ACM reference stlye** https://www.acm.org/publications/authors/reference-formatting

This is available in Citavi, Zotero, Endnote and many other reference managers.

Submissions Template

Submission template in Word can be downloaded here www.cdatp.org

Publication charges / Article processing charges

CDATP journal do **not** charge any fees for publication of articles. The costs for DOI and web hosting are covered by the Saxonia State and University Library (SLUB), Dresden and TU Dresden. The work of all editors and production team is voluntary.

Copyright

The authors retain the copyright of their paper without restrictions.

Licensing

All papers are published under Creative Common CC-BY-NC-ND License https://creativecommons.org/licenses/by-nc-nd/4.0/

Plagiarism and self-plagiarism

The editorial team checks first the manuscripts on google.com. In cases of any suspicion using plagiarism or self-plagiarism detection software available at TU Dresden to check the submissions. If plagiarism is detected, the COPE guidelines on plagiarism will be followed.

Publication Ethics and Publication Malpractice Statement

The CDATP journal is committed to maintaining the highest level of integrity in the content published.

This journal follows the COPE *Code of Conduct and Best Practice Guidelines for Journal Editors* and the *Code of Conduct for Journal Publishers*.

Preprint servers

Posting a manuscript on a preprint server or an author personal or institutional webpage (without DOI, publisher) does not count as previous publication. Once the manuscript is accepted and published, the author is responsible to update the preprint record with a publication reference, including the DOI and URL link to the published version.

Repository policy

The authors are encouraged to deposit a copy of their accepted manuscripts papers in an institutional or other repository of their choice, as Accepted version (Author Accepted Manuscript) and as Published version (Version of Record). Authors should provide a link from the deposited version to the DOI and URL of the publication article. The only purpose of this link is to ensure, that the journal's website is clearly identified as the definitive version of record. There is no embargo period for self archiving.

The journal is listed in Romeo Service https://v2.sherpa.ac.uk/id/publication/39565

COMMUNICATIONS IN
DEVELOPMENT AND ASSEMBLING OF TEXTILE PRODUCTS

Functionalization of medical textiles

Natalia Sadretdinova[1], Sergey Bereznenko[1], Larisa Bilotska[1], Maria Pawlowa[2], Halina Szafranska[2,*], Vitalii Bakal[3], Natalia Bereznenko[3,*]

[1] *Kyiv National University of Technologies and Design, Kyiv, Ukraine*
[2] *Kazimierz Pulaski University of Technology and Humanities in Radom, Radom, Poland*
[3] *State Research Institute of the Ministry of Internal Affairs of Ukraine, Kyiv, Ukraine*
* Corresponding author *E-mail address: h.szafranska@uthrad.pl, nmbereznenko@gmail.com*

INFO

CDAPT, ISSN 2701-939X
Peer reviewed article
2020, Vol. 1, No. 2, pp. 88-95
DOI: 10.25367/cdatp.2020.2.p88-95
Received: 11 May. 2020
Accepted: 21.07.2020
Available online: 23 November 2020

ABSTRACT

An important basis for the creation of medical clothing is realization of the influence of various factors that arise in the interaction of elements of the system "man–clothes–production environment". Given the increasing technogenic burden on health of both medical staff and hospital patients, the assessment of the role of medical clothing in forming the energy balance of direct consumers is extremely relevant. Previous studies have experimentally confirmed the presence of energy effects of textile materials on the human body. However, determination of the nature of the impact is a complex task, which solution depends on a number of factors, such as the raw material composition, its structure, surface characteristics, etc. The purpose of our paper is to study the development of textile multifunctional materials for medical purposes and to study their energy-information impact on the human body. The following tasks have been solved in the course of the study. For use in the medical field, several samples of textile materials with antimicrobial properties, modified by herbal preparations, were obtained. Properties of textile materials that determine the possibility of their use in medical practice have been investigated. The influence of the experimental samples on the functional state of the organs and systems of human organs by use of the methods of information-wave therapy is evaluated.

Keywords
medical clothing,
herbal modifiers,
antimicrobial properties,
energy-information state of organs

1 Introduction

Textile based products are widely used in modern medicine. First and foremost, it is clothing worn by patients and healthcare professionals, towels and tissues to hold and clean the fluid, wipes to maintain sterility during surgery, as well as interior items and linens. Considering the particularities of the consumption environment, textiles can be a potential source of infection by holding microorganisms and transmitting them during human contact. This is what we are watching in the worldwide pandemic caused by COVID 19, when personal antimicrobials for doctors and the general public have become one of the most important means of preventing the spread of infection. Therefore, as a response to the challenge of the present day, research related to antimicrobial treatments in the field of medical textiles is intensifying.

Analysis of research in the field of functionalization of medical textiles shows that today different ways of giving antimicrobial properties to textile materials have been developed and successfully used. The literature provides data on the bacteriostatic effect of textile materials on impregnation with a mixture of neomycin salts with propionic, tartaric, phthalic, stearic and some other acids, which were dissolved in water, butanol or methanol and applied to the material by spraying solutions. However, the antimicrobial action of such materials is short-lived. As biocides, metal salts have become quite widespread. The use of copper salts as an antibacterial agent leads to the dyeing of the textile material in yellow-green color. The use of zinc salts is limited by their weak biocidal action, and the salts of mercury, tin, arsenic increase toxicity to humans [2, 3]. Much attention is drawn to the functional activity of silver nanoparticles in terms of giving both bactericidal and bacteriostatic properties to various materials and products, but there are problems, caused by the leaching of ions into wastewater, which leads to environmental pollution [4].

One of the ways to increase the durability of antimicrobial processing on textiles is microencapsulation. Biocides are placed in nano-sized containers (cyclodextrin, liposomes – vesicles). In the case of vesicles, pathogenic bacteria that have an affinity for the vesicles attack them, destroy the vesicle membrane, and release molecules or nanoparticles of the biocide from it [10].

Finishing of textiles with hydrophobic agents (for example, silicones) can reduce the impact of microorganisms on materials by reducing the amount of adsorbed moisture, but does not completely eliminate them [5].

In the worsening global environmental crisis, another promising area of antimicrobial properties is the so-called “green technology”, which involves the production of new products with minimal environmental damage [6].

Thus, to obtain products with antimicrobial properties they use materials based on bast fibers, whose unique natural properties can be supplemented or enhanced by surface modification [7]. Natural dyes and pigments derived from plants, insects, animals and minerals also have antimicrobial activity [8]. Plant extracts can be used in the form of reducing agents in nanomodification, as well as independently, in the form of impregnations or sprays [9].

As we can see, modern science offers a large number of options for providing antimicrobial properties to textile materials. Given the scientific uncertainty and the emergence of more and more new data on the early signs of harm and the potential adverse health effects that may be associated with antimicrobial treatments, the precautionary approach seems to be most appropriate. There is a need to clarify information on the effect of physically or chemically modified materials on the human body. These are medical products whose operation involves many risk factors and it is therefore important to understand how the presence of a particular treatment will affect the overall condition of the potential consumer of such products in the traditional operating environment.

Nowadays, in the field of medical diagnostics, energy-information wave medicine is becoming more widespread, its main provisions are based on quantum mechanics and theoretical physics [10]. There are known about twenty methods and devices that use various physical effects: electropunctural diagnostics, electromagnetic wave therapy with the use of other energy types (UV radiation, torsion fields), SCENAR-therapy, mineral-, color-, sound and spectral therapy etc.

Previous studies [11], carried out using the methods of electrowave diagnostics, have detected a complex effect of materials and their components on the functional state of organs and organ systems. This indicates the significant role of materials for the clothes manufacturing, as important mean of protecting people from aggressive environment, pathogens of internal and external origin. In this case, the information-wave nature of the interaction of the elements of the system “man–clothes–microbial environment” can be realized due to standing waves that occur when interfering with the traveling wave from the pathogen and the oncoming wave reflected from the material. Therefore, conducting a comparative analysis of the results of registration of the functional state of the human body under the influence of the studied textile material and without its influence makes it possible to assess the degree of safety of using this material for the functioning of the body of potential consumers in the production environment.

Considering these aspects, the purpose of the study was the functionalization of medical textiles by providing them with long-lasting antimicrobial properties based on “green technologies” and the study of their energy-information impact on the human body.

The following tasks have been solved in the course of the study. For use in the medical field, several samples of textile materials with antimicrobial properties, modified by herbal preparations, were obtained. Properties of textile materials that determine the possibility of their use in medical practice are investigated. The influence of experimental samples on the functional state of organs and systems of human organs by use of information-wave therapy methods was evaluated.

2 Method

2.1 Description of the Subject of Research

A review of the literature has revealed that the main material used in the manufacture of medical clothing at present is mixed textile fabrics containing cotton. Therefore, as a textile basis for the application of the modifying agent, cotton fabric (65 PE / 35 of cotton) of weave was selected with a surface density of 125 g/m^2.

An antimicrobial drug used to modify the textile fabric is a peony infusion solution patented as an antimicrobial drug that have an active effect on gram-positive, gram-negative bacteria and fungi such as *Staphylococcus aureus*, *Candida albicans* and *Bacillus subtilis* [12]. The recommended concentration of the solution is 0.05 g/l.

2.2 Methods and Devices for Antimicrobial Coating

Traditional antimicrobial coatings can generally be considered as polymeric matrices. They are usually applied to the textile material by spraying or impregnating with a solution, followed by a drying process to remove the solvent. A common problem for such antimicrobial coatings is the instability to repeated wet treatments, which may be caused by limited adhesion.

To compare the stability of the antimicrobial properties of the textile material added as a result of the modification, two methods of applying the modifier to the textile material were used.

To provide antimicrobial treatment in the first way, aqueous nano-solution with infusion of peony medicinal is sprayed on the surface of the sample tissue using a steam brush.

The second method involves the impregnation of the textile material with citric acid and the subsequent spraying of the medicinal peony nano solution. Citric acid (2-hydroxy-1,2,3-propantricarboxylic acid, $C_6H_8O_7$, HOOC-CH_2-C(OH)COOH-CH_2-COOH) with a working concentration of 0.96 g / l was used for the preliminary impregnation of the textile. The essence of the modification is to create the necessary conditions for the reaction between the anhydride modifying agent (acid) and cotton cellulose textile material. For this purpose, the fabric is filled with a solution of citric acid of a given concentration. After stirring for 30 min. at 20 °C, the acid solution is drained, the fabric is placed in a vessel and dried at 50 °C in an oven for 4 hours. After drying, the thermochemical reaction between the acid and the cellulose occurs by raising the temperature to 120 °C, at which the acid is converted to the anhydride. Processing time is 2 hours. After cooling, the reaction products are washed with distilled water until neutral to remove excess acid. After drying, an aqueous solution of the herbal preparation – peonies drug concentration of 0.05 g / l nano solution – was sprayed with a Philips GC361 / 20 Steam & Go steam brush, repeating the first method. To dry the tissue samples, a ShS-3 drying cabinet was used to provide drying of the materials at a predetermined temperature (10 °C above room temperature and up to 200 °C).

Spraying was carried out by use of Philips GC361 / 20 Steam & Go household steam brush used for safe ironing of all kinds of fabrics, with a steady supply of 22 g / min [13]. To check the stability of the obtained antimicrobial effect, the samples were washed in an automatic washing machine according to the method of GOST ISO 6330-2011.

2.3 Methodology of Energy-Information Impact Assessment

Today, scientists [14–16] have proved the importance of biologically active points and biologically active zones in the perception of the influence of environmental factors: meteorological, solar activity, various electromagnetic fields, etc. And these achievements are already being used to create the latest functional clothing.

Previous studies conducted in collaboration with researchers of Khmelnitsky National University have shown that use of the hardware-software diagnostic complex “Intera-DiaCor” (Register of Medical Technology of Ukraine No 3277/2004 dated 30.10.2009) makes it possible to register the parameters of zonal conductivity from biologically active areas of the body that are functionally connected with organs, and to evaluate the functional status of the latter and the body as a whole at the cellular level [17].

The study was conducted according to the method described in [11]. According to the method, after two complete cycles of diagnosis, the results of diagnostics of the functional state of organs and systems of the human body were compared without the influence of the analyzed fabric and with it. The results of the diagnosis at the Intera-DiaCor are displayed on the monitor in the form of histograms showing the three main states of organs and systems of the human body: energy lability (normal state); energy instability (instability of energy processes in the body); energy failure (suppression of energy processes).

According to the developed methodology, the level of negative and positive energy-wave influence is suggested to be estimated by the numerical value of the comfort factor $К_к$:

$$Кк = \frac{Кс - Кн}{Кс} \cdot 100\%,$$

where $К_н$ – the number of organs (organ systems) of the human body, in which functional and energy state there were negative changes caused by the influence of the material; Kc – the number of organs (organ systems) of the human body that have been diagnosed.

The methodology for conducting comfort studies at the Intera-DiaCor APC is described in [17] and patented [18].

3 Results

In order to detect the effect of modified textile material on the human body, the functional state of the human body was investigated by use of the Intera-DiaCor APC. The study was performed with the involvement of two young people, whose functional state of the organism at the time of the study was not characterized with significant deviations. This number is sufficient because the determination of the functional state of the human body using the Intera-DiaCor APC has high accuracy (relative warranty error does not exceed 5%).

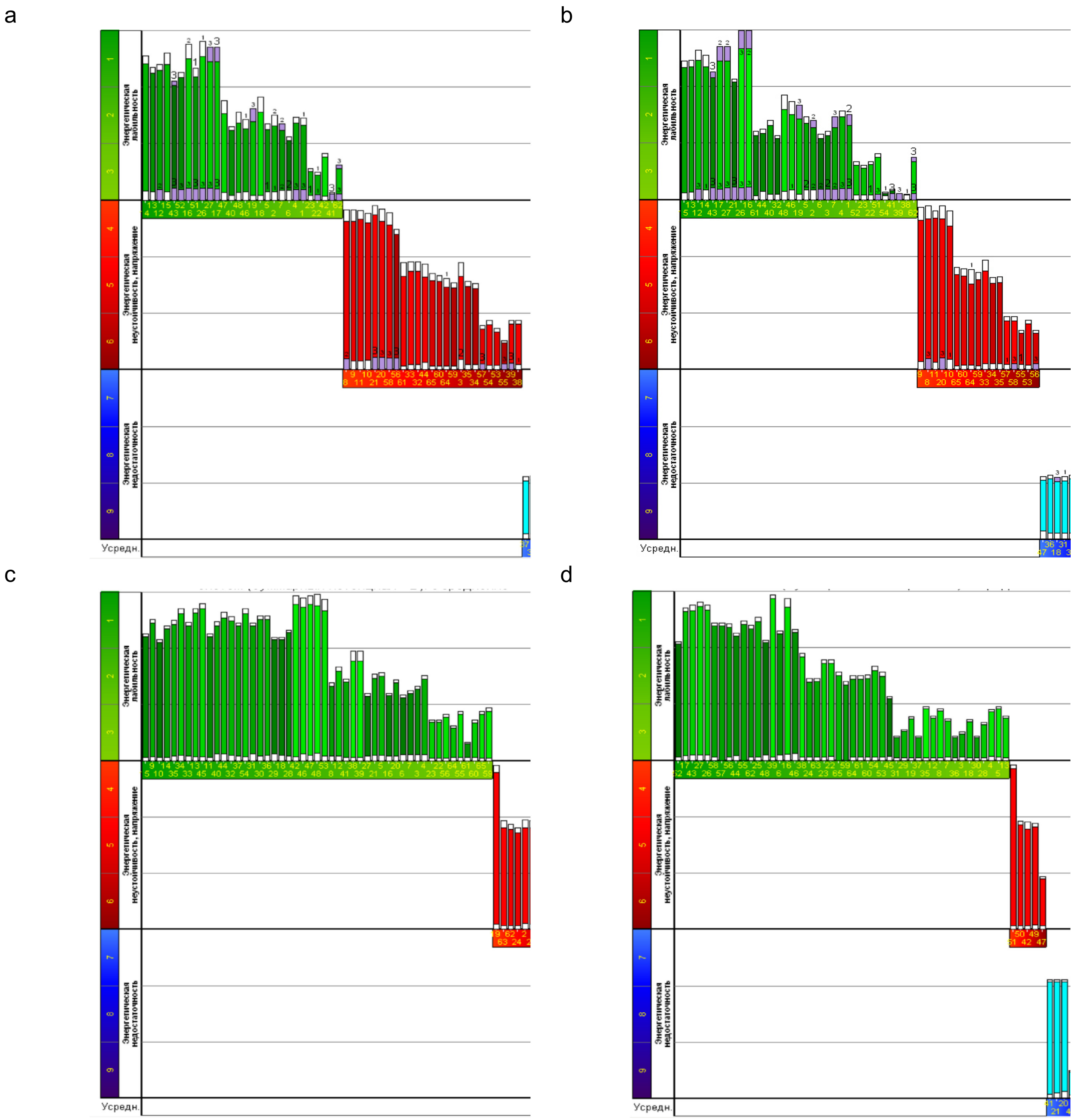

Fig. 1. Histograms of the Energy and Functional State of Organs: (a) – a person without a sample of material, C1; (b) – a person with an unmodified sample of material, C2; (c) – the person with the sample modified in the first way, C3; (d) – the person with the sample modified in the second way, C4.

The studies were conducted in four environments of interaction between humans (subjects) with textile material:

C1 – a person without a sample of material;

C2 – a person with an unmodified sample of material;

C3 – a person with a sample modified by spraying an aqueous peony drug solution (first method);
C4 – a person with a sample modified by impregnation of the textile material with citric acid and subsequent spraying of the medicinal peony nano solution (second method).

After two complete cycles of diagnosis, the results of the diagnostics of the functional state of the organs and systems of the human body were compared without the influence of the test cloth and with it. Examples of the obtained histograms are shown in Figure 1.

On the basis of the obtained histograms, the total number of organs and systems of organs of the human organism, which are in different energy states: energy lability (green column), energy instability (red column) and energy insufficiency (blue column) without the influence of the material and under their influence on the investigated persons was calculated. Based on these data, the coefficient of comfort was calculated using the formula above. The results are summarized in Table 1.

Table 1. Results of the calculation of the level of energy information impact of textile antimicrobial materials on the functional state of the human body.

Types of test environments	Number of human organs in condition:						Comfort coefficient	
	energy lability		energy instability		energy failure			
	person 1	person 2	person 1	person 2	person 1	person 2	person 1	person 2
C1	28	37	25	0	12	28	1.00	1.00
C2	33	37	17	0	15	28	1.08	1.00
C3	49	47	10	2	6	16	1.32	1.15
C4	46	60	5	5	14	0	1.28	1.35

As it can be seen from the table, an unmodified sample of material (C2) has a minor effect on the functional state of the organism, which makes it possible to weigh it inert to the effect on the body. At the same time, the samples modified with the nanoparticle of peony medicinal, applied in the first and second methods (C3, C4), have a significant effect on the correlation of the number of organs in different energy states. At the same time, there is a tendency to increase the number of organs in the state of energy lability and decrease their number in the states of energy instability and insufficiency.

To determine the resistance of antimicrobial treatments to the effects of service loads, similar studies were conducted for samples of modified materials after three washing cycles. The results are shown in Table 2.

Table 2. Results of the calculation of the level of energy information impact of textile antimicrobial materials on the functional state of the human body after three washing cycles.

Types of test environments	Number of human organs in condition:						Comfort coefficient	
	energy lability		energy instability		energy failure			
	person 1	person 2	person 1	person 2	person 1	person 2	person 1	person 2
C1	28	37	25	0	12	28	1.00	1.00
C2	30	37	20	0	15	28	1.03	1.00
C3	37	45	18	4	10	16	1.14	1.12
C4	45	52	10	13	10	0	1.26	1.23

A slight decrease in lability indicates that the result of the modification of the tissue with a solution of peony drug positive effect on the energy-functional state of the body, is quite resistant to the effects of washing. After three cycles of washing, citric acid modified with peony solution (C4) exert a more active effect on the organism of the subjects compared to those modified only with peony solution (C3).

This can be explained by the fact that under the action of citric acid increases the size of the capillaries inside the cellulose fibers, which in the further processing are filled with modifiers, extending the life of protective textiles.

To study the dynamics of the change in the coefficient of comfort for different test environments before and after washing, the diagrams are shown in Fig. 2. In determination of the tendency of change in comfort the control sample (C2) was not considered, since it does not have a clear effect on the human body.

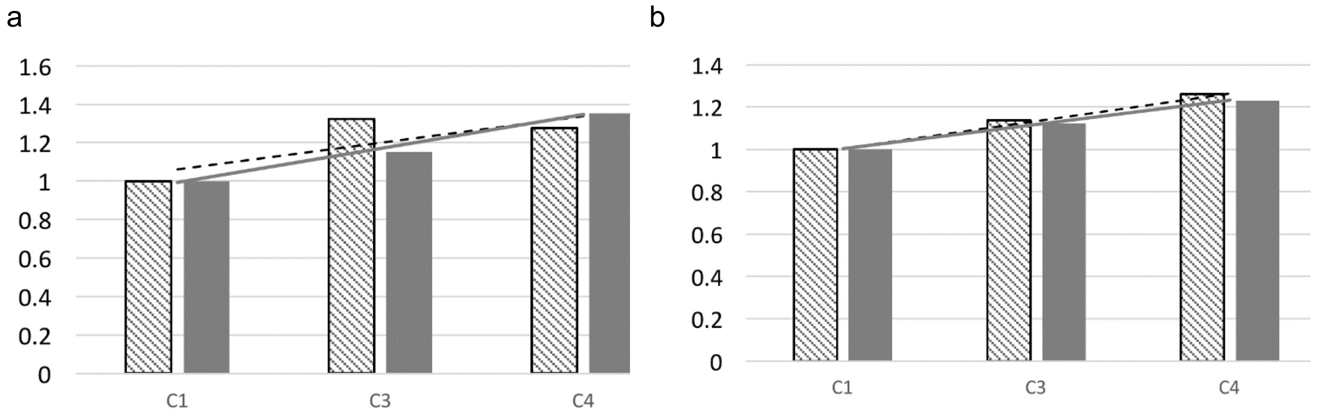

Fig. 2. Dynamics of change of comfort factor of investigated persons under the influence of samples of modified materials: (a) before washing; (b) after washing.

As it can be seen from the diagrams, after the modification of the samples, there is a tendency to the improvement of the comfort of the organism of the subjects. This tendency persists after three washing cycles as well.

It is established that all textile clothes in the environment of interaction with the person C2, C3, C4 exert energy and information influence on the organism of the studied persons. Given the purpose of these clothes, it is important to choose the clothes with the highest coefficient of comfort for the functional state of the body of the subjects (Tables 1, 2). As visible, this option is a sample modified by impregnation of the textile material with citric acid and subsequent spraying of the medicinal peony nano-solution.

4 Conclusions

The paper suggests the method of provision of antimicrobial properties to textile materials using the solution of medicinal peony tincture. The use of vegetable raw materials in the creation of antimicrobial textiles is advantageous due to its availability, as well as, in most cases, its low toxicity, lack of habituation and negative side effects.

The technique of applying a phyto-preparation to a textile canvas has been developed. It has been found that it is expedient to use the method of atomization of the solution and structural destruction of the fiber by acids for the stable fixing and uniform distribution of the nanoparticles of the preparation on the surface of the textile web. This method prevents the rapid leaching of nanoparticles from the fabric surface during operation and washing.

As textile materials play an important role in the formation of the energy flows of the "man–clothes–environment" system and such influence can be inert, positive or negative, the evaluation of the energy-related impact of modified materials on the functional state of organs and systems of human organs using the wave medicine method is carried out.

It has been established that the medicinal materials obtained as a result of the modification of the peony solution exert a positive influence on the energy state of the person and activate processes in the body responsible for the immune system. This makes it possible to believe that these materials actively protect the body from exposure to pathogenic microflora.

Also, the method of energy information diagnostics determines the resistance to washing achieved by the modification of the antimicrobial effect. After three cycles of washing, citric acid modified with peony solution exerts a more active effect on the organism of the subjects compared to those modified with only peony solution.

Therefore, the results obtained in this paper contribute to the spread of the use of “green technologies” for the manufacture of textile materials with antimicrobial properties. Considering the potential danger of modified materials for human health, it is also important to use the method of complex analysis of the influence of materials on the functional state of the body.

References

[1] Abaeva, L. F.; Schumskyi, V. I.; Petritskaya, E. N. Nanoparticles and nanotechnology in medicine today and tomorrow. *Clinical Medicine Almanac*, 2010, 22, pp. 10–17.

[2] Erokhina, E.V. Synthesis of ultrafine copper and silver particles to protect textile materials from biodegradation. *Physics of fibrous materials: structure, properties, high technology and materials*, 2015, 1, pp. 88–91.

[3] Krichevsky, G. E. Nano, bio, chemical technology and production of new generation of fibers, textiles and clothing: monograph; 2011, Moscow.

[4] Galik, I. S., Semak, B. D. The use of nanotechnology for the medical textiles production. *Bulletin of KNUTD,* 2014, 3 (77). pp. 176–186.

[5] Matveytsova, D. S. Development of technology of final processing in textiles using silica nanoparticles, Doctoral dissertation, Kherson national University. 2017, Kherson.

[6] Shahid-ul-Islam; Shahid, M.; Mohammad, F. Perspectives for natural product based agents derived from industrial plants in textile applications – a review. *Journal of Cleaner Production*, 2013, 57, pp. 2–18.

[7] Bereznenko, N. P.; Wislenko, V. G.; Bandura, N. G. Creation of antimicrobial textile materials based on bast fibers and modified synthetic threads. *Bulletin of KNUTD*, 2005, 5, pp. 22–24.

[8] Dobrovolskaya, A. V.; Paliy, G. K.; Kryzhanivska, A. V. Using of natural dye for destination color and antimicrobial properties to textile materials. *Light industry*, 2008, 4. pp. 46–47.

[9] Herbal antibiotics. Available online: http://www.disbak.ru/php/content.php?id=4080

[10] Fedotkin, I. M. Notes on the theory of information-wave medicine (IVT, BRT, Moro therapy, VRT, SCENAR-T, OLM-1, Fractal-metric applicators) / Fedotkin I.M. - K.: Publishing house “Himjest”, 2003, p. 40.

[11] Bereznenko, N.; Bereznenko, S.; Pawłowa, M.; Jancałowskij, O.; Vlasenko, V. Influence of textile materials on the functional state of human body – assessment; *Towaroznawcze Problemy Jakosci*, 2011, 4, pp. 59–65.

[12] Kislichenko, V. S., Zhuravel, I. O., Burda, N. E., Sakhatskaya, I. M. Antimicrobial drug; Utility model patent № 88422, МПК A61K 35/00, 11.03.2014.

[13] Manual evaporator Steam&Go. Available online: https://www.philips.ua/c-p/GC361_20/steam-go-handheld-garment-steamer.

[14] Zhdanova, O.; Bereznenko; S.; Bereznenko, N.; Novak, D. Textile materials manufacturing features with the use of antimicrobial additives. *Vlakna a Textil*, 2017, 4, pp. 41–46.

[15] Pashkin, O. V.; Soroka, S. O. Method for determination the influence of biologically active substances on human skin. 2018, pp. 362–365.

[16] Buhantsova, L.; Luschevska, O.; Troyan, O.; Krasniuk, L.; Yantsalovskyi, O. Formation of the package of materials of adaptive multifunctional clothing. *Technology Audit and Production Reserves*, 2017, 3.3 (35), 4–12.

[17] Bereznenko M. P.; Vlasenko V. I.; Yantsalovsky O. Y. Investigation of the influence of textile materials on the energy-information state of human body. *Collection of scientific works Sworld*, 4 (32), pp. 31–38.

[18] Luschevskaya, O. M.; Yantsalovsky, O. Y.; Trojan, O. M. Method for evaluation the comfort of textile materials; Patent №35944, МПК G01 N33/36, 10.10.2008.

COMMUNICATIONS IN
DEVELOPMENT AND ASSEMBLING OF TEXTILE PRODUCTS

Selected dynamic anthropometrics and body characteristics for posture corrector fit

Inga Dāboliņa[1]*, Jelizaveta Fomina[2], Eva Lapkovska[2], Liene Siliņa[2]

[1] *Head of Research Laboratory of Ergonomics Electrical Technologies, Institute of Industrial Electronics and Electrical Engineering, Faculty of Electrical and Environmental Engineering, Riga Technical University, Riga, Latvia*
[2] *Institute of Design Technologies, Faculty of Material Science and Applied Chemistry, Riga Technical University, Riga, Latvia*
*Corresponding author *E-mail address:* inga.dabolina@rtu.lv

INFO

CDAPT, ISSN 2701-939X
Peer reviewed article
2020, Vol. 1, No. 2, pp. 96-103
DOI 10.25367/cdatp.2020.1.p96-103
Received: 12 July 2020
Accepted: 11 November 2020
Available online: 22 November 2020

ABSTRACT

Correct body posture is a balanced musculoskeletal body position; however, today many people face severe posture defects, and their body posture may be far from normal, causing progressive musculoskeletal deformities and pain, as well as affecting the functionality and appearance of the body. Human daily habits, lack of physical activities and overall a sedentary lifestyle cause such phenomena. The research focuses on studies of human body measurements and body characteristics while wearing posture-corrective equipment for the assessment of the effectiveness of different posture correctors (PoC). Four test-persons were selected and scanned using 3D anthropometrical scanner in relaxed stand position wearing five different posture correctors for a prolonged period of time in order to determine the effectiveness and functionality of each PoC. Four distance (linear) human body measurements were gained to quantify postural changes – scapula position depth, upper torso position, shoulder projection height and hip-waist depth. General feedbacks on each subject impression of wearing PoCs were also received. Correction of posture could serve as a preventive or treatment for spine-related problems; though, commercially available correctors could negatively affect wearer's health due to non-conformity of the design and/or used material. Therefore, PoC selection and wearing procedures should be solved with more personalized and customized approaches.

Keywords
ergonomics,
anthropometrics,
posture,
posture corrector,
compression garment,
human body 3D scanning

1 Introduction

Almost every person faces posture defects. The main reason that leads to the wrong posture and resulting health problems is back muscle weakness caused by lack of body movements or physical activities (unless postural defects are congenital or caused by disease). The human body movement system is strengthened insufficiently due to the lack of physical activities. One of the symptoms is back pain, though discovering the cause of it is not always easy. Normalization of posture could serve as a preventive measure or treatment for back pain or sprains [1-3]. The main functions of posture correctors (PoCs) are to correct body posture, as well as to relieve back and neck pain [1]. Mostly such PoCs are intended to help a person maintain a correct body posture and, if necessary, for spinal support. The most obvious method for determination of posture garment effects on wearer's posture is the assessment of postural changes [4-7].

There are various types of belts, bandages, back supports and posture correctors available on the market that could help with correcting posture defects. However, the use of such commercially available products daily could be cumbersome due to unsuitable choice of textiles and design deficiencies; moreover, they could cause skin irritation and limited mobility [6]. To evaluate the effects of different PoC products, four test-persons were selected to test and analyze five posture correctors.

2 Posture disorders and means of their correction

Posture is defined as the relative position of body parts to a physical position, such as standing, lying, and sitting. Correct posture – a straight spine in relation to the medial plane that supports the natural curve of the spine, maintaining the balance of muscles and skeleton [4]. This balanced musculoskeletal position protects the supporting structures of the body and prevents damage or progressive deformation in all positions, including standing, lying, and sitting [2,4].

The importance of the right body posture and particularly emphasizing the right posture while sitting should be promoted. In most cases, the occurrence of poor posture is affected by human habits, such as back bending or leg crossing, sedentary work, use of smart devices, and generally sessile lifestyle without proper physical activities. If taking a poor posture becomes a habit at an early age, a person who maintains this posture becomes accustomed to it and even feels comfortable, thus causing tension in the spine, pelvis, muscles, tendons, joints, bones and discs, leading to fatigue and spine deformations [8]. Spinal injuries mostly occur in young and actively working people (as a result of high traumatic energies), relatively less often in older people with osteoporosis (as a result of minimal influencing energies).

2.1 Posture disorders

The spine of an adult has the shape of the letter “S”: in the neck and lumbar region the spine is curved forward (lordosis), while in the chest and sacrum the spine forms two curves backwards (kyphosis). Due to its curved shape, the spine can absorb pushes and convulsions, and therefore it oscillates flexibly as a person walks, jumps and runs. From a physical medicine point of view, a posture is a balance of muscles and skeleton that protects the body’s supporting structures from damage or progressive deformation regardless of its position (lying, sitting on a squat or leaning), in which these structures work or rest [8]. Posture asymmetries can be progressive and affect functional activities, as maintaining the wrong posture for a prolonged period of time causes significant strain on the spine [9-12]. Postural disorders can be caused by a variety of reasons:

spinal asymmetries (scoliosis, kyphosis, lordosis)

injuries/traumas (clavicle injury, axial skeleton injury, et al.)

diseases (Scheuermann’s disease, osteoporosis, et at.).

2.2 Posture correctors

Various methods are used to treat diseases of the spine and joints, including orthopedic products called orthoses. Orthoses are functional orthopedic aids to change the structural and functional properties of the musculoskeletal system, to immobilize, relieve or correct a diseased spine or limb, including various medical bandages, collars, corsets, belts, etc. The main task of orthoses is to ensure temporary and secure immobilization of certain muscles and skeletal system segments, as well as to compensate functionally deficient limbs and body parts. The period of wearing the orthoses is regulated by a doctor, and they can be produced individually or in series [9,13]. Orthoses (belts/corsets/vests) are used to reduce pain, protect against further damage, help weak muscles, and prevent or help to correct the deformity by maintaining torso alignment through passive force [13,14].

Various means are used to correct posture and relieve back pain:

sitting support devices (cushions, Swiss ball chairs, et al.)

kinesiology tape

Posture braces/Orthosis (full spine brace/reclinator, upper back brace/cross-back elastic brace, electronic posture reminder, et al.).

The variety of patents includes various posture correction solutions from textiles or partial use of textiles – such as posture correction girdles [15], spinal orthoses [16,17], posture vests [18], therapeutic garment systems [19] and other posture support devices [20,21,22].

In this study five posture correctors – three upper back brace and two full spine brace – were analyzed, see Fig. 1:

PoC # 1 cross-back elastic brace with wide straps

PoC # 2 cross-back elastic brace with narrow straps

PoC # 3 cross-back elastic brace with wide hemmed straps and narrowing of the straps in the area of the shoulders and armpits

PoC # 4 reclinator with half waist belt

PoC # 4 reclinator with full waist belt.

Fig. 1 (a-c) Upper back brace; (d,e) full spine brace.

3 Testing of posture correctors

3.1 Method

Test subjects were scanned using 3D human body scanning device Vitus Smart XXL ®. The scanning was performed six times in a time frame of one work-day for each posture corrector: at the beginning of the day without posture corrector and with posture corrector, three times every two hours while wearing posture corrector, the last time – after wearing period of six hours – without posture corrector. Each scanning set was conducted as follows: one set consisted of three scans; after each scan the test subject was asked to step off the scanner platform and step again back on it. All participants were scanned while wearing their underwear and standing in a natural/relaxed posture.

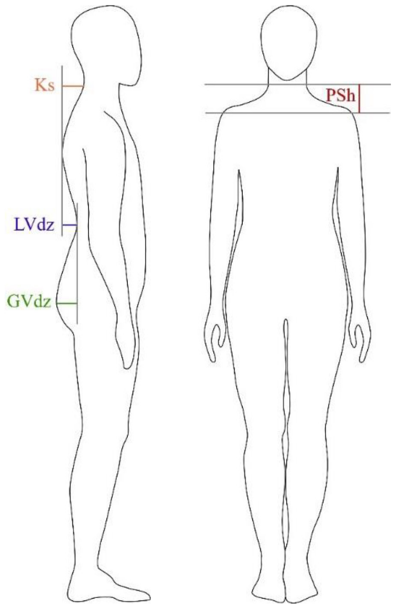

Fig. 2 Measurements determining the change of posture.

Four linear human body measurements were selected to determine postural changes – scapula position depth (LVdz), upper torso position (Ks), shoulder projection height (Psh) and hip-waist depth (GVdz), see Fig. 2. The obtained measurements were summarized, and the median value was selected (from all three scans of each test set). The use of an arithmetic mean value was not appropriate due to the uniformity of the human body. Selecting values that did not correspond in any of the cases was not in accordance with the methodology; therefore a scan with medial measurements from all three measurements was accepted as the calculation model.

The analysis of the data took into account both – the effect of each posture corrector on the test subject and the effect on individual measurements.

3.2 Test-persons

To determine the effects of each PoC on wearer's posture, four test subjects were selected – women aged 25 to 35 years (each was assigned a letter designation: A to D). All test subjects have a slender body structure (see Table 1) and moderately developed musculature. The test-person A has no posture or spine defects, is physically well developed, but not trained. As for other test subjects, this person has mild back problems – the prominence of the scapula, scoliotic and/or kyphotic changes.

Test-person A was a reference test-person without back problems and with the best trained (but not athlete's) body; respectively, posture certainty and repeatability for this person was the highest, while test-person C had the most uncertain physical fitness and could be the most easily influenced, and posture correctors are expected to give the best result to test-person C.

Table 1. *Characteristics of test-persons.*

Person:	A	B	C	D
Body height (cm)	173	159	167	164
Horizontal bust girth (cm)	97	88	93	90
Hip girth (cm)	95	93	93	93
Weight (kg)	64	51	58	51

3.3 Analysis of data

After testing the posture correctors, graphs were drawn up for each test subject, including all stages (scanning sets) of the experiment, showing the changes of the four previously selected human body measurements (LVdz, Ks, Psh, GVdz) (see Fig. 3).

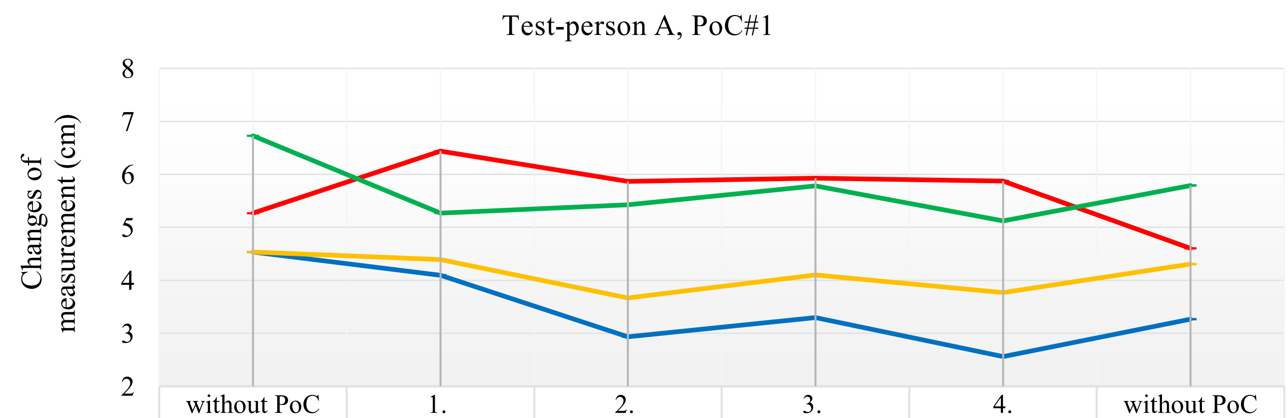

	without PoC	1.	2.	3.	4.	without PoC
LVdz A	4,5	4,1	2,9	3,3	2,6	3,3
Ks A	5,3	6,4	5,9	5,9	5,9	4,6
Psh A	6,7	5,3	5,4	5,8	5,1	5,8
GVdz A	4,5	4,4	3,7	4,1	3,8	4,3

Fig. 3 Effect of PoC#1 to the test-person A.

According to the change in the measurement visible from the graph, the effect of PoC was evaluated in comparison to the first scan without PoC. If the value is greater than or equal to the original (a positive value indicates a bent posture, a negative value indicates that no change was observed), then the stage was marked with 0, if less, then with 1. The obtained binary scores were summed to describe the extent to which the PoC affects the particular measurement. The last column “without PoC” determines how the test-subject’s posture as a whole was affected by evaluating it without posture corrector at the end of the experiment – positively or negatively according to the same comparison method (see Table 2).

Table 2. Analysis of effect of PoC#1 to the test-person A

Test # / Measurement	1.	2.	3.	4.	∑	without PoC
LVdz	1	1	1	1	**4**	1
Ks	0	0	0	0	**0**	1
Psh	1	1	1	1	**4**	1
GVdz	1	1	1	1	**4**	1

Such comparison method was used for all measurements and the overall impact of PoC. After a binary comparison which is to assess all properties in pairs – if one is evaluated as better than other, it is marked as 1, if properties (PoCs) are with equal impact, both are marked as 0.5 (see Table 3), it was concluded that regardless of whether or not there is a narrowing of the straps in the area of shoulders and armpits, PoC # 1 and PoC # 2 affected the test subjects in the same way and that the result for each test-person was more dependent on their physiological features.

To support the data, a posture test was performed on test subjects A and C without PoC. The experimental procedure was the same as using PoC. These tests showed only insignificant changes in stature (also posture), which confirms the effect of PoC on test subjects.

Table 3. Binary comparison of the effect of PoC on the test-person.

Effect on the test-person	PoC#1	PoC#2	PoC#3	PoC#4	PoC#5	∑
PoC#1 person A		1	1	1	1	**4**
PoC#2 person A	0		0	0	0	**0**
PoC#3 person A	0	1		0.5	1	**2.5**
PoC#4 person A	0	1	0.5		1	**2.5**
PoC#5 person A	0	1	0	0		**1**
PoC#1 person B		0	0	0	0.5	**0.5**
PoC#2 person B	1		1	1	1	**4**
PoC#3 person B	1	0		0.5	1	**2.5**
PoC#4 person B	1	0	0.5		1	**2.5**
PoC#5 person B	0.5	0	0	0		**0.5**
PoC#1 person C		0.5	0	0.5	0	**1**
PoC#2 person C	0.5		0	0.5	0	**1**
PoC#3 person C	1	1		1	0.5	**3.5**
PoC#4 person C	0.5	0.5	0		0	**1**
PoC#5 person C	1	1	0.5	1		**3.5**
PoC#1 person D		1	1	1	0.5	**3.5**
PoC#2 person D	0		1	0.5	0	**1.5**
PoC#3 person D	0	0		0	0	**0**
PoC#4 person D	0	0.5	1		0	**1.5**
PoC#5 person D	0.5	1	1	1		**3.5**

According to the binary comparison and its summary results, it could be concluded that there were no favorites among posture correctors – each PoC reacts to each test-person differently.

Similar conclusions could be drawn from listening to test subjects, for example, test subject A had a good impression of the effects of PoC # 1 on posture and well-being, while test subject C immediately felt uncomfortable when putting on PoC # 1. The same could be said for all PoCs.

4 Conclusions

Based on the medical literature and research on posture improvement, it has been concluded that an ideal or correct posture requires a balanced body position and proportion. Today, on the other hand, people's social and private lives are dominated by bad habits, such as bending over while studying and working, using computers and smart devices too often, carrying heavy bags, using desks and stools that are not appropriate in height for a person's body, lack of health education and physical activity. All these factors affect muscle shape, deform skeleton and cause malformations that prevent proper posture. A good, correct posture helps a person to participate in active and healthy life, as well as to achieve a good body appearance.

Compression of soft tissues while wearing a posture corrector negatively affects certain aspects of the normal psychological balance of the human body and can also become a health risk factor. When choosing PoC, the patient must pay attention to the design aspects of PoC that could determine wearing comfort – narrowing of the straps in the area of shoulders and armpits. To avoid skin irritation, PoC is recommended to be worn on tight-fitting garments.

Measurements confirm that the proportional relationships of human lordosis and kyphosis do not change correlatively; therefore, spinal change analysis is a task with a lot of room for data interpretation. Regardless of the design (pattern) and type of PoC, the back muscles relax after just a few hours, which rapidly reduces the product's effectiveness and functional properties, meaning that not only the PoC itself must be personalized, but also the wearing time, regularity and intensity must be coordinated for each individual.

Future studies should include a method to correlate test-persons' views with the effects of the tested PoC on a person's posture. The trend of the currently analyzed statements suggests that if the test subject has psychological and physiological objections, this results in a worse effect of PoC on the test subject's posture corrections. To refine the experimental data, the measurements should be repeated under the same conditions for several days to exclude the effects of a particular mood. Such measurements are very time consuming and place limitations on test subjects to perform their casual routine duties.

Acknowledgements

This work has been supported by the European Regional Development Fund within the Activity 8.2.2 "To Strengthen Academic Staff of Higher Education Institutions in the Areas of Strategic Specialization".

References

[1] Saemee, L. Posture Modification Effects Using Soft Materials Structures. Dissertation, University of Minnesota, Minneapolis, USA, 2016.

[2] Kim, D.; Cho, M.; Park, Y.; Yang, Y. Effect of an exercise program for posture correction on musculoskeletal pain. *J. Phys. Ther. Sci.*, 2015, 27 (6), 1791–1794. DOI: 10.1589/jpts.27.1791.

[3] Watkins, S. M.; Dunne, L. E. Functional clothing design. From sportswear to spacesuits. Bloomsbury, 2015.

[4] Lyu, S.; LaBat, K. "Shapewear" for women as a postural improvement garment. *International Textile and Apparel Association Annual Conference Proceedings*, 2014, 71 (1), 1–2.

[4] Liu, P. Y.; Yip, J.; Yick, K. L.; Yuen, C. W. M.; Tse, C. Y.; Ng, S. P.; Law, D. Effects of a tailor-made girdle on posture of adolescents with early scoliosis, *Textile Research Journal*, 2015, 85 (12), 1234–1246. DOI: https://doi.org/10.1177/0040517514561928.

[5] Liu, S. The effects of an innovative posture garment technology on the scapular and lumbar muscle activity and scapular alignment. *International Journal of Physical Medicine & Rehabilitation*, 2018, 6, p.14.

[6] McRoberts, L. B.; Black, C. M.; Cloud, R. M. Evaluation of a prototype soft-structured thoracic posture support garment. *Clothing and Textiles Research Journal*, 2016, 34 (2), 143–158. DOI: 10.1177/0887302X15622571.

[7] McRoberts, L. B., et al. Evaluation of the New York posture rating chart for assessing changes in postural alignment in a garment study. *Clothing and Textiles Research Journal*, 2013, 31, 81–96. DOI: 10.1177/0887302X13480558.

[8] Kendall, F. P.; McCreary, E. K.; Provance, P. G.; Rodgers, M. M.; Romani, W. A. Muscles: Testing and function with posture and pain, 5th ed.; Lippincott Williams & Wilkins: Baltimore, MD, USA, 2005, 512.

[9] Kouwenhoven, J. W; Castelein, R. M. The pathogenesis of adolescent idiopathic scoliosis: review of the literature. *Spine*, 2008, 33 (26), 2898–2908. DOI: 10.1097/BRS.0b013e3181891751.

[10] Chow, D. H.; Kwok, M. L.; Cheng, J. C.; Lao, M. L. Holmes, A. D., Au-Yang, A., Wong, M. S. The effect of backpack weight on the standing posture and balance of schoolgirls with adolescent idiopathic scoliosis and normal controls. *Gait Posture*, 2006, 24 (2), 173–181. DOI: 10.1016/j.gaitpost.2005.08.007.

[11] Mahaudens, P.; Thonnard, J. L.; Detrembleur, C. Influence of structural pelvic disorders during standing and walking in adolescents with idiopathic scoliosis. *The Spine Journal*, 2005, 5(4), 427–433. DOI 10.1016/j.spinee.2004.11.014.

[12] Jaworski, P. Postural defects – correct posture, pathological posture, pathogenesis and consequences, *Journal of education, health and sport*, 2019, 9 (8), 452–460.

[13] ISO 13404:2007 "Prosthetics and orthotics – Categorization and description of external orthoses and orthotic components".

[14] Bazzarelli, M.; Durdle, N.; Lou, E.; Raso, J. A low power portable electromagnetic posture monitoring system. *Conference Proceedings (Cat. No.01TH8555) of Canadian Conference on Electrical and Computer Engineering* 2001, Toronto, Ontario, Canada, 2001, Vol. 2, 1373–1377. DOI: 10.1109/CCECE.2001.933652.
[15] Yip, Y. W. J.; Yick, K. L.; Tse, C. Y.; Yuen, C. W. M.; Ng, S. P.; Liu, P. Y.; Law, K. M., inventors, Hong Kong Polytechnic University HKPU, assignee, Posture correction girdle and the method of correcting spinal deformity, United States Patent 9,398.972 B2, Jul. 26, 2016.
[16] Mills, A. J., inventor, SPINECORPORATION Ltd., assignee, Spinal orthosis, United States US 2010/0217166 A1, Aug. 26, 2010.
[17] Ingimundarson, A. T.; Bakken, N.; Omarsson, B.; Romo, H. D.; Nemeth, J., inventors, Ossur hf, assignee, Spinal orthosis, United States US 2017/0156911 A1, Jun. 8, 2017.
[18] Lai, W.; Mao, K., inventors, Mao, K.; Lai, W. C., assignees, Posture vest, United States Patent US 7,842,000 B2, Nov.30, 2010.
[19] Taylor, B. C., inventor, Thera Togs Inc., assignee, Elasticized garment and strapping system to aid in body mobility support and maintenance, United States Patent US 8,007,457 B2, Aug. 30, 2011.
[20] Pollack, J., inventor, Pollack, J., assignee, System, method, and device for posture support, United States Patent US 9,456,919 B2, Oct. 4, 2016.
[21] Brown T. W., inventor, ALIGNMED Inc., assignee, Posture improvement device and method of use, United States US 2011/0213283 A1, Sep. 1, 2011.
[22] Ingimundarson, A. T.; Robertson, B., inventors, Ossur hf, assignee, Orthopedic device for treatment of the back, United States Patent US 9,414,953 B2, Aug. 16, 2016.

CDATP

COMMUNICATIONS IN
DEVELOPMENT AND ASSEMBLING OF TEXTILE PRODUCTS

The influence of thermal after-treatment on the adhesion of 3D prints on textile fabrics

Daniel Görmer, Jannik Störmer, Andrea Ehrmann*

Bielefeld University of Applied Sciences, Faculty of Engineering and Mathematics, Bielefeld, Germany
*Corresponding author *E-mail address:* andrea.ehrmann@fh-bielefeld.de

INFO

CDAPT, ISSN 2701-939X
Peer reviewed article
2020, Vol. 1, No. 2, pp. 104-110
DOI 10.25367/cdatp.2020.1.p104-110
Received: 16 August 2020
Accepted: 06 September 2020
Available online: 22 November 2020

ABSTRACT

3D printing belongs to the emerging technologies of our time. While it enables producing new structures and makes individualized products affordable, 3D printed objects still suffer from low production speed and often insufficient mechanical properties. Both these problems can be tackled by combining 3D printing with substrates prepared by conventional technologies, e.g. textile fabrics. In this case, the adhesion between both partners is most challenging and defines for which possible applications such composites are suitable. Here, we report on a new approach to increase the adhesion between 3D printed materials and warp knitted fabrics, showing that in some cases a thermal after-treatment, in the simplest case performed by ironing, is able to significantly increase the adhesion between both materials.

Keywords
3D printing,
warp knitted fabrics,
ironing,
thermal after-treatment,
adhesion,
nozzle-textile distance

1 Introduction

While 3D printing was originally mostly used for rapid prototyping, nowadays these techniques are more and more often used for preparing real objects with real applications. While some of these applications, such as 3D printing of microfluidics of microelectromechanical systems (MEMS), mostly strive for high resolution and accuracy [1], other applications necessitate especially good mechanical properties [2-4].

One of the possibilities to increase the tensile properties and at the same time reduce production time is 3D printing on textile fabrics, in this way adding a desired stiffness to certain areas of textiles due to functional or design purposes [5], while the main fabric is produced in a conventional way. Such composites, however, often suffer from lacking adhesion between both partners.

This is why several research groups investigated the adhesion between 3D printed parts and textile fabrics. In most cases, 3D printing was performed using the fused deposition modeling (FDM) process, while most recently the first proof-of-principle showed that stereolithography (SLA) can also be applied to print 3D objects on many textile fabrics [6]. Here, however, we concentrate on the common FDM technology.

In recent studies, several material and printing parameters were found to influence the adhesion of 3D printed layers on textile fabrics. Eutionnat-Diffo *et al.* reported the printing bed temperature as well as woven fabric parameters to have an impact on the adhesion [7]. Generally, the structure of the textile fabric, especially pores and hairs as possibilities for the 3D printing polymer to penetrate into the fabric or to build other form-locking connections, is an important parameter [8-11]. One of the most important parameters is the distance between nozzle and fabric surface, defining with how much force the molten polymer is pressed into the fabric pores [12,13]. For a broader overview of the influence of diverse parameters on the textile-polymer adhesion, the reader is referred to References 14 and 15.

Besides these parameters, chemical and physical surface treatments of the textile fabric before printing and the composite afterwards were investigated. According to the Korger law [16], in most cases hydrophilic surfaces support 3D printing on them, while hydrophobic ones often result in lower adhesion [17]. On the other hand, thermal after-treatments were examined, printing with poly(lactic acid) (PLA) on jeans-like cotton woven fabrics [17]. In this previous study, ironing slightly decreased the adhesion force, without showing a significant difference.

Here, we report on 3D printing especially on warp knitted fabrics with four different polymers. While some of the aforementioned relations are underlined by the recent study, ironing as a simple way of thermal after-treatment unexpectedly showed a large impact in some cases, opposite to our previous study.

2 Materials and Methods

3D printing was performed using the FDM printer CR-10S Pro (Creality, Shenzhen, China) with nozzle diameter 0.4 mm. In all experiments, rectangles of 120 mm x 25 mm x 0.8 mm were printed, using a layer height of 0.2 mm and 100 % infill with ± 45° orientation.

For the tests, four different filaments were printed (nozzle and printing bed temperatures in brackets): PLA (white, from Creality, 200 °C / 45 °C); co-polyester (CPE) (black, from Filamentworld, 260 °C / 85 °C); polyethylene terephthalate glycol (PETG) (green, from Filamentworld, 215 °C / 70 °C); and thermoplastic polyurethane (TPU) (orange, from Recreus, 230 °C / 30 °C). In addition to the “raw” printed samples, further samples were ironed after 3D printing, using an electric iron Quigg DB 2016.19/5218 (Globaltronics GmbH & Co. KG, Hamburg, Germany), at grade 10 (“jeans”), equivalent to the common setting *** and defining a temperature of (185 ± 15) °C, according to the producer. Ironing was performed with a rotating movement from the back of the sample, i.e. on the textile side, for 15 s, letting the sample cooling down for 2 min and afterwards again ironing for 15 s, to avoid overheating and at the same time to average over a relatively long duration due to the well-known temperature variation of bimetal irons. The iron was not pressed down during ironing; its mass without the power cable is approx. 1240 g.

The warp knitted fabrics on which printing was performed were prepared on different machines (all by Karl Mayer, Obertshausen, Germany), using different warp knitted structures and yarns. Table 1 depicts scans of the four samples with corresponding machines, machine gauges and yarn materials.

Examinations were performed by a Sauter universal testing machine at a speed of 100 mm/min. Tests were performed according to DIN 53530 and evaluated according to ISO 6133, using the method for more than 20 peaks. This means that one end of the fabric was manually separated from the fabric so that these separated ends could be clamped in the testing machine, allowing for measuring the force-displacement curves. The test process is sketched in Fig. 1.

Table 1. Warp knitted fabrics used for printing.

Sample WK1	Sample WK2	Sample WK3	Sample WK4
	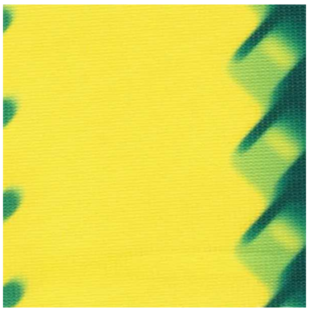		
HKS 2-3 E, E40 Elastane / polyamide 6	HKS 3-M, E28 Polyester, flat, dull	RSE 5 EL, E28 Elastane / polyamide 6	HKS 4-M EL, E28 Polyester, semi-dull

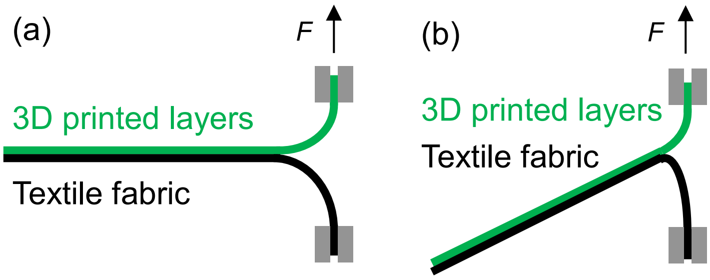

Fig. 1 (a) Test process according to DIN 53530. (b) For the rigid filaments, the 3D printed layers are more linearly shaped than the textile fabric.

Photographs of the samples were taken by a Nikon D750 with an objective Sigma 105 mm 1:2.8 DG Macro HSM.

3 Results and Discussion

The results of the first test series, testing combinations of all four polymers with the four warp knitted fabrics, are depicted in Fig. 2.

Comparing these graphs, it is obvious that the adhesion on the samples WK 1 and WK 3 is smaller than on samples WK2 and WK4. Both samples WK1 and WK3 are prepared from elastane and polyamide 6 yarns, correspondingly these two samples are elastic, while the others have a very low elasticity. Possible explanations for this finding are, on the one hand, the sample structure – samples WK2 and WK4 have larger pores and thus allow the molten polymer to penetrate deeper into the fabric. On the other hand, the elasticity of WK1 and WK3 make it harder to press the polymers into the fabrics since they are fixed only along the sample borders and thus can be moved by the moving nozzle. Finally, samples WK2 and WK4 are highly hydrophilic, with water drop penetration times below 1 s, while the drop penetration time on samples WK1 and WK3 is in the order of 2-3 s. Apparently here different reasons can be found why a higher adhesion can be reached on samples WK2 and WK4.

Next, the different polymers can be compared. Here it can be recognized that TPU and CPE give the best results, while PETG and PLA show in most cases much lower adhesion. While it is known from the literature that elastic filaments, such as TPU, usually show a high adhesion [18], no reports can be found about 3D printing CPE on textile fabrics. Our first test of this polymer suggests that CPE may have a high potential for direct printing on textile fabrics, e.g. for applications in orthoses where a very high adhesion is necessary [19]. This is especially important since PLA is often regarded as the rigid polymer with the highest adhesion, compared with nylon (polyamide), acrylonitrile butadiene styrene (ABS) and other polymers [12], and here it is outperformed by CPE in most cases.

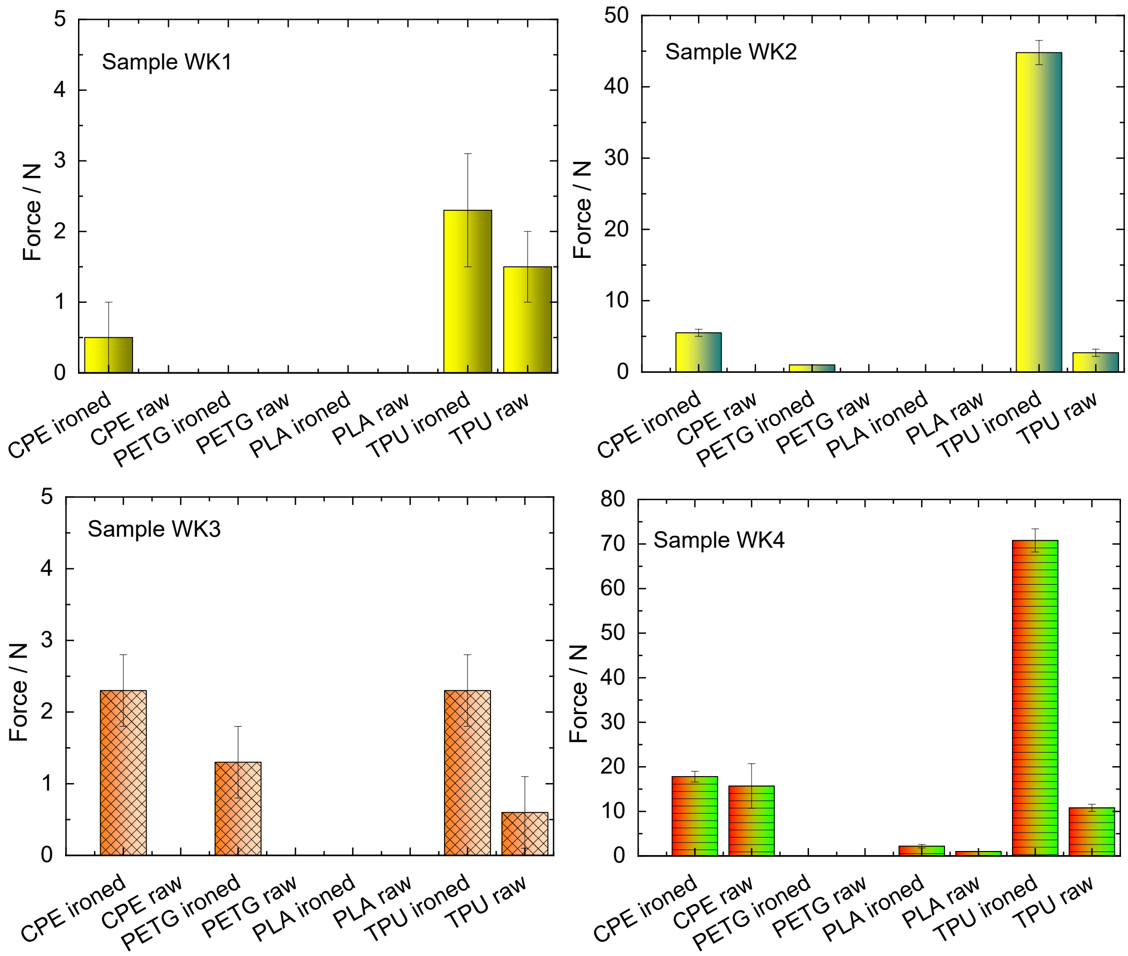

Fig. 2 Adhesion forces, measured for the four textile fabrics under investigation, measured in combination with different 3D printing polymers.

Besides, the influence of ironing shall be examined. While our former study showed a small reduction of the adhesion due to ironing, this finding is different here. For CPE, ironing is supportive on samples WK1-3 and not disadvantageous on samples WK4. PETG in most cases fall apart from the textile substrates before testing; only after ironing, it shows a very low adhesion on samples WK2 and WK3. For PLA, ironing does not seem to make a difference, which is similar to the finding of the previous study. Finally, for TPU, only on the finest sample WK1 ironing does not make a significant difference, while on the other substrates, ironing increases the adhesion approximately by a factor of 4-17.

Apparently, the influence of ironing is worth a deeper investigation. This is especially valid since in the tests depicted in Fig. 2, the distance between nozzle and printing bed was optimized manually for each sample without performing a full test series. This means that the impact of ironing on the adhesion may also depend on this distance – it can be imagined that ironing is especially supportive if the nozzle-textile distance was too large during printing so that the filament has not yet been pressed into the fabric with enough pressure, which could be finalized by ironing.

This is why the next test series concentrated on sample WK4 which showed a strong impact of ironing TPU printed samples, comparing the impact of ironing for different distances between nozzle and printing bed. Fig. 3 depicts the results of the corresponding adhesion tests. A distance of 0.2 mm is automatically set by the printer for a first-layer thickness of 0.2 mm. Printing slightly below this value would be typical for printing on the pure glass bed. Here, however, a textile fabric of thickness 0.62 mm is placed on the printing bed, meaning that a distance of approx. 0.8 mm would be comparable to the usual distance for printing on the glass bed. As already pointed out in former publications [12], printing "below" the surface of the textile fabric is necessary to optimize the adhesion.

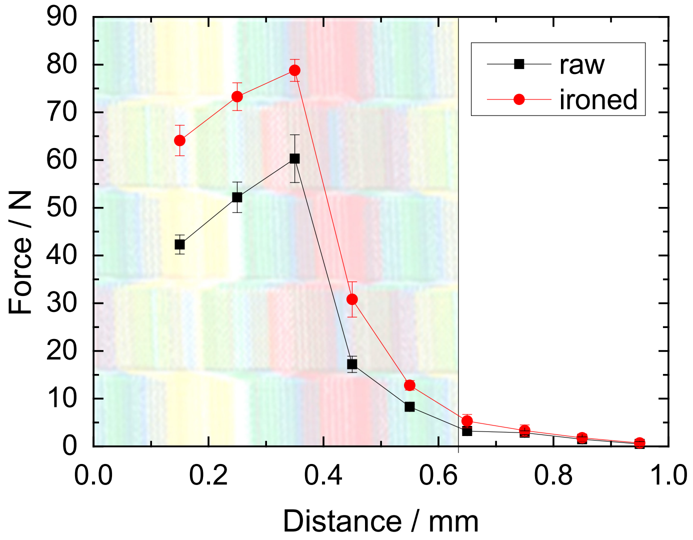

Fig. 3 Adhesion forces, measured for sample WK4, in dependence of the distance between nozzle and printing bed for raw and ironed samples.

As Fig. 3 clearly shows, ironing cannot be used as a substitute for this first creation of a form-locking connection. Instead, this thermal after-treatment always increases the adhesion force, independent from the original printing distance. This means that, at least in this combination of TPU with relatively dense, inelastic polyester warp knitted fabric, the adhesion between both materials should be optimized by controlling the distance between nozzle and printing bed as well as by an additional thermal after-treatment.

To investigate the reasons for this effect more in detail, Fig. 4 depicts the back of different samples after the adhesion tests.

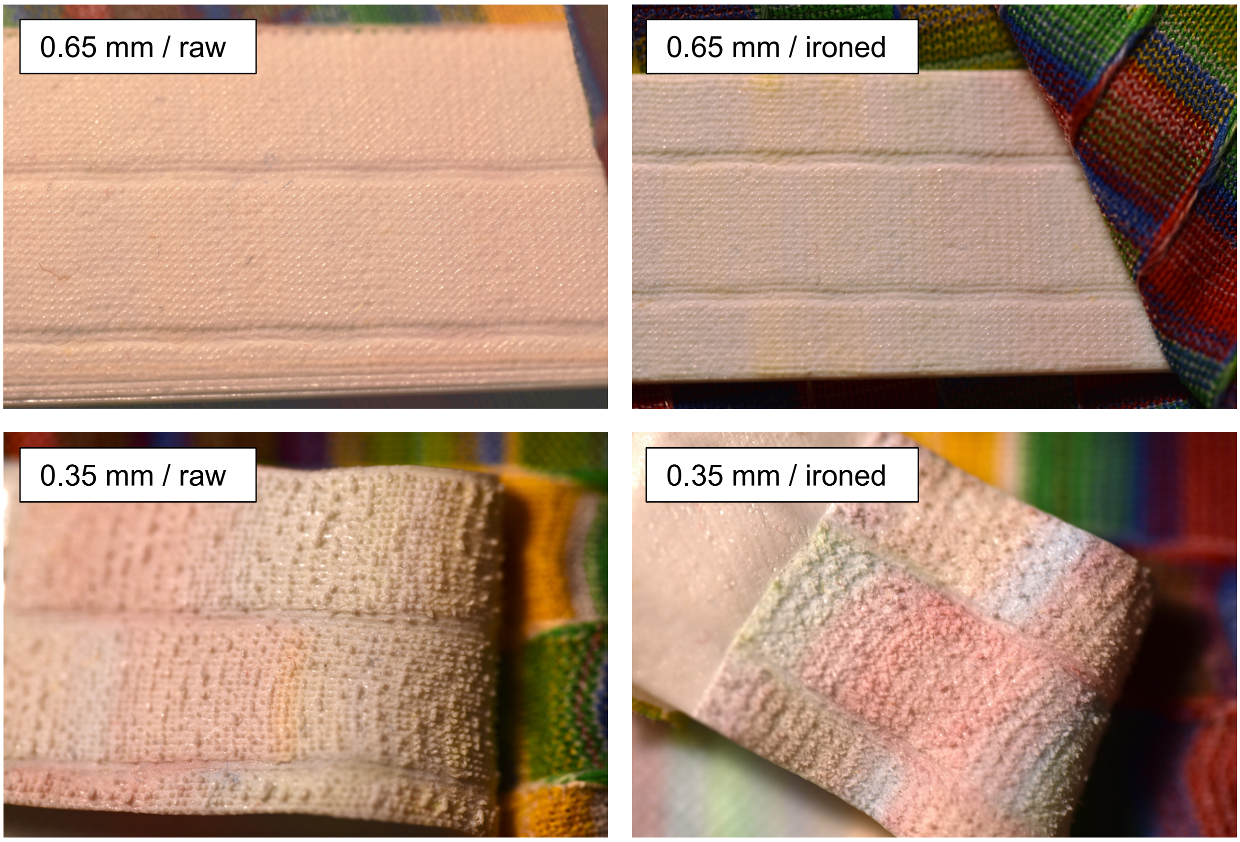

Fig. 4 Back of different samples (cf. insets) after the adhesion test.

On the one hand, comparison between the samples printed at distances of 0.35 mm (optimum distance, cf. Fig. 3) and 0.65 mm (slightly “outside” the fabric) clearly shows that only a slight imprint of the textile surface is visible on the latter, while at the optimum distance, the polymer was pressed into the fabric, after the adhesion test clearly showing small spikes which were pulled out of the pores of the fabric. This finding is identical to previous experiments where different z-distances were compared by cross-sectional images [12].

On the other hand, due to the colored warp knitted fabric, it is also possible to investigate the color transferred to the white polymer. Comparing both samples printed at the larger distance of 0.65 mm, no significant differences are visible, while the ironed sample may show slightly more colors. For the samples printed at the optimum distance of 0.35 mm, however, the ironed one is clearly more colored.

We can thus assume that the relatively high ironing temperature – near to the melting temperature of polyester of typically 230-260 °C – was sufficient to start softening and slightly melting the textile material. In this way, a chemical bonding may have been formed during ironing, while the previous pressure during printing, applied by an optimized z-distance, results in a form-locking (physical) bonding. Apparently, here two different mechanisms interact, both able to increase the adhesion between polymer and textile fabric independently.

Comparing the values in Fig. 3 with those depicted in Fig. 2 for TPU printed on sample WK4 again underlines the importance of optimizing the distance. While for precisely controlled distances, the forces between raw and ironed composites (Fig. 3) differ maximally by approx. a factor of 1.5, this difference is much higher for the comparison given in Fig. 2, clearly showing that it is not possible to control the distance well enough manually. This finding can be explained from Fig. 3, showing that a small distance reduction from 0.45 mm to 0.35 mm approximately triples the adhesion force.

Generally, as this study shows, printing on textile fabrics in the optimum distance cannot be optically supervised as easily, as it is possible for an experienced user for printing on the common printing bed. Since each textile fabric behaves differently, has different mechanical properties, hairiness, surface structure etc., it is strongly recommended for researchers working in this field to optimize and control the distance carefully, to avoid conclusions of parameter modifications which may be at least partly based on erroneous distance variations.

4 Conclusions

3D printing with four different polymers was performed on four warp-knitted fabrics. We report on the first experiment to perform 3D printing with CPE on textile fabrics, showing that this polymer may be advantageous in comparison to PLA which is most often used in such studies. In addition, opposite to a previous study, a significant influence of a thermal after-treatment, performed by ironing, on the adhesion was found in most cases. Finally, the strong impact of the distance between nozzle and textile surface, revealed in previous studies, was underlined.

Future investigations will concentrate on the impact of ironing on different material combinations to examine whether the correlation found here for TPU and relatively thin fabrics with narrow pores translated to other structures and materials, besides differentiating further between physical and chemical effects.

Acknowledgements

The authors are grateful for the warp knitted textiles provided by Karl Mayer Textilmaschinen AG, Obertshausen, Germany.

References

[1] Blachowicz, T.; Ehrmann, A. 3D printed MEMS technology – recent developments and applications. *Micromachines*, 2020, 11(4), 434. DOI: 10.3390/mi11040434.

[2] Arunothayan, A. R.; Nematollahi, B.; Ranade, R.; Bong, S. H.; Sanjayan, J. Development of 3D-printable ultra-high performance fiber-reinforced concrete for digital construction. *Construction and Building Materials,* 2020, 257, 119546. DOI: 10.1016/j.conbuildmat.2020.119546.

[3] Afshar, A.; Mihut, D. Enhancing durability of 3D printed polymer structures by metallization. *J. Mater. Sci. Technol.,* 2020, 53, 185-191. DOI: 10.1016/j.jmst.2020.01.072.

[4] Oviedo, A. M.; Puente, A.H.; Bernal, C.; Perez, E. Mechanical evaluation of polymeric filaments and their corresponding 3D printed samples. *Polym. Test.*, 2020, 88, 106561. DOI: 10.1016/j.polymertesting.2020.106561.

[5] Spahiu, T.; Fafenrot, S.; Grimmelsmann, N.; Piperi, E.; Shehi, E.; Ehrmann, A. Varying fabric drape by 3D-imprinted patterns for garment design. *IOP Conf. Ser.: Mater. Sci. Eng.,* 2017, 254, 172023. DOI: 10.1088/1757-899X/254/17/172023.

[6] Grothe, T.; Brockhagen, B.; Storck, J. L. Three-dimensional printing resin on different textile substrates using stereolithography: A proof of concept. *J. Eng. Fibers Fabr.,* 2020, 15, 1558925020933440. DOI: 10.1177/1558925020933440.

[7] Eutionnat-Diffo, P. A.; Chen, Y.; Guan, J. P.; Cayla, A.; Campagne, C.; Zeng, X. Y.; Nierstraz, V. Stress, strain and deformation of poly-lactic acid filament deposited onto polyethylene terephthalate woven fabric through 3D printing process. *Sci. Rep.,* 2019, 9, 14333. DOI: 10.1038/s41598-019-50832-7.

[8] Narula, A.; Pastore, C.; Schmelzeisen, D.; El Basri, S.; Schenk, J.; Shajoo, S. Effect of knit and print parameters on peel strength of hybrid 3D printed textiles. *J. Text. Fibrous Mater.,* 2018, 1, 2515221117749251. DOI: 10.1177/2515221117749251.

[9] Meyer, P.; Döpke, C.; Ehrmann, A. Improving adhesion of three-dimensional printed objects on textile fabrics by polymer coating. *J. Eng. Fibers Fabr.*, 2019, 14, 1558925019895257. DOI: 10.1177/1558925019895257.

[10] Calvo, J. O.; Martin, A. C.; Ferradas, M. I. R.; Morcillo, P. L. F.; Munoz, L. M.; Camo, P. M. Additive manufacturing on textiles with low-cost extrusion devices: Adhesion and deformation properties. *Dyna*, 2019, 64, 8893. DOI: 10.6036/8893.

[11] Mpofu, N. S.; Mwasiagi, J. I.; Nkiwane, L. C.; Njuguna, D. Use of regression to study the effect of fabric parameters on the adhesion of 3D printed PLA polymer onto woven fabrics. *Fashion and Textiles*, 2019, 6, 24. DOI: 10.1186/s40691-019-0180-6.

[12] Grimmelsmann, N.; Kreuziger, M.; Korger, M.; Meissner, H.; Ehrmann, A. Adhesion of 3D printed material on textile substrates. *Rapid Prototyp. J.,* 2018, 24(1), 166-170. DOI: 10.1108/RPJ-05-2016-0086.

[13] Spahiu, T.; Al-Arabiyat, M.; Martens, Y.; Ehrmann, A.; Piperi, E.; Shehi, E. Adhesion of 3D printing polymers on textile fabrics for garment production. *IOP Conf. Ser.: Mater. Sci. Eng.,* 2018, 459, 012065. DOI: 10.1088/1757-899X/459/1/012065.

[14] Sitotaw, D. B.; Ahrendt, D.; Kyosev, Y.; Kabish, A. K. Additive manufacturing and textiles – state of the art. *Appl. Sci.,* 2020, 10, 5033. DOI: 10.3390/app10155033.

[15] Kozior, T.; Blachowicz, T.; Ehrmann, A. Adhesion of three-dimensional printing on textile fabrics: Inspiration from and for other research areas. *J. Eng. Fibers Fabr.,* 2020, 15, 1558925020910875. DOI: 10.1177/1558925020910875.

[16] Korger, M.; Bergschneider, J.; Lutz, M.; Mahltig, B.; Finsterbusch, K.; Rabe, M. Possible Applications of 3D Printing Technology on Textile Substrates. *IOP Conf. Ser.: Mater. Sci. Eng.,* 2016, 141, 012011. DOI: 10.1088/1757-899X/141/1/012011.

[17] Kozior, T.; Döpke, C.; Grimmelsmann, N.; Juhász Junger, I.; Ehrmann, A. Influence of fabric pretreatment on adhesion of three-dimensional printed material on textile substrates. *Adv. Mech. Eng.,* 2018, 10, 792316. DOI: 10.1177/1687814018792316.

[18] Korger, M.; Glogowsky, A.; Sanduloff, S.; Steinem, C.; Huysman, S.; Horn, B.; Ernst, M.; Rabe, M. Testing thermoplastic elastomers selected as flexible three-dimensional printing materials for functional garment and technical textile applications. *J. Eng. Fibers Fabr.,* 2020, 15, 1558925020924599. DOI: 10.1177/1558925020924599.

[19] Ahrendt, D.; Karam, A. R. Development of a computer-aided engineering–supported process for the manufacturing of customized orthopaedic devices by three-dimensional printing onto textile surfaces. *J. Eng. Fibers Fabr.,* 2020, 15, 1558925020917627. DOI: 10.1177/1558925020917627.

COMMUNICATIONS IN
DEVELOPMENT AND ASSEMBLING OF TEXTILE PRODUCTS

Approximation of a function describing a quality criterion of the thermo-mechanical fusible interfacing process

Snezhina Andonova[1]*, Silvia Baeva[2]

[1]Faculty of Engineering, South-West University "Neofit Rilski", Blagoevgrad, Bulgaria
[2]Faculty of Applied Mathematics and Informatics, Technical University of Sofia, Sofia, Bulgaria
*Corresponding author *E-mail address:* andonova_sn@swu.bg

INFO

CDAPT, ISSN 2701-939X
Peer reviewed article
2020, Vol. 1, No. 2, pp. 111-120
DOI 10.25367/cdatp.2020.1.p111-120
Received: 29 August 2020
Accepted: 21 September 2020
Available online: 23 November 2020

Keywords
approximation,
thermo-mechanical
fusible interfacing process,
quality criterion

ABSTRACT

The present work aims to investigate the function describing the relationship between a quality criterion and input factors of the thermo-mechanical fusible /TMF/ interfacing process and to derive its effective approximation. An approximation by interpolation was applied for the purpose of the study.

A numerical realization of a linear and exponential approximation of the mathematical model describing the TMF interfacing process was performed. An effective linear approximation of the function connecting the quality criterion with the input factors of the TMF interfacing process was found. This creates conditions for replacing the relatively complex function (describing the TMF interfacing process) with its linear approximation. The linear approximation gives the possibility easier and faster to determine the relationships between the input factors and the quality criterion. This created conditions for ignoring the subjective factor and for optimizing and automating the studied technological process.

1 Introduction

Nowadays, the achievements of mathematics allow the application of mathematical modeling for various objects and processes. Mathematical modeling and optimization acquires special significance in the modern conditions of accelerated scientific and technical progress, in the need to achieve high efficiency with limited financial, material, labor, energy and time resources.

The mathematical methods for analysis, modeling and optimization are increasingly used in the sewing and textile technologies [1-4]. This allows avoiding the subjective factor and creates real conditions for automation of the processes.

One of the effective methods for study a given function is the method of approximation [5-7].

With this method the investigation of various (unknown or extremely complex) numerical characteristics and qualitative properties of the original objects reduces to working with other objects whose characteristics and properties are already known or more convenient to work with [5-7].

After the analysis of the literature survey, it can be summarized that the methods of approximation are applied to a number of technological processes in the textile and clothing industry [8-12].

For example, [8] presents the mathematical and computer simulation of multiparameter systems. The simulation is based on experimental data and is achieved by modifying the one-dimensional approximations of splines. The method is used in the study of some technological conditions of fabric lamination systems and gives good results.

In [9] mathematical and computer models are developed for predicting effective elastic properties for a complex periodic cell and a representative volume (fragment) of spatially amplified composite material (SRCM). Numerical experiments are performed to predict the effective elastic properties of a cell with SRCM periodicity with an orthogonal tissue pattern with two variants of the structure and the representative volume cell using the local approximation method.

An approximation of a mathematical model of the thermo-mechanical fusing process is proposed in [13].

The thermo-mechanical fusing process is one of the main technological processes in the sewing production. The quality and productivity achieved in this process significantly affect the quality and productivity of the entire production in the sewing company. Therefore, it is important to investigate the thermo-mechanical fusing process, to create mathematical models describing the process [14,15], and to search for opportunities for their approximation [13].

In [13], an approximation of the function connecting an output criterion for performance with input factors of the thermo-mechanical fusing process is proposed.

It is especially important to study and analyze an output quality criterion as well. Several studies [16,17, 18] analyze the influence of input factors on various quality criteria of the thermo-mechanical fusing process. In [15] a function is derived connecting an output quality criterion with factors influencing the fusing conditions.

Finding an approximation of this function [15] which describes the thermo-mechanical fusible /TMF/ interfacing process in a simpler way is of particular interest.

This work aims to investigate the function describing the relationship between a quality criterion and input factors of the TMF interfacing process and to derive its effective approximation.

2 Research work

2.1 Methods

The standard algorithm for approximating functions, described in detail in [5, 6, 7, 13], is used in the research.

Taking into account the conditions for conducting the present studies, interpolation is used as a method of approximation [5, 6, 7].

The main steps in applying the interpolation method are [5, 6, 7]:

- let the function $y = f(x)$ be defined in some interval and a table of its values be known for the respective x_i [x, ш];

- an approximate function $\varphi(x)$ is sought such that

$\varphi(x_i) = y_i, i = 0,1, \dots, n.$ (1)

This problem is solved by setting the class of functions $\varphi(x)$.

Graphically, condition (1) means that the approximating function $\varphi(x)$ passes through the points (x_i, y_i), since x_i has the same values as $f(x)$ (Figure 1).

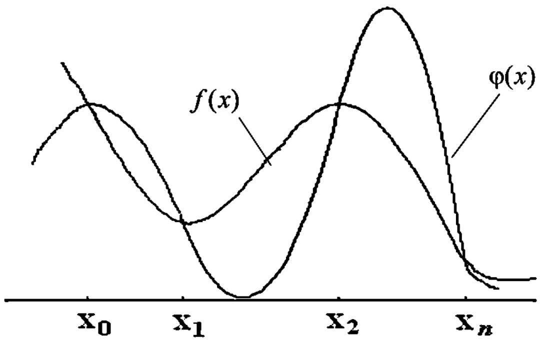

Fig. 1 Indicative graphical representation of the condition (1).

After performing the interpolation, it is necessary to determine the coefficient of determination R^2 [6]. It measures how much of the approximation error is eliminated. The coefficient of determination is a measure of the quality of the approximation model and varies in the range [0;1], or in percentages [0; 100]. The closer R^2 is to 1 (up to 100%), the greater the efficiency of the approximation model.

Specialized software Maple and Matвab is used for the research in the present work.

2.2 Materials

Materials produced by the company NITEX-50 - Sofia were used for basic textile materials /TM/. They are 100% wool fabrics. Their characteristics are described in detail in [14].

Material produced by the company Kufner-B121N77 was used for an auxiliary TM (interlining). Their characteristics are described in detail in [14] as well.

2.3 Conditions for conducting the study

For the numerical realization of the research the experimentally obtained function (2) is used [15]:

$$Y = 1.255 + 0.3225.x_1 + 0.21.x_2 + 0.155.x_3 - 0.0175.x_1.x_2 - 0.04.x_2.x_3 + 0.0175x_1.x_2.x_3 \quad (2)$$

The function (2) describes the relationship between a quality criterion Y (The change of the color shade of the TM after TMF interfacing process) and manageable process factors X_1 – Pressure, P [N/cm^2], X_2 - Temperature of the pressing plates, T [°C] , X_3 - Mass per unit area of the basic textile materials, M [g/m^2].

The correlation field from the experimental data that are processed with the specialized software Maple and MatLab is used.

The best approximation to the experimentally derived function (2) is sought. An approximation of function (2) is applied by interpolation in linear and exponential form. The investigations were performed with the coded values of the factors. The relationship between the natural and coded values of the factors is given in [14]. Three variants are investigated. In each variant, one of the factors assumes values in the range [-1; +1], and the other two factors are constants. The constant values are the values of the factors at which the function Y(X_1, X_2, X_3) is optimal.

The optimal value of the selected quality criterion $Y_{opt} = Y_{min} = 0.4975$ is reached at the following values of the input factors: the pressure P = 10 [N/cm^2], the temperature of the pressing plates T = 120 [°C] and the mass per unit area of basic textile materials M = 173 [g/m^2] [18]. The coded values of the factors in which Y_{min} is obtained are X_1 = (-1); X_2 = (-1); X_3 = (-1) [18].

A linear and exponential approximation of the function (2) is made for the following three variants:

- variant I - $X_1 \in [-1; 1]$; $X_2 = (-1)$; $X_3 = (-1)$;

- variant II - $X_2 \in [-1; 1]$; $X_1 = (-1)$; $X_3 = (-1)$;

- variant III - $X_3 \in [-1; 1]$; $x_1 = (-1)$; $x_2 = (-1)$.

3 Results and discussion

3.1 Results of the approximation

The numerical results of the linear and exponential approximation of the function (2) for the first variant are given in Table 1.

Table 1. Numerical results of the approximations of the function (2) for variant 1.

$\mathbf{X_1}$	**Linear Approximation** $\mathbf{Y = 0.93 + 0.3225x_1}$	**Exponential Approximation** $\mathbf{Y = 0.9059e^{0.3577x_1}}$
-1.00	0.607500	0.633481
-0.75	0.688125	0.692739
-0.50	0.768750	0.757542
-0.25	0.849375	0.828406
0.00	0.930000	0.905900
+0.25	1.010625	0.990643
+0.50	1.091250	1.083313
+0.75	1.171875	1.184652
+1.00	1.252500	1.295470

The graphical results of the linear and exponential approximation of the function (2) for the first variant are presented in figure 2.

For 1st variant: the linear and exponential approximation coincide, i.e.

$$Y_{LinAppr} = Y_{ExpAppr}, \quad (3)$$

where:

$$Y_{LinAppr} = Y = 0.93 + 0.3225x_1 \quad (4)$$

$$Y_{ExpAppr} = Y = 0.9059e^{0.3577x_1}, \quad (5)$$

when:

$$0.93 + 0.3225x_1 = 0.9059e^{0.3577x_1} \quad (6)$$

only for values for X_1:

$X_1 = -0.6857666234$;

$X_1 = 0.6092238139$.

The function Y (for these values for X_1) takes values accordingly:

$$Y(X_1 = -0.6857666234) = 0.7088402640 \quad (7)$$

$$Y(X_1 = 0.6092238139) = 1.126474680 \quad (8)$$

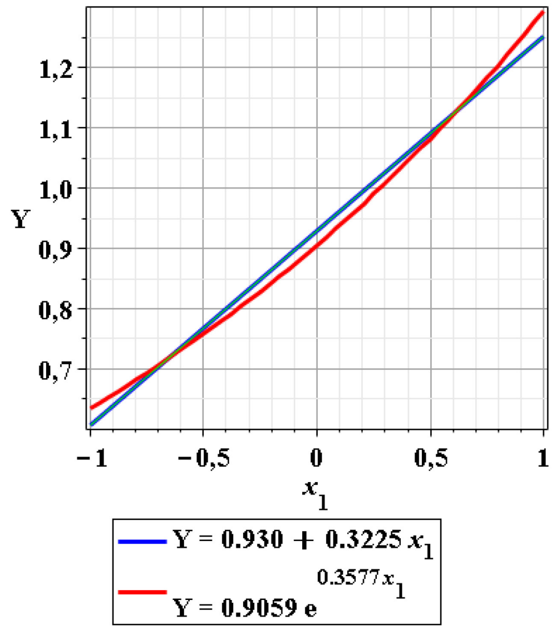

Fig. 2 Graphical results of the approximations of the function (2) for variant 1.

The numerical results of the linear and exponential approximation of the function (2) for the second variant are given in Table 2.

Table 2. Numerical results of the approximations of the function (2) for variant 2.

X_2	**Linear Approximation** $Y = 0.7775 + 0.2500x_2$	**Exponential Approximation** $Y = 0.7603e^{0.3302x_2}$
-1.00	0.52750	0.546488
-0.75	0.59000	0.593515
-0.50	0.65250	0.644589
-0.25	0.71500	0.700058
0.00	0.77750	0.760300
+0.25	0.84000	0.825726
+0.50	0.90250	0.896782
+0.75	0.96500	0.973953
+1.00	1.02750	1.057765

The graphical results of the linear and exponential approximation of the function (2) for the second variant are presented in figure 3.

For 2nd variant: the linear and exponential approximation coincide, i.e.

$$Y_{LinAppr} = Y_{ExpAppr}, \quad (9)$$

where:

$$Y_{LinAppr} = Y = 0.7775 + 0.2500x_2 \quad (10)$$

$$Y_{ExpAppr} = Y = 0.7603e^{0.3302x_2}, \quad (11)$$

when:

$$0.7775 + 0.2500x_2 = 0.7603e^{0.3302x_2} \quad (12)$$

only for values for X_2:

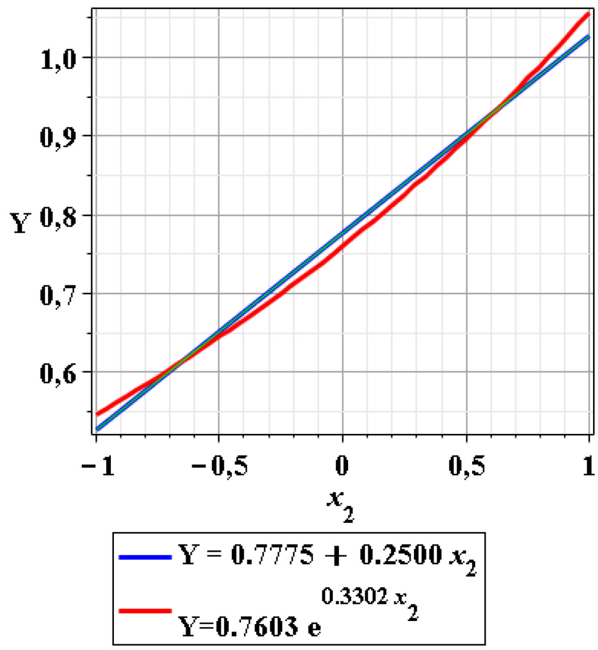

Fig. 3 Graphical results of the approximations of the function (2) for variant 2.

$X_2 = -0.6821481353;$

$X_2 = 0.6108059334.$

The function Y (for these values for X_2) takes values accordingly:

$$Y(X_2 = -0.6821481353) = 0.6069629662 \quad (13)$$

$$Y(X_2 = 0.6108059334) = 0.9302014834 \quad (14)$$

The numerical results of the linear and exponential approximation of the function (2) for the third variant are given in Table 3. The graphical results of the linear and exponential approximation of the function (2) for the third variant are presented in figure 4.

For 3rd variant: the linear and exponential approximation coincide, i.e.

$$Y_{LinAppr} = Y_{ExpAppr}, \quad (15)$$

Table 3. Numerical results of the approximations of the function (2) for variant 3.

X_3	**Linear Approximation** $Y = 0.74 + 0.1775x_3$	**Exponential Approximation** $Y = 0.731e^{0.2434x_3}$
-1.00	0.56250	0.573073
-0.75	0.60688	0.609028
-0.50	0.65125	0.647238
-0.25	0.69563	0.687845
0.00	0.74000	0.731000
+0.25	0.78438	0.776863
+0.50	0.82875	0.825603
+0.75	0.87313	0.877400
+1.00	0.91750	0.932448

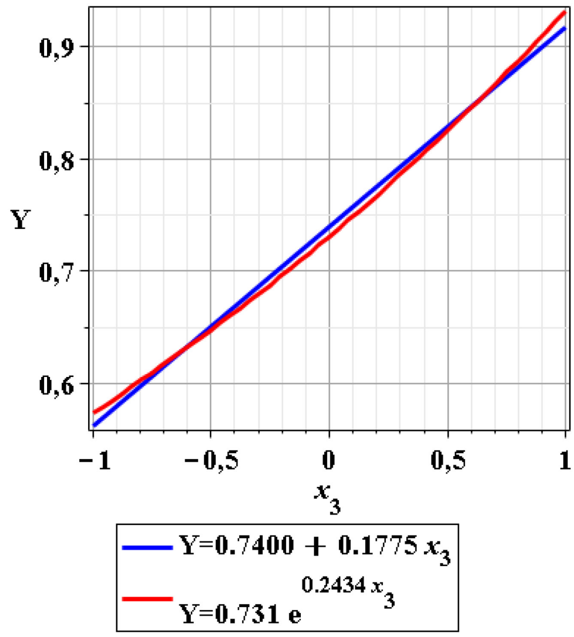

Fig. 4 Graphical results of the approximations of the function (2) for variant 3.

where:

$$Y_{LinAppr} = Y = 0.74 + 0.1775x_3 \quad (16)$$

$$Y_{ExpAppr} = Y = 0.731e^{0.2434x_3}, \quad (17)$$

when:

$$0.74 + 0.1775x_3 = 0.731e^{0.2434x_3} \quad (18)$$

only for values for X_3:

$X_3 = -0.6727381075$;

$X_3 = 0.6192396062$.

The function Y (for these values for X_3) takes values accordingly:

$$Y(X_3 = -0.6727381075) = 0.6205889859 \quad (19)$$

$$Y(X_3 = 0.6192396062) = 0.8499150301 \quad (20)$$

The summarized numerical results for the value of the investigated function (2) for linear and exponential approximation are presented graphically in Figure 5.

3.2 Discussion of the obtained numerical results

The investigation shows that the optimal value of the function Y is reached at a point with coordinates (-0.9999;-1;-1) and this value is 0.49249999, i.e.,

$$Y_{min} = Y(X_1 = -0.99999999999999988; X_2 = -1; X_3 = -1) = 0.49249999 \quad (21)$$

The differences in the values at the local minimum of the studied function (2) and the local minima of the function in the considered variants are insignificant of the order of at most 10^{-1}.

This is due to rounding one of the variables X_1 from -0.99999999999999988 to -1. (The used software rounds the data.)

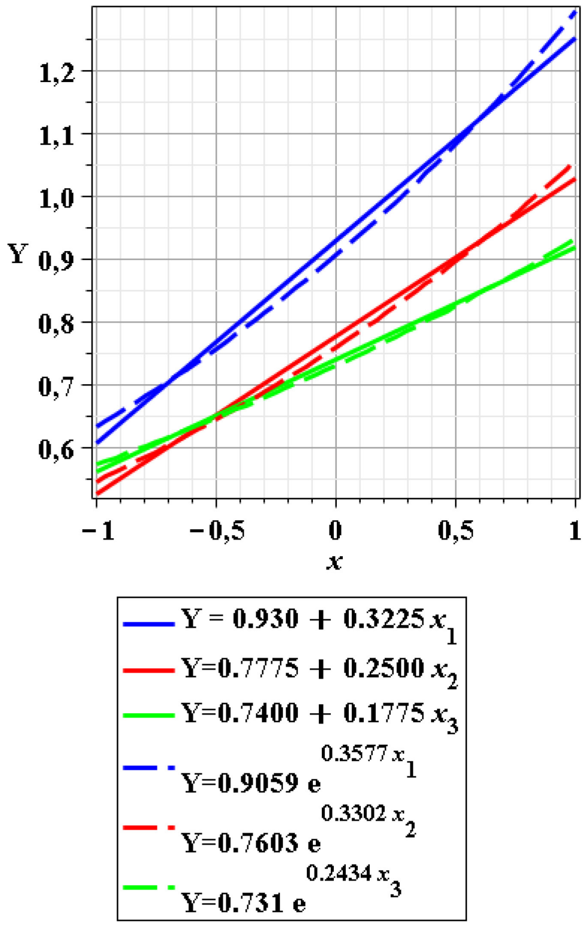

Fig. 5 Movement of the value of the objective function Y.

For each of the considered variants the coefficient of determination R^2 is determined /table 4/ for the linear and exponential approximation of the function (2) respectively. The results for R^2 show the high efficiency of both approximation models /linear and exponential/.

The data in Table 4 mean that:

- the model in the linear approximation explains between 99.07% and 99.63% of the experimental data;

- the exponential approximation model explains between 98.96% and 99.52% of the experimental data.

Therefore, the linear approximation of the investigated function (2) is more efficient.

Table 4. Values of the coefficient of determination R^2 in the linear and the exponential approximation.

	1st variant	2nd variant	3rd variant
$R^2_{LinAppr}$	0.9907	0.9932	0.9963
$R^2_{ExpAppr}$	0.9896	0.9912	0.9952

4 Conclusions

The present work investigates the nature of a function describing the TMF interfacing process. The function gives the relationship between the quality criterion Y (the change of the color shade of the textile material after TMF interfacing process) and the input factors X_1 - the pressure P, [N / cm^2]; X_2 - the temperature of the pressing plates T, [° C]; X_3 - the mass per unit area of basic textile materials M, [g / m^2] [15]. An approximation by interpolation was applied for the purpose of the study.

A numerical realization of a linear and exponential approximation of the mathematical model describing the TMF interfacing process was performed. Three generalized variants with different values of the input factors were taken into consideration. For each of the studied variants, the corresponding values for the change of the color shade of the TM after TMF interfacing process were obtained.

An effective linear approximation of the function connecting the quality criterion with the input factors of the TMF interfacing process was found. This creates conditions for replacing the relatively complex function (describing the TMF interfacing process) with its linear approximation. The linear approximation makes it easier and faster to determine the relationships between the input factors and the quality criterion. This is of essential importance for the quality and efficiency of the TMF interfacing process.

Of course, the proposed mathematical model of the process and its linear approximation can be applied to the described operating conditions / for the respective type of press used, for the respective types of textile materials, etc./. The principles and methods of research of TMF interfacing process / used in the present work / can also be applied in the research of other textile materials, when working with another type of press, etc.

It can be summarized that the proposed methodology for research and analysis of the TMF interfacing process is applicable to different operating conditions.

In the present work, a specific technological process was studied and analyzed using mathematical methods and modern software products. An effective approximation of a mathematical model of the process was applied. This created conditions for facilitating the work, for ignoring the subjective factor and for optimizing and automating the studied technological process.

References

[1] Gries, T.; Lutz, V.; Niebel, V.; Saggiomo, M.; Simonis, K. 14: Automation in quality monitoring of fabrics and garment seams. In *Automation in Garment Manufacturing*, 1st ed.; Rajkishore, N., Rajiv, P.; Woodhead: 2018, pp. 353-376. https://doi.org/10.1016/B978-0-08-101211-6.00014-8

[2] Watcharapanyawong, K.; Sirisoponsilp, S.; Sophatsathit, P. A Model of Mass Customization for Engineering Production System Development in Textile and Apparel Industries in Thailand. *Systems Engineering Procedia,* 2011, 2, pp. 382-397. https://doi.org/10.1016/j.sepro.2011.10.052

[3] Quezada-García, S.; Espinosa-Paredes, G.; Polo-Labarrios, M.; Espinosa-Martínez, E.; Escobedo-Izquierdo, M. Green roof heat and mass transfer mathematical models: A review. *Building and Environment*, 2020, 170, Article 106634. https://doi.org/10.1016/j.buildenv.2019.106634

[4] Dimitrienko, Yu. I.; Dimitrienko, I. D. Modeling and simulation of textile composite plates under a punching load. *Applied Mathematics and Computation,* 2020, 3641, Article 124660. https://doi.org/10.1016/j.amc.2019.124660

[5] Agarwal, B.L. *Basic statistics*, e-book, 4th ed.; New Age International (P) Limited: 2006; pp. 523–563. https://books.google.bg/books?id=qT2srNLLxB0C&printsec=frontcover#v=onepage&q&f=false

[6] Giri, P.; Banerjee, J. *Introduction to statistics*, e-book, 6th ed.; Academic Publishers: 2008; pp. 1-90. https://books.google.co.in/books?id=1CiL9H7mO7wC&printsec=frontcover#v=onepage&q&f=false

[7] http://db.cs.duke.edu/courses/fall01/cps150/lectures/Interpolation.pdf (27 July 2020).

[8] Chizhik, M.; Yurkov, V.; Litunov, S.; Skuba, P. Nonlinear net models of multi-parametrical systems and processes. Journal of Physics: Conference Series of XIII International Scientific and Technical Conference "Applied Mechanics and Systems Dynamics", Omsk, Russian Federation, IOP: 2019; 1441. https://iopscience.iop.org/article/10.1088/1742-6596/1441/1/012053/pdf

[9] Anoshkin, Al.; Pisarev, P.; Ermakov, D.; Roman, Ks. Forecasting Effective Elastic Properties of Spatially Reinforced Composite Materials Applying the Local Approximation Method. AIP Conf. Proc. 2216 of the 28th Russian Conference on Mathematical Modelling in Natural Sciences, Perm, Russia, 2–5 October 2019; Matveenko, Trusov, Yants, Faerman; AIP Publishing: 2020, 020008-1–020008-7, https://doi.org/10.1063/5.0004078

[10] Kosheleva, M.; Golykh, R.; Novikova, T.; Dorovskikh, R.; Khmelev, V.; Shalunov, A. Ultrasonic drying of textile materials. Proceedings of 18th International Conference of Young Specialists on Micro/Nanotechnologies and Electron Devices, Erlagol, Russia, 29 June-3 July 2017; IEEE: 2017; INSPEC Accession Number: 17042461. https://doi.org/10.1109/EDM.2017.7981757

[11] Yu-xian, Zhang; Yong, Li; Bin, Cheng. A nonlinear approximation for size moisture regain using moving least squares method. Proceedings of 24th Chinese Control and Decision Conference, Taiyuan, China, 23-25 May 2012; IEEE: 2012; INSPEC Accession Number: 12881023. https://doi.org/10.1109/CCDC.2012.6244142

[12] Kosheleva, M.; Dornyak, O.; Novikova, T.; Tsintsadze, M. Approximation of Sorption Isotherms of Fiber Materials by Various Equations. *Fibre Chemistry*, 2019, 51, 268–271. https://doi.org/10.1007/s10692-020-10092-y

[13] Andonova, Sn.; Baeva, S. Approximation of a mathematical model of the thermo-mechanical fusing process in the sewing industry. *Fibres and textiles* under review.

[14] Andonova, Sn. Mathematical modelling of the thermo-mechanical fusing process. *Fibres and textiles*, 2020, 2, 3-7.

[15]Andonova, Sn. An influence of fusing conditions on the change of color shade in the production of clothing. *Tekstilec* accepted.
[16]Motejl, V. *Machines and equipment in clothing production*; SNTL: Praha, Czech Republic, 1984; pp. 206-213.
[17]Andonova, S.; Stefanov, A.; Amudzhev, I. An investigation of the thermo-mechanical fusing process of innovative textile material. *Industria Textila Journal* accepted.
[18]Andonova, Sn.; Baeva, S. Optimizing a function linking an quality criterion to input factors on the thermo-mechanical fusing process. *Fibres and textiles* under review.

CDATP

COMMUNICATIONS IN
DEVELOPMENT AND ASSEMBLING OF TEXTILE PRODUCTS

Innovative clothing system for protection against perforation

G. Santos[1,*], R. Marques[1], M. Pinto[2], F. Pinheiro[3], P. Ferreira[4]

[1] *CITEVE – Technological Center for the Textile and Clothing Industries of Portugal, V. N. Famalicao, Portugal*
[2] *LEMAR – Leandro Magalhaes de Araujo (Filhos), Lda., Guimaraes, Portugal*
[3] *OLDTRADING S.A., V. N. Famalicao, Portugal*
[4] *DAMEL – Confeccao de Vestuario Lda., Povoa de Varzim, Portugal*
*Corresponding author *E-mail address:* gsantos@citeve.pt

INFO

CDAPT, ISSN 2701-939X
Peer reviewed article
2020, Vol. 1, No. 2, pp. 121-129
DOI 10.25367/cdatp.2020.1.p121-129
Received: 30 July 2020
Accepted: 31 October 2020
Available online: 3 December 2020

ABSTRACT

Opuntia ficus-indica is a cactus species that has a large potential in several applications. Despite its enormous potential, the production process is still a concern. The harvest process is still mostly manual and implies a dangerous exposure of the human being not only to harsh environmental conditions such as high temperatures but also to the big and resistant spines of the Opuntia ficus-indica. To fulfill the lack of suitable protection equipment for this specific activity, a project emerged with the aim of producing an innovative clothing system composed by textile structures that can act as a barrier to spines and glochids without compromising breathability and presenting a suitable fitting, ergonomics and freedom of movements. This paper will focus on the development of a multilayer clothing system in which the outer layer provide protection against perforation and the inner layer acts like a second skin providing thermal comfort and freedom of movement, so the producers can withstand high temperatures. Concerning the inner layer, several textile structures were developed to analyze the impact on breathability, moisture management and thermal regulation. For the outer layer more than 20 fabrics were developed and submitted to laboratory tests to study their perforation and tearing resistance (according to EN 388). Afterward two structures were selected to proceed and new finishings were developed to prevent the adhesion of the glochids to the textile substrate and simultaneously to give water repellency. Results achieved for the clothing solution from laboratory and field tests with end-users will be presented.

Keywords
protective clothing,
comfort and well-being,
innovative clothing system,
thermo-physiological comfort,
advanced textiles

1 Introduction

Originally from México, *Opuntia ficus-indica* is a cactus species which widespread in both hemispheres and all the continents in arid and semi-arid regions and has been domesticated due to the large potential of these crops in several applications. In fact, *Opuntia ficus-indica* exploitation potential is almost integral. The cladodes can be used as food for animals and human (juice, jam, pickles etc.) or as natural dyers and thickeners. Concerning *Opuntia ficus-indica* fruit, it is most widespread uses as a fresh fruit although it can be processed into jam, juice, liquors, vinegar among others. From the seed, oil is extracted used in the cosmetic industry, and from this extraction a by-product is obtained used as animal feed. Finally, after drying the flower it is utilized for infusions with several therapeutically applications [1-3].

The perennial shrub *Opuntia ficus-indica* can grow up to 5 meters height. It presents succulent stems called cladodes that when they are 1-2 years old can produce flowers. These flowers may have three distinct colors, white, yellow and red, start to appear in May and go through early summer, concerning Northern Hemisphere productions. The *Opuntia ficus-indica* fruit harvest season is from August to October [4,5]

Since *Opuntia ficus-indica* is typically produced in arid and semi-arid regions and the harvest season goes from August to October, the farmers are exposed to harsh environmental conditions such as high temperatures. Additionally, the farmers are exposed to the cladodes as they may present big and resistant spines as well as glochids, air like spines that easily detach from the plant and lodge in the skin and eyes, causing irritation upon contact [6] [7].

Due to the lack of protection equipment's for this specific activity and in order to improve *Opuntia ficus-indica* producers' protection and comfort, a Portuguese consortium composed by three Portuguese companies and coordinated by CITEVE has joined synergies. Therefore, the main goal of this project is to develop a two-layer protection clothing system in which the outer layer provides main protection against perforation and the inner layer acts like a second skin providing thermal comfort and freedom of movements.

Concerning the inner layer, in order to achieve the thermal comfort needed for the *Opuntia ficus-indica* producers, after a body mapping analysis, the seamless technology was selected. Several prototypes were made for both men and women with different fiber compositions and different structures designed to each body region needs (ventilation, compression, moisture management, etc.). Besides thermal comfort, it is also important that the underwear provides freedom of movement and practicality to dress and undress. To evaluate the characteristics mentioned above, potential end-users tested the underwear garment during the harvest season of *Opuntia ficus-indica* fruit, which resulted in the selection of the suitable composition/structures for the underwear garment. The proof of concept was developed in collaboration with Confraria do Figo da Índia (Serpa) and Cactacea (Sesimbra).

In addition of providing protection against perforation, the outer layer will also have easy care features as waterproof and water repellency in order to make it easier to remove the glochids that get attached to the apparel. At first, more than 20 fabrics were developed to analyze the influence of using different parameters (composition, structure and titer of the yarn). Since the main goal is to achieve simultaneously protection and breathability, after submitted to laboratory tests to study their perforation and tearing resistance (according to EN 388) two different structures were selected to proceed and new finishings were developed to prevent the adhesion of the glochids to the textile substrate and simultaneously to give water repellency.

2 Method

The research and development process of the materials and textile components of the outer layer initially involved the development of several textile samples with good mechanical performance (tearing and perforation resistance), followed by the optimization of the repellent finishing and, finally, the optimization of the combined solution (waterproof and water repellence).

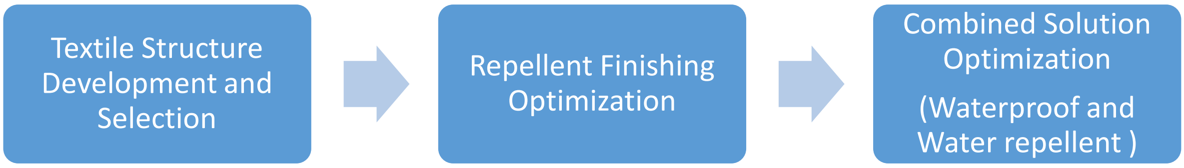

Figure 1. Outer layer development process

On the other hand, the research and development process of the inner layer began with the selection of interesting fibers that could be incorporated in the underwear garment, succeeding with the development of textile structures and afterwards the development of several prototypes that were evaluated by potential end users.

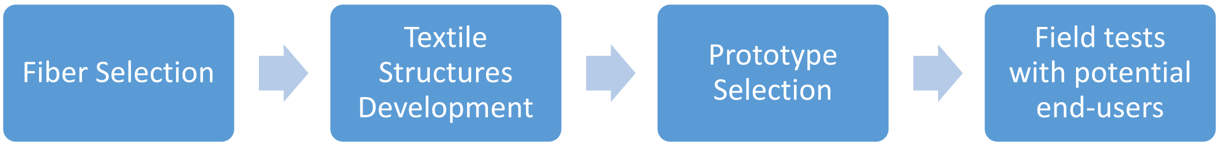

Figure 2. Inner layer development process

With the purpose of evaluating the characteristics required for the outer layer, several laboratorial tests were carried out. Regarding the protection against perforation, there is not currently a standard suitable for protection against spine perforation by *Opuntia ficus-indica*, thereby for this project was selected the standard EN 388 that is used to certify protective gloves against mechanical hazards. On the other hand, to evaluate easy clean functionalities (waterproof/water repellency), the method selected was the Bundesmann test. Regarding the fabric breathability, it was evaluated by the water vapor resistance. The most important evaluation techniques considered for the outer layer fabric are described in Table 1.

Table 1. Evaluation Techniques for the outer layer

Factor	**Property**	**Evaluation Techniques / Tests / Standards**
Physical and mechanical textile properties	Tearing Resistance	EN 388 Protective gloves against mechanical risks
	Puncture Resistance	EN 388 Protective gloves against mechanical risks
	Waterproofness / Water Repellence	EN 29865 Bundesmann
Thermophysiological wearer comfort	Water-vapor resistance	ISO 11092 Skin Model

Regarding the inner layer, due to the use of a seamless garment with several structures, key features of this layer as thermal regulation, moisture management, breathability, ergonomics and fitting were tested in a real environment with *Opuntia ficus-indica* workers. For that CITEVE performed comfort, ergonomics and fitting tests in cooperation with Confraria do Figo da Índia (Serpa) and Cactacea (Sesimbra) using questionnaires and interviews as the main techniques.

3 Results

The research and development process of the materials and textile components of the outer layer consisted, during the initial stage, in the development of several textile samples, changing the construction parameters, such as fiber/composition, title and filament number of the warp and weft yarns and the structure.

Besides the variation regarding construction parameters, the development of several textile samples was based on some initial considerations. In order to ensure good mechanical properties, namely good perforation and tearing resistance, it was established that the textile structures in the developed samples should have fabric coverage values near 100%. With this consideration, it is intended to guarantee low fabric porosity and consequently increase the mechanical resistance of the fabric. With the purpose of ensuring good mechanical properties without compromising weight and comfort of the textile structures, it was also established that the mass per unit surface area should be between 140 and 220 g/m^2. Finally, for economic and technological reasons, the use of 100% polyester (PES) for the warp and 100% polyamide (PA) for the weft yarns in the fabric was considered in all the developed structures.

After the evaluation of the fabric construction parameters regarding the mechanical properties (perforation and tearing resistance), the most promising samples were selected and are described in Table 2.

Table 2. Key construction parameters for the most promising textile structures

	Sample 4.5	**Sample 6.2**
Warp Composition	100 % PES 150 den 52 yarns/cm	100 % PES 150 den 52 yarns/cm
Weft Composition	PA 6.6 HT 235 dtex 29 yarns/cm	PA 6.6 HT 180 dtex 30 yarns/cm
Structure	Twill 2/1	Twill 2/1
Mass per unit area	184 g/m^2	165 g/m^2

With the purpose of evaluating the level of protection guaranteed by the chosen fabrics laboratorial tests were carried out according to the standard EN 388 – Protective gloves against mechanical risks. The results obtained for the fabric samples developed are presented in Table 3.

Table 3. Tearing and perforation resistance of the most promising structures and performance level

		Sample 4.5	**Sample 6.2**
Tearing Resistance (N)	**Warp**	32.4	49
	Weft	55.7	54
Perforation Resistance (N)		69.3	38
Performance Level	**Tearing**	**2**	**2**
	Perforation	**2**	**1**

Despite presenting lower values regarding perforation resistance, sample 6.2 is lighter and has better tearing resistance when compared with sample 4.5. Thereby both of the samples can be used with success for the development of the protective clothing for *Opuntia ficus-indica* producers.

Posteriorly, on a second stage of the process, after selecting the most promising textile structures, the study of functional finishes began. Functional finishings were applied to impart easy clean properties (waterproofness / water repellency) to the fabric, so that the protective clothing developed can be easily cleaned with a shower. Additionally, to prevent the adhesion of glochids to the textile, it is intended that the functional finishing grants a “paper touch” to the fabric. With this in mind, the study and development of functional finishings began by studying the functional property of water repellency and later on obtaining a combined solution, that is, water repellent and waterproof.

In order to develop a textile with water repellence characteristics four repellent products were chosen and applied in the selected fabric samples (trial 6.2 and trial 4.5), with different concentrations suggested by each supplier. Between the chosen repellents, two of them have fluorocarbons (repellent 1 and repellent 3) and the other two are fluorocarbon free (repellent 2 and repellent 4). To evaluate the influence of the selected products and the product concentration regarding the level of repellence imparted to the fabric, the contact angle was measured. To ensure water repellency to the fabric, the contact angle measured using water should be 90º or superior. The contact angle measuring results have shown that all the selected repellent products impart water repellence to the fabric regardless the concentration used, as can be seen in Figure 3.

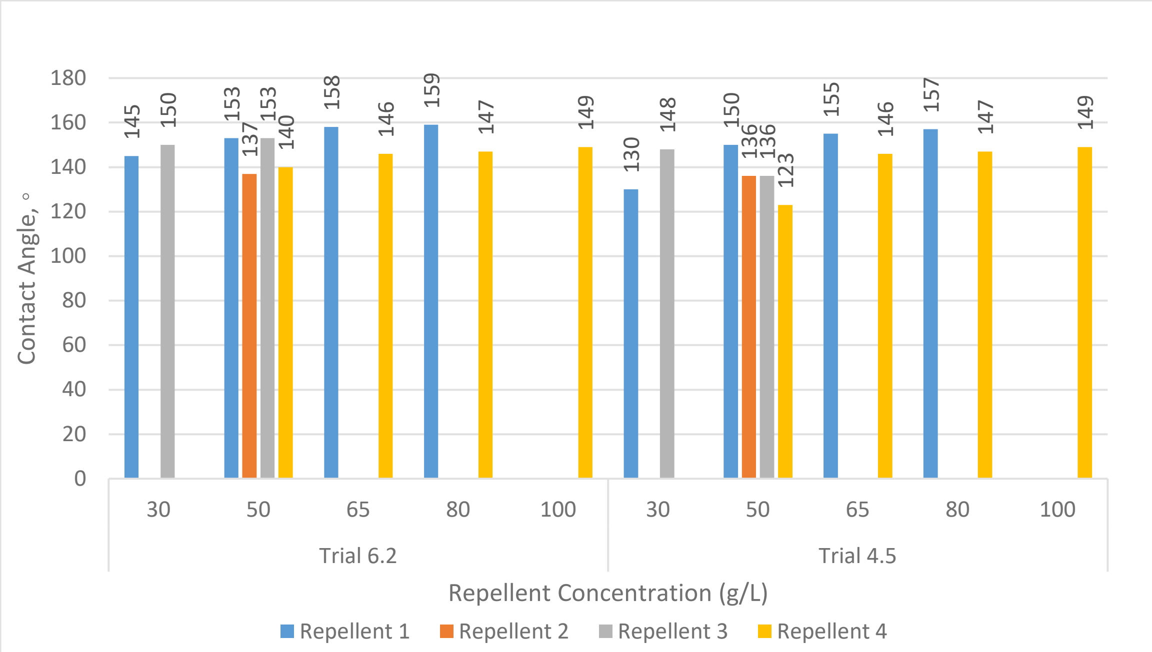

Figure 3.Contact angle measuring results for the repellent products applied with different concentrations

The analysis of the results allowed to conclude that as the concentration increased, the contact angle also increased. Additionally, it was also possible to conclude that fluorocarbon based repellent products present higher contact angles.

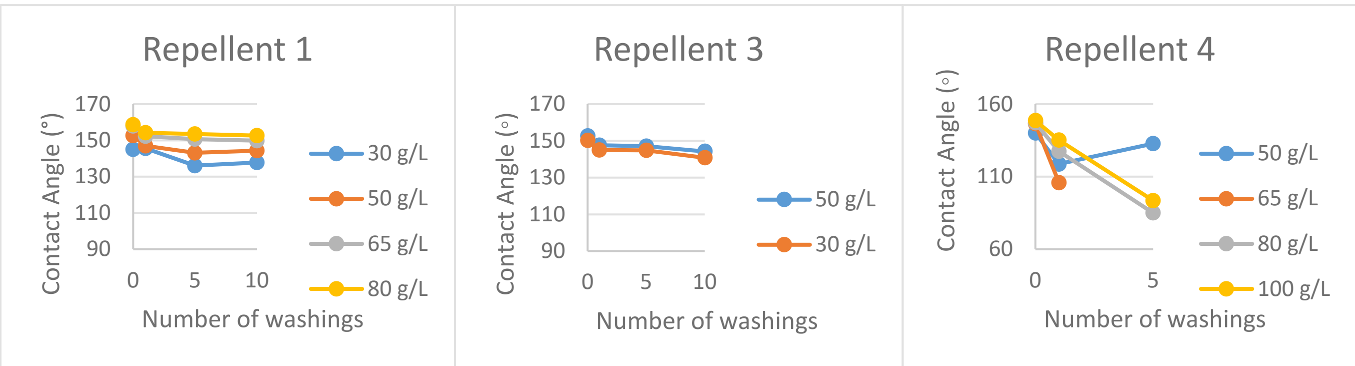

Figure 4. Contact angle results regarding fastness to wash trials for repellent 1, 3 and 4.

Afterwards, fastness to wash trials was carried out in order to understand the influence of washes on fabric repellency after one, five and ten washes. Regarding fluorocarbon free product impregnated samples, the contact angle results have shown a continuous decrease wash after wash. On the other hand, for the fluorocarbon based product impregnated samples after one wash, the contact angle decreased despite staying constant in the remaining washes. Thereby it was possible to conclude that fluorocarbon based product impregnated fabrics present better results and the sample impregnated with 30 g/L of repellent 3 achieved the most promising result, as can be verified in Figure 4.

Posteriorly, after selecting the water repellent product, the second stage of functional finishing study began. In this stage, the main goal was to obtain a combined solution using the water repellent product selected in the early stage and a waterproof coating that could also improve the mechanical characteristics of the fabric, being a barrier between the worker and the cactus spines.

The waterproof functionality can be obtained through foam or paste coating using a knife over roll system. Paste coating is used when the need exists to cover all the interstices of textile surface in order to achieve a waterproof surface. On the other hand, when there is a need to obtain a textile surface that can be simultaneously breathable and waterproof, foam coating is recommended. Both possibilities were studied; however, since one of the key features is to achieve a paper touch surface to prevent the adhesion of the glochids, the foam coating possibility was discarded since this method grants a smooth touch to the textile surface and the preliminary field tests have shown that it does not prevent the glochids' adhesion. Thereby, regarding paste coating applications, two alternative methods of application were carried out, one of which consists in the application of the coating over the fabric impregnated with water repellent product, and the other in the application of the coating with the water repellent incorporated in the paste formulation. In this stage of the process the two water repellent products with the best results were tested, repellent 1 and repellent 3. No samples were made with repellent 3 incorporated in the paste formulation, as its incorporation resulted in foam formation.

Table 4.Tearing and perforation resistance results for the coated samples

Trial	**Sample**	**Impregnation Formulation**	**Paste Formulation**	**Tearing Resistance (N)**			**Perforation Resistance (N)**	
				Warp	Weft	Level	Maximum strength	Level
6.2	1	Repellent 1	Binder 1 Thickener 1	43.4	35.0	2	56.0	1
6.2	2	Repellent 3	Binder 1 Thickener 1	62.8	54.1	3	65.2	2
6.2	3	n. a.	Binder 1 Thickener 1 Repellent 1	25.0	18.0	1	65.0	2
4.5	1	Repellent 1	Binder 1 Thickener 1	48.0	75	2	36.8	1
4.5	2	Repellent 3	Binder 1 Thickener 1	34.5	57.8	2	71.4	2
4.5	3	n. a	Binder 1 Thickener 1 Repellent 1	38.0	69.3	2	62.0	2

The best result was achieved by sample 2 for 6.2, since in this sample a compromise was reached between the tearing and perforation resistance. Afterwards the selected samples were submitted to new laboratorial assays in order to assess whether the coating is waterproof/water repellent (Bundesmann) and at the same time provides thermal comfort (water-vapor resistance) for the end-users. The results obtained are summarized in Table 5.

Despite satisfactory results regarding water penetration resistance, the selected sample did not achieve good results concerning water-vapour resistance, which translates into not obtaining the required thermal comfort for the end-users. Therefore, as the final solution an impregnated fabric will be used as the coverall solution and a coated fabric will be used on the critical areas, in order to reach a compromise between thermal comfort and tearing/perforation resistance.

Table 5. Water penetration resistance (Bundesmann) and water-vapor resistance results for the coated samples

Trial	**Sample**	**Water penetration resistance – Bundesmann Test**				**Water-Vapor Resistance (m^2Pa/W)**
		Water Absorption (%)	Hydrophobicity Level	Back side Wetting	Amount of water that passes through the specimen (mL)	
6.2	2	0.85	2	No	0.28	≥ 200

Regarding the inner layer development, initially a preliminary selection of structures and materials was made in order to achieve the required properties for this layer such as breathability, moisture management, thermal regulation, microbial protection, odor neutralization, hydration, compressibility, localized ventilation, high resistance to wash, movement freedom and comfort. The multi-functionalities required can be obtained from one or more competing variables in the construction of textiles substrates. These variables can be permanent, which are derived from the material and/or structure, or temporary, derivate from the finishing process, by addition of chemical substances.

For the inner layer, in order to achieve the main features previously described, the development began with the selection of interesting fibers that could be incorporated in the construction of the underwear garment. The selected fibers for the underwear were polyester, polypropylene, wool and polyamide. Polyester and polypropylene fibers have good elasticity, fast dry properties and low humidity absorption. On the other hand, wool fibers are known for their good thermal and humidity management. Easy care properties are associated to both polyester and polyamide fibers. Polyamide fibers are also known for having good chemical resistance, tenacity, high abrasion resistance, low humidity absorption and good touch. All the selected fibers have good dimension stability and durability. The possibility of using elastane fibers was also studied since these fibers have good elongation and recuperation properties in addition of being recommended for seamless technology technic.

Relative to textile structures, in order to achieve the required multi-functionalities, samples using different fibers and yarns were produced. The developed samples were made varying the textile structure and consequently the associated functionality. Afterwards, based on the developed structures, the most appropriate yarns and fibers were selected to be integrated in underwear for both male and female. These prototypes were developed taking in consideration the most suitable functionality for each body part as can be verified by the analysis of Figure 5.

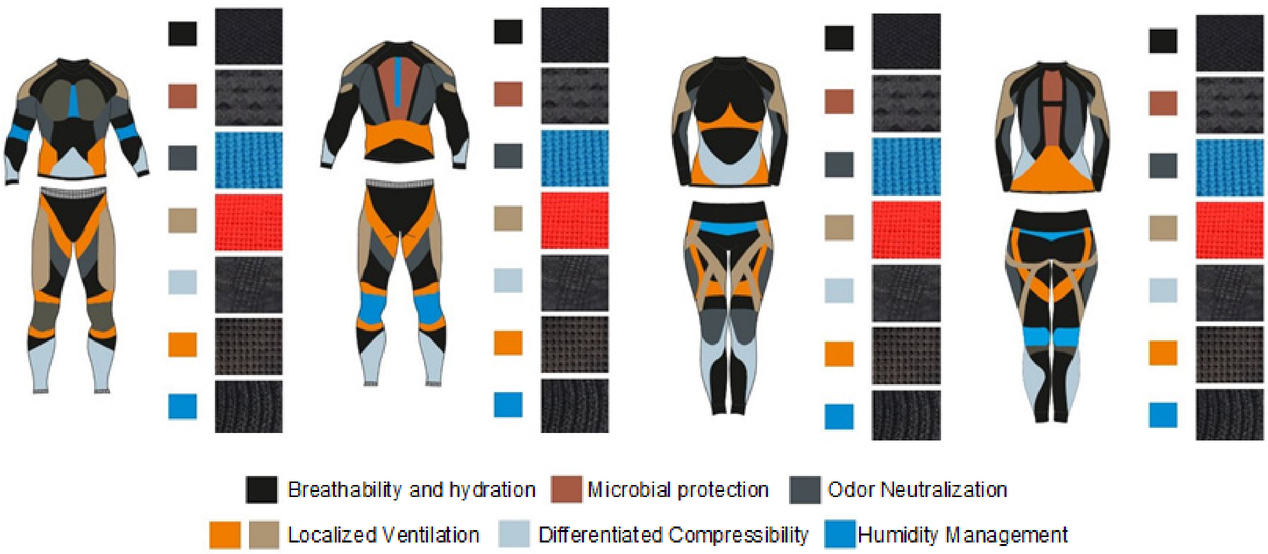

Figure 5. Proposal of design regarding the inner layer accordingly to the location of the functionalities provided by the different structures.

On an early stage, several prototypes were made using different fiber composition, described in Table 6. These prototypes were evaluated by potential end-users that considered the most promising composition being 53% WO, 21% polypropylene, 24% PA (12% PA, 12% PAQ-Skin) and 2% elastane.

Table 6. Inner layer prototypes compositions

Prototype	Composition
1	63 % WO 37 % PA Q-SKIN
2	70 % PES Coolmax 27 % PA Q-Skin 3 % EA
3	54 % WO 44 % PA Q-Skin 2 % EA
4	47 % WO 53 % PP
5	53 % WO 21 % PP 24 %PA (12 % PA, 12 % PA Q-Skin) 2 % EA

The chosen underwear has functional properties such as breathability, thermal regulation, humidity management, microbial protection, odor neutralizer, hydration and localized ventilation. The final prototype was evaluated by twenty six potential end-users that tried the underwear between six and ten times.

In Figure 6, it is possible to verify the obtained results regarding the main characteristics of the underwear garment. All the users agreed that the underwear has a very good touch and provides a very good sensation of freshness. At the same time, it was also considered by the users that the underwear garment has good durability and allows freedom of movements. The underwear was also found comfortable and breathable without compromising its wearability with other equipment used on the Opuntia-ficus harvest. On the other hand, the main problem pointed out was the difficulty for dressing and undressing which will be sorted out by adjusting the size charts.

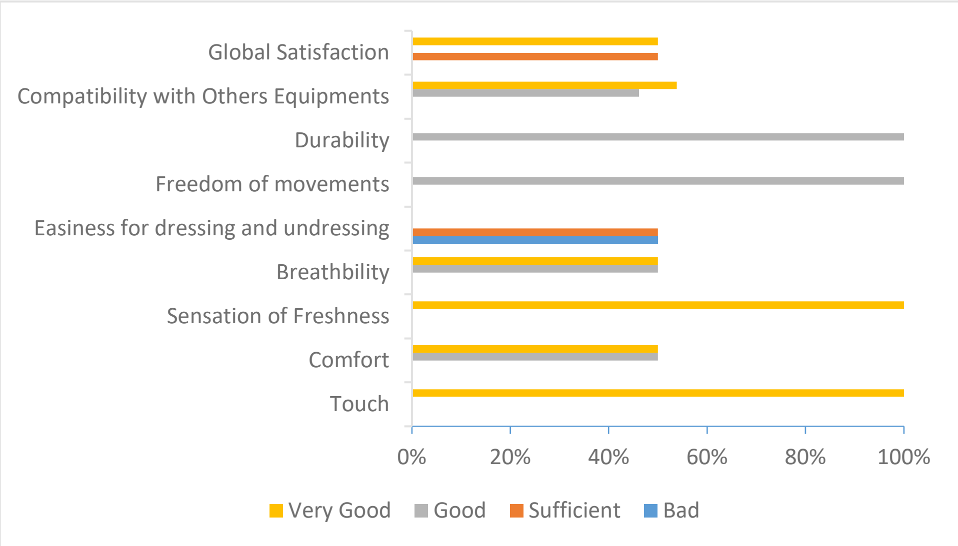

Figure 6. Results obtained regarding the main characteristics of the underwear garment

The survey also questioned about the underwear durability, namely about the fabric elasticity resistance to wash. The underwear was washed by the users from six to ten times and was not reported to show a loss of fabric elasticity.

Currently, the prototype selected by the end-users is being tested regarding the thermal comfort and moisture management accordingly to the thermal manikin test in order to measure the effect of the materials and textile structures developed.

4 Conclusions

In order to fulfill the lack of suitable protection equipment regarding the harvest of *Opuntia ficus-indica*, it is intended to develop a multilayer suit that can offer both protection and comfort to the workers.

The research regarding the outer layer started with the study of multiple structures in order to achieve a fabric with high tearing and puncture resistance. Afterwards, to grant easy care properties to the selected fabric, four different repellent products were studied (two of them without fluorocarbons). In this study it was possible to conclude that fluorocarbon based products present better results and that the sample impregnated with 30 g/L of repellent 3 achieved the most promising result. After selecting the water repellent product, the second stage of functional finishes study began which consisted of obtaining a combined solution using the selected water repellent product and a waterproof coating that can additionally improve the mechanical characteristics of the fabric, being a barrier between the worker and the cactus spines. The selected coating improved the tearing and perforation resistance as well as provided satisfactory water penetration resistance. On the other hand, the selected sample did not achieve good results concerning water-vapor resistance, which translates into not obtaining the required thermal comfort for the end-users. Therefore, the final solution will consist of the use of an impregnated fabric as the coverall solution and a coated fabric on the critical areas, in order to reach a compromise between thermal comfort and tearing/perforation resistance.

Regarding the inner layer development, initially a preliminary selection of structures and materials was made in order to achieve the required properties for this layer. On an early stage several prototypes were made using different fiber composition that were evaluated by potential end-users that selected as final composition 53% WO, 21% polypropylene, 24% polyamide (12% PA, 12% PA Q-Skin) and 2% elastane. The final prototype was evaluated by potential end-users which considered the underwear presents a very good touch and sensation of freedom as well as good durability. The users also found the underwear comfortable and breathable without compromising its wearability with other equipment used on the Opuntia-ficus harvest. The main complaint about the underwear was the difficulty for dressing and undressing which will be sorted out by adjusting the size charts.

Acknowledgements

This study was supported by COMPETE 2020 / PORTUGAL 2020/ FEDER within TexBoost Project – Less Commodities more Specialties and was made possible thanks to a team of Portuguese partners (CITEVE, DAMEL, LEMAR and OLDTRADING).

References

[1] Sá, P.; Ramos, J.; Mesquita, A.; Lopes, F., Virgínia Pereira, et al., A. Pela promoção da fileira do figo-da-índia, 2016.
[2] Sáenz, C. Opuntias as a natural resource. In: Sáenz, C. (Ed.) Agro-industrial utilization of cactus pear, Food and Agriculture Organization of the United Nations, Rome, 2013, 1-5.
[3] Barbera, G.; Inglese, P.; Pimienta, E. Agro-ecology, cultivation and uses of cactus pear, Food and Agriculture Organization of the United Nations, Rome, 1995.
[4] da Silva, R. R.; de Sa Barretto Sampaio, E. V. Palmas forrageiras *Opuntia fícus-indica* e *Nopalea cochenillifera*: sistemas de produção e usos, *Revista GEAMA* 2015, 1 (2), 151–161.
[5] Sáenz, C. Chemical composition and characteristics of Opuntia spp, In: Sáenz, C. (Ed.) Agro-industrial utilization of cactus pear, Food and Agriculture Organization of the United Nations, Rome, 2013, 7-16.
[6] Saha, S.; Banerjee, D.; Khetan, A.; Sengupta, J. Epidemiological profile of fungal keratitis in urban population of West Bengal, India, *Oman J. Ophthalmol.* 2009, 2 (3), 114-118.
[7] Goodheart, H. P.; Huntley, A. C. Rash after visiting Tucson, *Dermatology Online Journal*, 2001, 7 (2), 10.

COMMUNICATIONS IN
DEVELOPMENT AND ASSEMBLING OF TEXTILE PRODUCTS

Investigation of usability and measurement accuracy of 3D body scanning mobile applications

Ekaterina Strunevich[1,*], Ute Detering-Koll[1], Bastian Quattelbaum[1]

[1]*Faculty Textile and Clothing Technology, Niederrhein University of Applied Sciences, Moenchengladbach, Germany*
* Corresponding author *E-mail address: ekaterina.strunevich@hsnr.de*

INFO

CDAPT, ISSN 2701-939X
Peer reviewed article
2020, Vol. 1, No. 2, pp. 130-140
DOI 10.25367/cdatp.2020.1.p130-140
Received: 2 September 2020
Accepted: 28 September 2020
Available online: 03 December 2020

ABSTRACT

In this research project an independent case study on the new contactless 3D body measuring native mobile applications has been carried out. The presented approach allows combination of three different measurement methods: the manual body measuring with the help of traditional instruments, 3D full body scanning technology, and the contactless body measuring via smartphone applications. This paper discusses results of the investigation of usability of the measurement process via 3D body scanning apps on the Gage R&R methodology and the examination of their measuring accuracy. The current research provides analysis of body data obtained by the mobile scanning apps with the help of various methods.

Keywords
3D body scanning technology,
body measuring mobile applications,
body scanning position,
body shape,
body posture,
body measurements,
3D avatar

1 Introduction

Several years ago, an era of new-app & smartphone commerce [1] has begun. The “explosion” of apparel e-commerce has led to overwhelming number of online returns, which exacerbate the problem of sustainability in the fashion industry. 3D body scanning mobile applications based on 3D body data acquisition and its reconstruction are intended to solve the sizing problem during online shopping. And, particularly, at the current “turbulent” time caused by COVID-19, the contactless mobile body measurement technologies, which can greatly facilitate the consumers’ online fashion experience in the quarantine isolation, acquires a new urgency and importance. Nowadays, the investigations on comparing the anthropometric data on living humans using different body measuring methods including smartphone apps are carried out, the results will be released in 2020 [2].

From a scientific perspective, the main challenge is to study the usability, the body measuring accuracy of these new native mobile applications, especially on persons in the group of large sizes, to analyze the quality of body shape recognition, and above all, on figures having nonstandard asymmetrical body posture.

This research consists of two phases based on the systematic analysis. In the 1st phase, the analysis of more than 25 existing 3D body scanning mobile applications was performed and a comprehensive classification of the apps was worked out [3]. The systematic analysis allowed identifying the most important criteria for categorization of the body measuring apps. Table 1 demonstrates the short extracts of the developed classification criteria.

Table 1. Criteria for categorization of the body measuring apps (extracts).

	Criteria name	**Criteria value**	**Comment**
1	Focus of the application regarding to the measuring part of the human body	Body measuring/ foot measuring	This research exclusively concerns the native mobile applications for contactless body measuring.
2	Set of body measurements, measurement up to existing ISO standard	From minimum 8 body control dimensions in the app to maximum 128 in the web application programming interface (Web API)	Most of the investigated apps offer different sets of body control dimensions, which are named and measured with very different methods and under different requirements regarding body position of the measured subject.
3	Measuring mode	Snapshot mode / selfie mode / both	The app can be used alone or/and with the help of another person.
4	Clarity of the body measuring process	Voiceover, animated and/or video user instructions	Simplicity and visibility of the app usage should be provided.
5	Need for subsequent manual calibration for recognition of contours of a human figure	Yes/ No	The additional manual adjusting for more accurate recognition of body contour slows down the process of work with the app.
6	Technical requirements to the mobile device	Smartphone operating system: iOS from the version 7.0 or Android from the version 5.0	Some applications have additional technical requirements, e.g. special depth sensor or 3D-scanner.
7	Default input information		
7.1	Initial anthropometrical information	Gender: female or male, body length, body mass	The initial anthropometrical information is required at the beginning of the app processing. Correctness of default anthropometrical information has large impact on the measuring results.
7.2	Graphical information	Pictures of the measured person or short video of a person moving around	
7.3	Necessary number of pictures of the measured person	One / two	One picture (one front photo of a person and one photo of a background) or two pictures (the front and side photos of a person).
8	Position of the measured person	Five different body positions according to the requirements of the investigated 3D body scanning mobile apps	The analysis revealed that the apps require special body positions which differ from the standard anthropometric position. The body positions were fixed and coded for developing the anthropometric measuring program.
9	Requirements to the clothing and background	Skin-tight clothing, clean and contrast background / scan suit / special measuring kit	Almost all the investigated 3D body measuring apps need skin-tight clothing and clean background in contrast to the color of the clothing.
10	Position of smartphone in the process of graphical data capturing	Fixed on the support surface / in the hand of the operator, approx. on the hip level of the	

		measured figure / on the floor	
11	Place of business or location of the developer	Europe, Asia, North America	Countries: Austria, China, Denmark, Finland, Germany, India, Israel, Japan, Spain, Sweden, Switzerland, Ukraine, USA
12	3D-avatar of the measured figure	Yes / no	Generating of 3D-avatar in one of accepted file formats (e.g. *.obj) via Web API allows to download and analyze it with 3D CAD software.
13	Additional functions	Size recommendation/ Body tracking/ Elements of augmented reality/ Implementation of a virtual dressing room via Web API	Various additional functions depend on the target market: online commerce, final consumer, industry or research purposes [4]. Visualization of the generated 3D avatar in the app allows entertaining the user with the elements of augmented reality (Fig. 1).

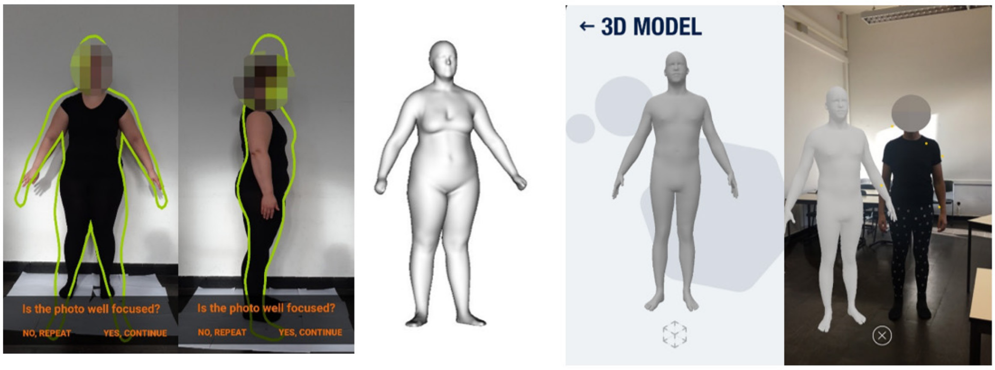

a b

Fig. 1 (a) Visualization of the generated 3D avatar in the mobile app interface; (b) Entertainment of the user with the elements of augmented reality

2 Research methodology

Considering the classification criteria, a set of body control dimensions and the requirements to the position of the measured subject the anthropometric measuring program was developed. This program contains totally 25 body control dimensions which represent 4 following groups:

- girths (U)
- breadths to be measured across the body surface (B)
- vertical and horizontal lengths (L)
- width dimensions / body projections (P).

The program provides descriptions on the measurement method for every control dimension and the information about the necessary body position (Fig. 2).

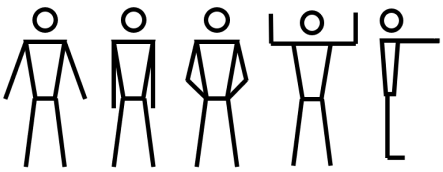

1 2 3 4 5

Fig. 2 Five default body positions according to the requirements of the investigated 3D body scanning mobile apps

In the first phase a preliminary measuring study on 10 female and male participants of different body sizes and figure types has been carried out. The analysis of usability of 3D scanning apps in a combination with their measurement results allowed choosing only 5 reliable apps for the next phase of the research project. The apps were selected considering the following main criteria:

- Duration of the measuring and calculation procedure should trend to minimum.
- The reliability of the app: only fault-free operation was acceptable.
- Measuring operation on plus size figures must be provided.
- Measuring accuracy of the app: the standard deviation of the measuring results and the relative error (RE, %) in comparison with the traditional manual measuring method should trend to minimum.

In the second phase the investigations have been performed on 20 female and male subjects covering the age range from 18 to 55 years old. The measuring figures belong to different groups of sizes: small, medium/normal and large, and to different groups of body lengths: small, normal and long. There were also participants having individual asymmetric body postures.

The main research challenge was to estimate the measuring process and results on plus size figures and also on figures with nonstandard body posture.

2.1 Measurement technologies

The body measuring was realized with the help of three various technologies:

- 3D full body scanning laser technology: Anthroposcan, Human Solutions GmbH, Virtual Lab at Niederrhein University of Applied Sciences
- Contactless body measuring using one specific selected smartphone and 5 chosen native mobile applications installed. For the process of body measurement via apps the special guidelines on the Gage Repeatability and Reproducibility methodology were developed (see Chapter 2.2 below).
- Manually measuring with the help of traditional technique and instruments according to the previously developed anthropometric measurement program. Herewith, the standard measuring instruments were implemented: tape measure, girths measuring tape with an adjustable fastening and a spreading caliper for measuring width dimensions/ body projections. Every measurement was taken manually and fixed 3 times by the same examiner. The calculated average value was considered as a real value.

2.2 Gage Repeatability and Reproducibility

In the second phase, the usability and the reliability of the measuring process via 3D body scanning apps were investigated. The feasibility of every app was examined with the help of the Gage Repeatability and Reproducibility methodology (Gage R&R or GRR). The GRR methodology requires using of the same measuring system (the same smartphone and the same app), two independent examiners measuring at least twice in random order the same study participants. These requirements were strictly fulfilled.

The practical measuring tests on the GRR methodology have been planned and carried out under the general guidelines:

- Two different examiners/ operators use the same mobile device and measure with the same apps.
- Under gage the measuring system is taken: mobile device with all 5 apps installed.
- The measurement procedure with every app is to be performed twice by operator.
- The operator cannot see the measuring results of the other operator.
- Regular rotation of the operation order, so that the examiners cannot remember the results of the previous measurement procedure.

- The operators 1 and 2 should be always the same by measuring every study participant.

3 Results and discussion

The following chapter presents only a short extract from the results of the independent study. The results can be divided up into three groups:

- Usability of the apps on the methodology GRR
- Measuring accuracy of the apps based on mathematical analysis
- Quality estimation of body posture and shape of the avatars.

3.1 Usability of the apps on the methodology GRR

GRR considers an evaluation of the combined variation of repeatability and reproducibility, see Equation (1). In other words, GRR is the variance equal to the sum of within-system and between-system variances [5].

$$\sigma_{GRR}^2 = \sigma_{reproducibility}^2 + \sigma_{repeatability}^2 \qquad (1)$$

Gage Repeatability and Reproducibility data were collected and evaluated. GRR data results show no obvious problems with the tested measurement systems. The difference between repeatability (Equipment Variation) and reproducibility (Appraiser Variation) is considered to be significant. It was found that the Appraiser Variation can be equated to 0 in most cases (Equation (2)). This allows drawing the conclusion that the influence of the examiner is small enough by measuring via mobile apps.

$$GRR = \sqrt{EV^2 + AV^2},\ AV = 0 \qquad (2)$$

Total GRR percentage was calculated for every control measure by capturing female and male figures using every app separately. This approach enabled evaluating the measurement systems independently and regardless of a set of body measures taken.

Figure 3 shows percentages of body measures obtained by every app with the corresponding acceptance ranges in three colors: green – acceptable, yellow – may be acceptable, and red – unacceptable.

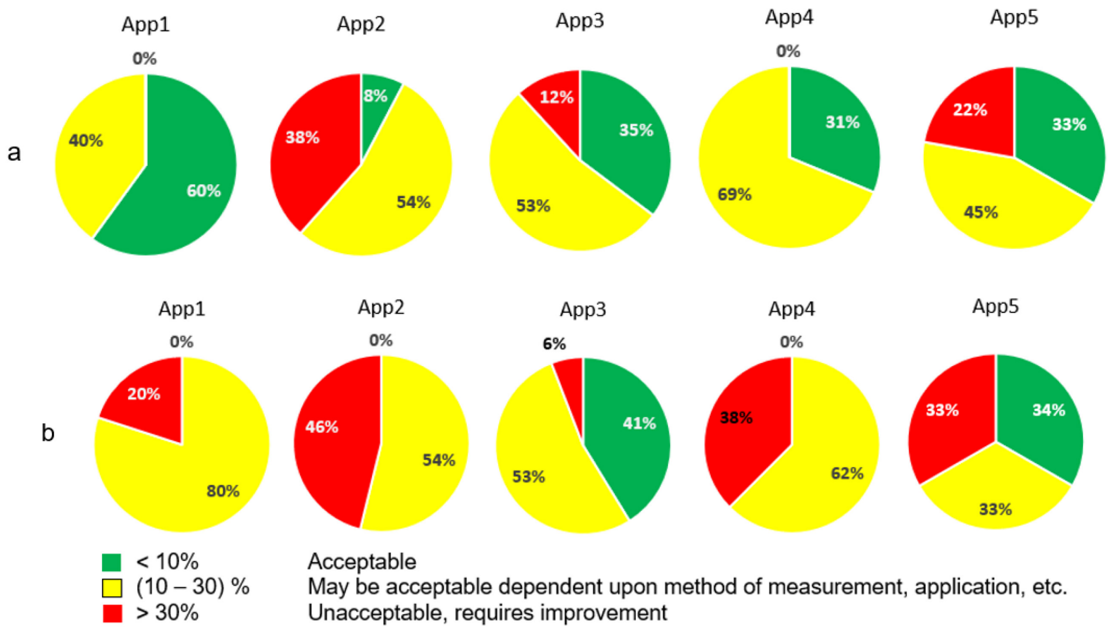

Fig. 3 Total GRR percentage for 5 investigated apps by measuring (a) female, (b) male figures

Total GRR percentage allows concluding that the investigated applications can be generally considered as the acceptable measurement systems (Equation (3)):

$$GRR < 10\% \; or \; GRR \in \; (10; 30)\% \qquad (3)$$

3.2 Measuring accuracy of the apps based on mathematical analysis

The accuracy of body measuring process via 3D body scanning apps was examined by means of the relative error (RE, %) in comparison with the traditional manual measuring method, see Equation (4).

$$RE,\% = \frac{x - x_{real}}{x_{real}} \times 100 \qquad (4)$$

x – average of the body measure gained using every app twice by 2 operators

x_{real} – average of the body measure obtained 3 times by the same examiner manually

The following function (Equation (5)) was calculated and the graph curves are discussed by the method of mathematical analysis.

$$RE,\% = f(x), \qquad (5)$$

where x takes the values of bust girth (g Bu), waist girth (g Wa) and hip/posterior girth (g Po) in cm.

The research results show that RE-distribution of g Bu of women in the medium group of sizes is almost symmetrical with respect to the x-axis and does not exceed ± 5%. RE,% increases maximum to 8% in the group of small sizes. Furthermore, the RE-distribution of g Bu of women in the group of large sizes trends to the area of negative values, see Fig. 4 and Table 2.

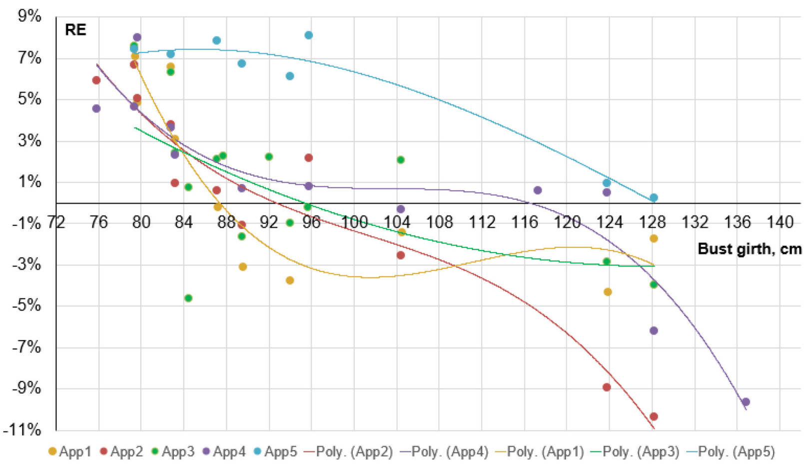

Fig. 4 RE-distribution of g Bu of female figures measured using 5 chosen apps

Table 2. Overview of RE,% in various groups of sizes (g Bu), female.

	Domain of function g Bu (cm)	**RE (%)**
Group of small sizes	$g\,Bu \ll 84$	$RE \in [4; 8]\%$
Group of medium sizes	$84 < g\,Bu \ll 96$	$RE \in [-5; 3]\%$
	$g\,Bu = 104$	$RE \in [-3; 3]\%$
Group of large sizes	$116 < g\,Bu < 136$	$RE \in [-11; 1]\%$

Figures 5-6 and Tables 3-4 provide results of mathematical analysis of RE,% for g Wa and g Po of various female figures measured with the help of 5 chosen apps.

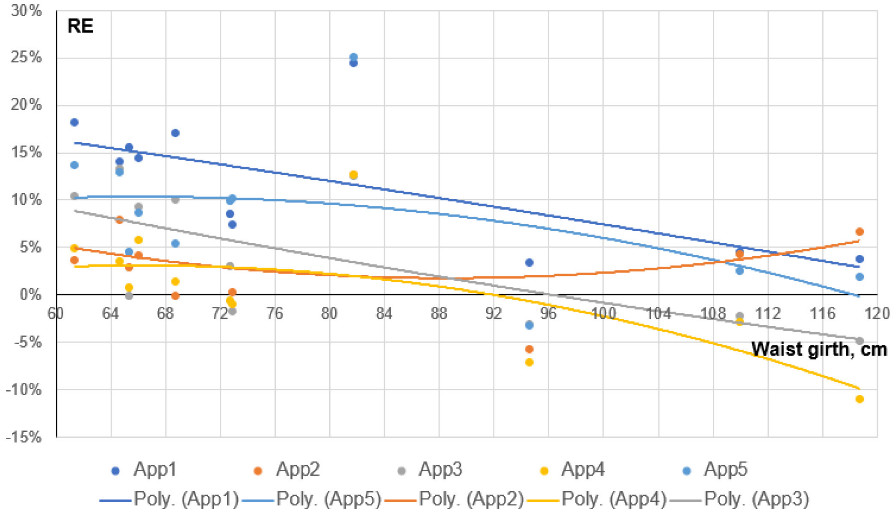

Fig. 5 RE-distribution of g Wa of female figures measured using 5 chosen apps

Table 3. Overview of RE,% for various g Wa, female.

	Domain of function g Wa [cm]	**RE [%]**
Small values g Wa	$60 < \mathrm{g\,Wa} \ll 73$	$\mathrm{RE} \in [0; 15]\%$
	$\mathrm{g\,Wa} = 94$	$\mathrm{RE} \in [-7; 4]\%$
Large values g Wa	$110 < \mathrm{g\,Wa} < 120$	$\mathrm{RE} \in [-11; 6]\%$

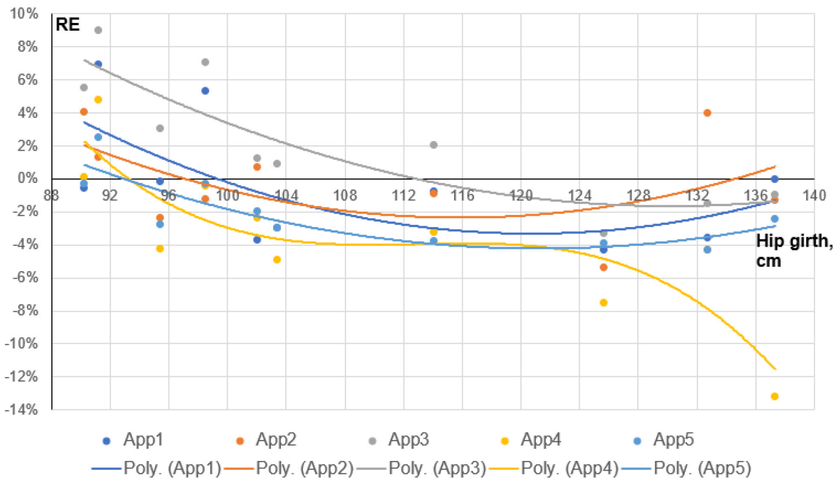

Fig. 6 RE-distribution of g Po of female figures measured using 5 chosen apps

Table 4. Overview of RE, % for various g Po, female.

	Domain of function g Po [cm]	**RE [%]**
Small and medium values g Po	$90 < \mathrm{g\,Po} \ll 104$	$\mathrm{RE} \in [-5; 8]\%$
	$\mathrm{g\,Po} = 114$	$\mathrm{RE} \in [-4; 2]\%$
Large values g Po	$126 < \mathrm{g\,Po} < 138$	$\mathrm{RE} \in [-12; 4]\%$

The study suggests that the measuring accuracy in the group of medium/normal sizes can be generally considered as acceptable. The relative error trends to negative values to -12% by measuring primary girths in the group of large sizes. These results were confirmed by comparison of body measurements using different measuring systems including 3D body scanning technology, see an extract in Table 5 for one female figure, plus size.

Table 5. Comparison of body measurements from different measuring systems, female plus size.

Measurement	**Measuring Technology**						
	Anthroposcan	Manually	App1	App2	App3	App4	App5
Bust girth	141.7	141	138	124	118	128	133
Waist girth	135.0	134	131	113	118	119	119
Hip girth	143.2	144,5	141	134	127	136	136

3.3 Quality estimation of body posture and shape of the avatars

The surface of a human body can be characterized as an object having a sophisticated 3D shape. The fundamental anthropometrical information about the human figure can be obtained from various informational sources:

- Set of primary body control measures: the body length and the main girths: g Bu, g Wa, g Po.
- Body back posture in side view which is determined by side spinal contour. The spinal contour outlines are characterized by cervical and lumbar lordoses and thoracic kyphosis. It is well known that the individual figures are often asymmetric. Figure 7 shows a scanned individual body with a sideways curvature of the spine. Photogrammetry and 3D body scanning technology capture the individual body posture sufficiently, so that the corresponding posture parameters can be investigated with the help of graphics software.

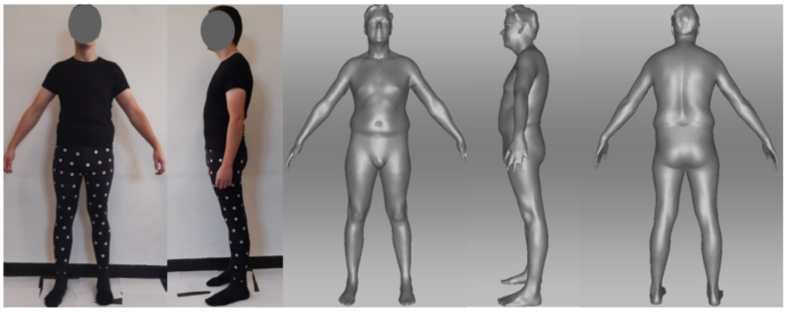

Fig. 7 Scanned individual figure with a sideways curvature of the spine

The front median contour in the side view determines the shape of the bust and trunk areas and delivers balance characteristics and parameters of 3D forming elements (e.g. length and breadth of darts) into garment construction [6].

The individual body shape can be validated with the help of horizontal sections of the scan on the horizontal control planes, e.g. bust plane, waist plane and hip plane.

In this research the detailed graphical analysis of body shapes of scanatars obtained from 3D full body scanner and of simplified 3D avatars generated via Web API was carried out.

Figure 8 shows the substantial differences of body shape of the 3D scan (a) and the 3D avatars (b, c) generated via Web API for one female figure in the group of medium/ normal sizes. The corresponding bust, waist and hip horizontal sections indicate apparent differences of the outlines and the circumference values. For the large group of sizes, these differences become much more significant, see Fig. 9.

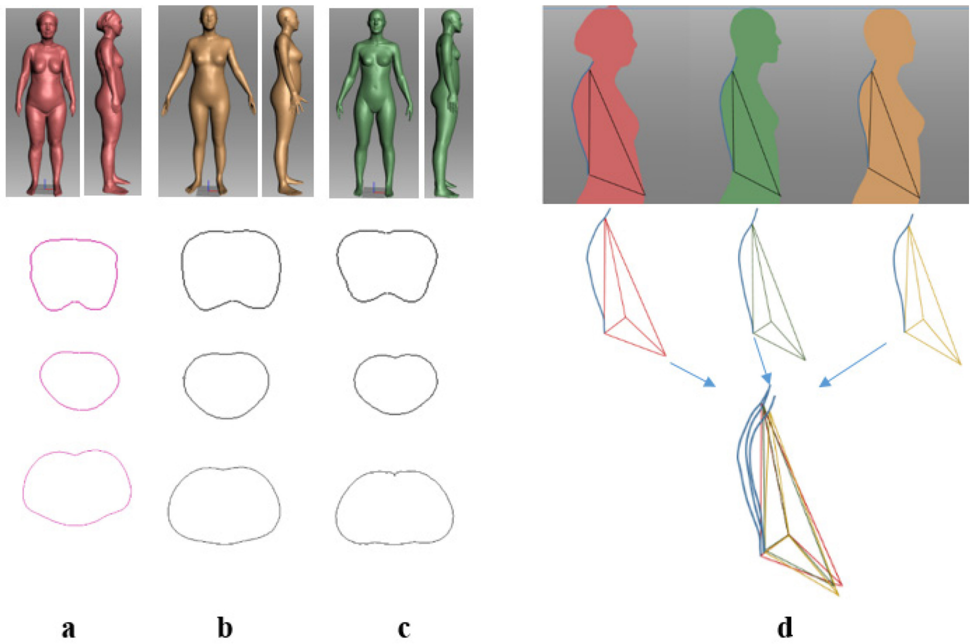

Fig. 8 Comparative graphical analysis of scanatar (a) and two different 3D avatars (b, c), female figure in the group of medium sizes

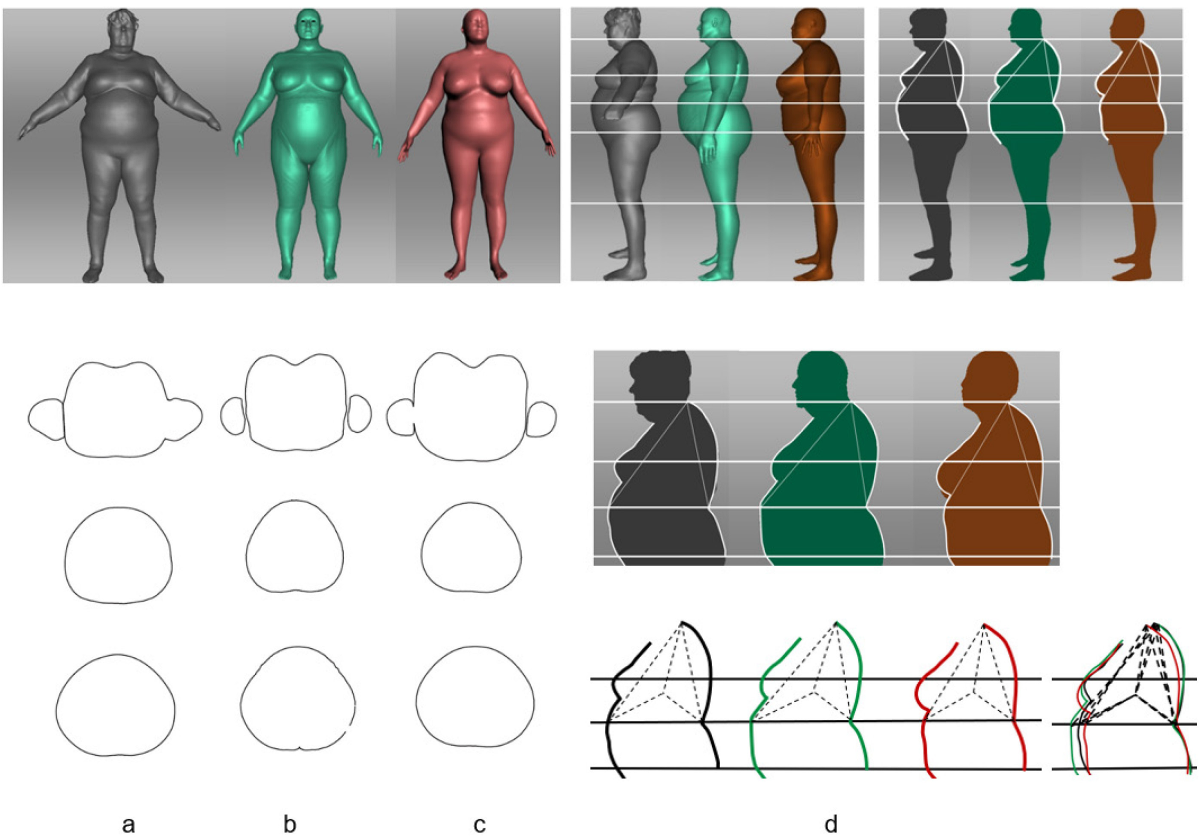

Fig. 9 Comparative graphical analysis of scanatar (a) and 3D avatars (b, c), female figure in the group of large sizes

Comparative graphical analysis of back spine contour based on back posture triangle (Fig. 8 d, Fig. 9 d) and the differences of posture angles characterizing lordosis and kyphosis show, that the 3D avatars do not repeat properly the back posture of the sufficiently precise individual 3D scanatars.

The individual figures with nonstandard configuration of back spine contour were repeatedly scanned with the help of different apps. Figure 10 shows the result of graphical analysis of the generated 3D avatars in comparison with the individual scanatars.

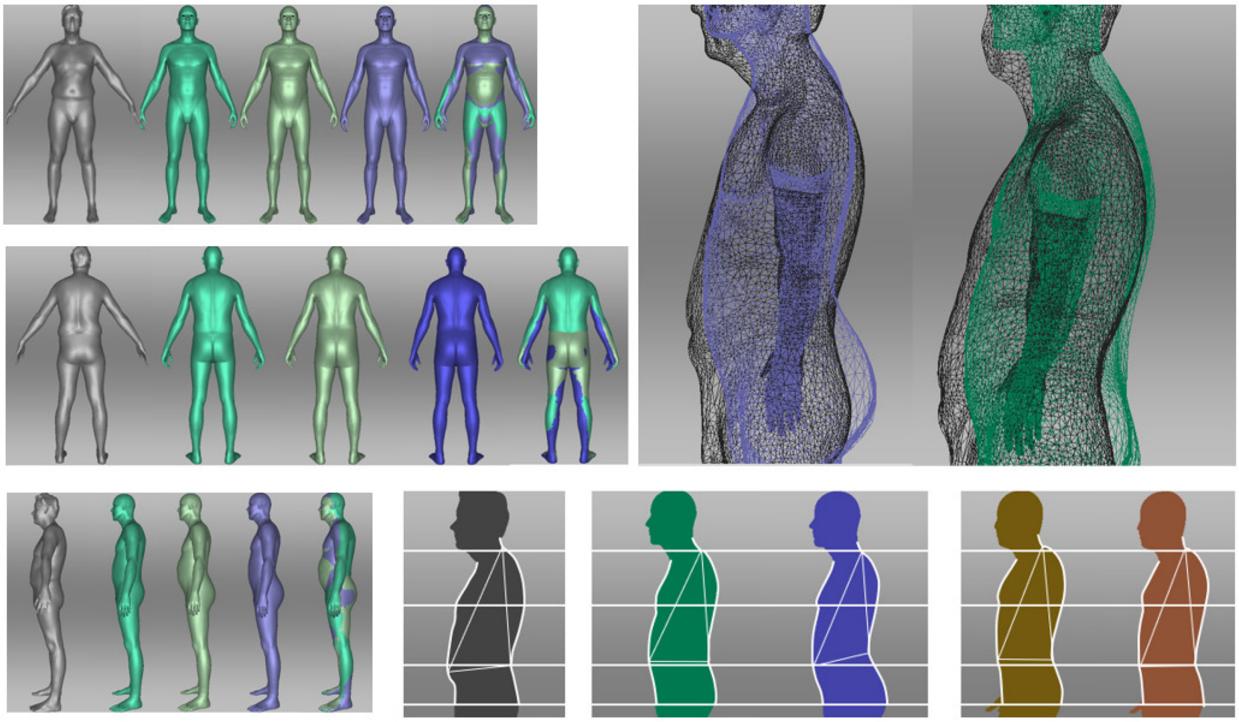

Fig. 10 Comparative graphical analysis of scanatar and repeatedly generated 3D avatars

4 Conclusions

The investigated technology of body measuring and scanning via applications for mobile devices is exclusively useful, relatively fast and easy in usage, and becomes particularly relevant in a wide variety of potential areas, e.g. apparel personalization, made-to-measure, virtual try-on of individualized garments, fitness, medicine, etc.

The examination of usability of the mobile body measuring apps by the methodology GRR showed that the investigated applications can be considered as acceptable measurement systems.

Moreover, the study suggests that the measuring accuracy of body measuring process via 3D body scanning apps in the group of medium/normal sizes can be generally considered as acceptable. The relative error of measuring increases significantly by capturing primary girths of the subjects in the group of large sizes.

The detailed body shape analysis of different 3D avatars generated repeatedly via various Web API shows that they do not correspond sufficiently and do not describe the individual body shape with the required quality. The analyzed 3D avatars differ greatly in the body shape, back posture and front median outline from the sufficiently precise scanatars and accordingly from the real human figures as well. The findings of the research allow highlighting that the algorithm of 3D body data capturing using mobile scanning technology is still not sufficient and there is a demand for great enhancement. Accordingly, from the anthropometrical point of view, there is a need for the continuation the current research in one fundamental study.

Acknowledgements

The authors would like to express appreciation for the support of the Niederrhein University of Applied Sciences (Project "Investigation of contactless process for determination of body measures with the help of digital media", Internal Project Number 362), Virtual Lab at the Faculty of Textile and Clothing Technology, the students Katarina Winands, Markus Bünnemeyer, Iarina Myroniuk, Vanessa Petzold, Natalia Fischer and all voluntary participants of the study.

References

[1] Heinemann, G. *Der neue Online-Handel: Geschäftsmodelle, Geschäftssysteme und Benchmarks im E-Commerce*, 9th ed.; Springer: Wiesbaden, Germany: 2018.

[2] McDonald, C.; Ballester, A.; Rannow, R. K.; Fedyukov, M.; Dabolina, I. *Working Group Progress for IEEE P3141 – Standard for 3D Body Processing, 2018-2019.* Proceedings of 3DBODY.TECH 2019 - 10th Int. Conf. and Exh. on 3D Body Scanning and Processing Technologies, Lugano, Switzerland, 22-23 October 2019, pp. 185–195, DOI: 10.15221/19.185.

[3] Strunevich, E.Y.; Detering-Koll, U., Ernst, M. *Investigation of New Technologies for Retail Returns Solutions in Apparel E-commerce.* Proceedings of the International Scientific and Technical Symposium "Modern Engineering Problems in the Production of Consumer Goods". Kosygin International Forum "Modern Challenges of Engineering Sciences", Moscow, Russia, 29-30 October 2019; Russian State University named after A.N. Kosygin (Technology. Design. Art), Part 3, pp. 172–175.

[4] Ballester, A.; Parrilla, E.; Piérola, A.; Uriel, J.; Pérez, C.; Piqueras, P.; Nácher, B.; Vivas, J. A.; Alemany, S. Data-driven three-dimensional reconstruction of human bodies using a mobile phone app. *Int. J. Digital Human*, 2016, 1 (4), pp. 361–388. DOI: 10.1504/IJDH.2016.10005376.

[5] Chrysler Group LLC, Ford Motor Company, General Motors Corporation. Measurement Systems Analysis. Reference Manual. 4^{th} ed.; Available online: http://www.rubymetrology.com/add_help_doc/MSA_Reference_Manual_4th_Edition.pdf (accessed on 18.08.2020).

[6] Martynova A.; Andreeva E. *Constructive Modelling of the Clothing*, Moscow State University of Design and Technology: Moscow, Russia, 2002; pp. 81–82.

COMMUNICATIONS IN
DEVELOPMENT AND ASSEMBLING OF TEXTILE PRODUCTS

Testing the car seats' comfort

Adnan Mazari[1], Funda Buyuk[1], Antonin Havelka[1]

[1] Technical University of Liberec, Faculty of Textile Engineering, Department of Textile Clothing, Studentska 2, Liberec, 461 17, Czech Republic
*Corresponding author *E-mail address:* adnan.ahmed.mazari@tul.cz

INFO

CDAPT, ISSN 2701-939X
Peer reviewed article
2020, Vol. 1, No. 2, pp. 141-147
DOI 10.25367/cdatp.2020.1.p141-147
Received: 30 June 2020
Accepted: 11 December 2020
Available online: 13 December 2020

ABSTRACT

In this paper, four commonly used car seat covers, made from leather as well as from woven, knitted and 3D spacer fabrics are tested as sandwiched and separate layers to determine the effect of the lamination and layers on air and water vapor permeability. Different combinations of interlining materials are also tested to obtain the optimum comfortable car seat cover. This analysis gives us a real idea of which layer negatively affects the breathability of the car seat. The focus of this part of research was to identify the issues within the car seat material instead of factors like external cooling or the clothing of the driver. It was observed that the polyurethane (PU) foam and lamination significantly reduce the permeability of the car seats. The 3D spacer fabric shows the best top layer properties as compared to classical woven, leather or knitted car seat covers. The research shows how layers and lamination cause thermo-physiological discomfort of car seats.

Keywords
Comfort,
heat transfer,
car seat

1 Introduction

Car seats are meant to be safe, comfortable and durable. The comfort part is usually neglected because of complex structure of the seat and hesitation of experimenting new materials, as durability and safety are much more important for the car producers. During the last two decades, the demand of the customers forced the producers to prioritize the development of the car seat considering better ergonomics and breathability [1]. In this research the focus remains on the thermo-physiological comfort, neglecting the other factors like ergonomics, external cooling, etc.

Car seats do not only have to be designed for safety, they must also have ideal comfort properties. But seat comfort is much more than just passenger convenience. Scientific findings show that the performance of a driver over long distances significantly decreases if the car seats do not support posture and heat balance as required. This leads to exhaustion and loss of concentration, which, in extreme cases, could result in serious accidents [2, 3].

There are multiple factors which make up the comfort seat, but in this research we will keep the focus on the thermo-physiological comfort. From the physiological point of view, comfort of car seat has 4 phases [4]:

i. The first touch: This is the first warm-cool feeling which the driver gets on initial touch.

ii. The long-term comfort: The transfer of dry heat from driver through the car seat.

iii. Breathability of the material: The transfer of moisture and air through the car seat.

iv. Heavy perspiration: In the event of heavy perspiration (a car in the summer heat, stressful traffic situations) the ability to absorb perspiration without the seat feeling damp.

Liquid and moisture transfer in the textile materials includes [5-8]:

- diffusion,
- sorption,
- forced convection.

In this research, two classical ways are used to determine the breathability of the car seats. Moisture vapor transmission parameters are calculated by following different standard methods [9]:

i. The sweating guarded hot plate, skin model (ISO 11092)

ii. Air permeability by FX3300 (ISO7231)

The objective of this research is to analyze the thermo-physiological properties of car seat covers as sandwiches and separate layers and to find the optimum combination of layers for a better comfort performance.

In this research all the sandwiched car seats and each layer separately are obtained from the company MARTUR to determine the effect of each layer and the lamination.

2. Methodology

The experimental part of the research included different combination of car seats cover and the lining material including poly-urethane foam. The classical car seat is made of multiple layers as shown in Figure 1.

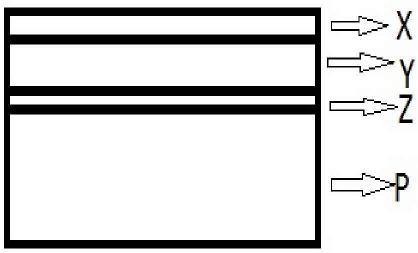

Figure 1. Layers of car seats

The layer details are listed below:
X is the upper fabric layer which is in contact with the person/driver
Y is the following layer made of thin polyurethane (PU) foam
Z is a thin porous polyester mesh (used to decrease friction during the sewing process)
P is a dense PU-foam (8 cm thick)

A set of samples was obtained from the company MARTUR (Turkey), which is a famous car seat cover producer in Europe. All these layers are obtained as sandwiched as well as single layers to identify the effect of lamination. The constructions of woven top layers are shown in Table 1.

Table 1. Car seat cover sandwich combinations

Car seat sandwich	Layer X	Layer Y	Layer Z	Layer P
1	Knitted	Perforated PU-foam, 5 mm	100% Polyester mesh 1.5 mm	8 cm PU foam
2	Woven	Perforated PU-foam, 5 mm	100% Polyester mesh 1.5 mm	8 cm PU foam
3	Leather	Perforated PU-foam, 5 mm	100% Polyester mesh 1.5 mm	8 cm PU foam
4	3D spacer fabric	Perforated PU-foam, 5 mm	100% Polyester mesh 1.5 mm	8 cm PU foam

As shown in Table 1, besides layer X, all other layers are identical. The properties of the layer X are shown in Table 2.

Table 2. Properties of car seat cover layers

Layer X	Material	Thickness (mm)	Areal mass (g/m^2)
1	Knitted, 100% polyester	5.1	245
2	Woven, 2/1 twill, 100% polyester	5.2	230
3	Natural leather, porous	4.8	297
4	3D spacer fabric, warp knitted	5.4	280

3. Results

Car seats are made of multiple layers and each layer has unique importance for the comfort, durability or lifetime of the car seat. The top layer is mostly made permeable to air and moisture, while the bottom and middle layers made up from PU-foam are known for being impermeable to moisture or air. But PU-foams are easy to use, cheap to produce, durable and long-living, so they are an essential part of the car seat. For this research all material types mentioned in Table 1 are tested for air and moisture permeability. Table 3 shows the air permeability of each layer of the car seat cover separately. It was measured by a device FX 3300 according to the standard ISO 7231.

Table 3. Air permeability of each layer separately

Air permeability (L/m^2/s) ± standard deviation				
Car seat sandwich	Layer X	Layer Y	Layer Z	Layer P
1	3200 ± 86	780 ± 60	9400 ± 420	14 ± 2
2	2400 ± 72			
3	1260 ± 41			
4	4900 ± 52			

All these layers are attached together using a copolymer polyamide powder. This is a very economical way, and the majority of the car seat cover producers use this technique. To see the effect of the lamination on the air permeability, the sandwiched car seat (already received as laminated by the producer) which is a combination of layers X, Y and Z was tested by the device FX 3300 (Table 4).

Table 4. Air permeability of laminated and non-laminated car seat's cover

Air permeability ($L/m^2/s$) ± standard deviation		
Car seat sandwich	Layer X + Y + Z by lamination	Layer X + Y + Z without lamination
1	220 ± 8	510 ± 12
2	180 ± 7	407 ± 18
3	120 ± 4	310 ± 14
4	310 ± 5	620 ± 22

These results clearly show that the lamination (to stick each layer together) significantly affects the air permeability of the car seat cover, as the lamination closes the pores of the woven or knitted textile layer and blocks the flow of air. The lamination is mostly a polymeric material which melts to connect the two layers.

Figure 2 shows the percentage change for the air permeability of the car seat cover after lamination. It is more than 50% of change and the highest was recorded for the leather material.

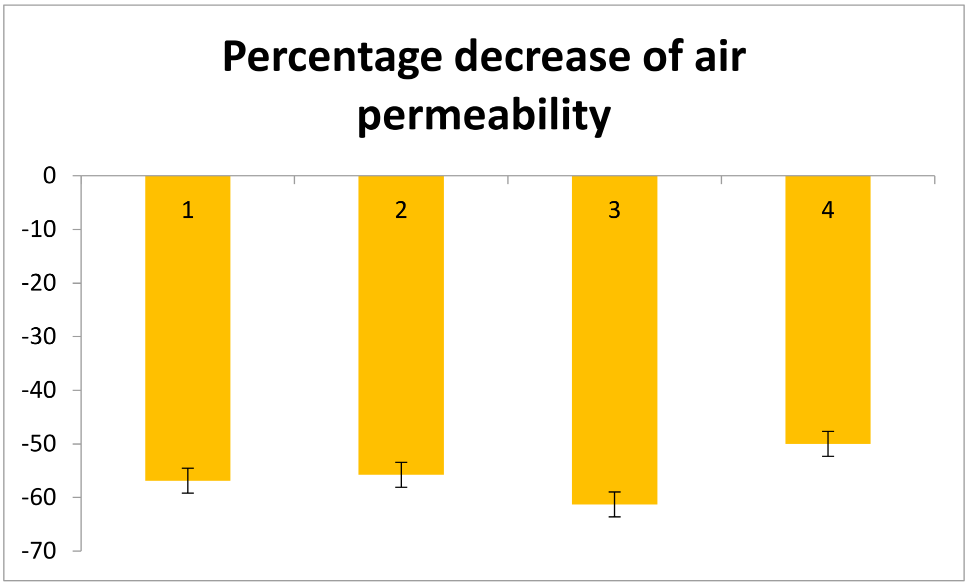

Figure 2. Percentage change of air permeability

The set of sample was also tested for the water vapor resistance with the machine Atlas Sweating Guarded Hot Plate (SGHP using standard ISO 11092. Each experiment is repeated 5 times for mean value.

To measure the water vapor permeability, the device Sweating Guarded Hot Plate was used according to standard ISO11092. Each sample was tested for 5 times. It is visible from Table 5 that the layer 4, i.e. the 3D spacer fabric, is very permeable to water vapor, followed by the knitted fabric, the woven fabric and finally leather.

Table 5. Water vapor permeability of each layer separately

Water vapor permeability (m^2Pa/W) ± standard deviation				
Car seat sandwich	Layer X	Layer Y	Layer Z	Layer P
1	5.56 ± 0.89	12.6 ± 1.5	2.2 ± 0.5	(not permeable)
2	6.37 ± 0.97			
3	12.2 ± 1.23			
4	4.2 ± 0.56			

Similarly as for the air permeability test, the water vapor permeability test was also performed for sandwiches (X + Y + Z) with laminated and non-laminated layers to see the effect of lamination on water vapor permeability (Table 6). The results show that lamination significantly decreases the water vapor permeability by approximately 30-70%.

Table 6. Water vapor permeability of laminated and non-laminated cover

Water vapor permeability (m^2Pa/W) ± standard deviation		
Car seat sandwich	Layer X + Y + Z by lamination	Layer X + Y + Z without lamination
1	19.5 ± 0.9	15.2 ± 1.2
2	22.7 ± 0.7	17.1 ± 1.7
3	27.4 ± 0.3	19.4 ± 1.3
4	15.3 ± 0.4	12.6 ± 2.7

The standard rating for comfortable water vapor resistance values is shown in Table 7.

Table 7. Water vapor resistance and comfort grading

Water vapour resistance (m^2Pa/W)	Performance
0-6	Extremely breathable
6-13	Very Breathable, comfortable at moderate activity rate
13-20	Satisfactory but uncomfortable at high activity rate
20-30	Unsatisfactory
30+	Uncomfortable and short tolerance time

There are multiple interlining materials (Layer Y) available in the market that differ in properties and thickness. The research was further extended to see the effect of different interlining on the car seat cover. In this part the most permeable top layer X, which was the 3D spacer fabric, was taken to measure the effect of interlining on the overall performance of the car seat cover. From the previous experiment, we know that that lamination causes more than 50% decrease of air and water vapor permeability, so this test was performed with the lamination.

Table 8 shows the thickness of different interlinings which are commonly used in car seats. It is easily seen that 3D spacer fabric shows minimum thermal resistance, water vapor resistance and the highest air permeability; both these factors plays a significant role for the thermal comfort of the car seat

The top layer X used in this experiment is the most permeable one, i.e. a 3D-spacer fabric with an air permeability of (4900 ± 52) $L/m^2/s$, combined with different interlining materials (Table 9).

Table 8. Thickness of interlinings

Samples	Interlining materials (layer Y)
1	3.6 mm PU-foam
2	5.6 mm PU-foam
3	6.7 mm PU-foam
4	8.5 mm PU-foam
5	3D spacer 3.6
6	3D spacer 4.8 mm
7	3D spacer 6.5 mm
8	Non-woven felt 4.5 mm
9	Non-woven felt 8.5 mm

Table 9. Air permeability of car seat covers with different interlining materials

Air permeability (L/m^2/s) ± standard deviation		
Samples	**Interlining materials (layer Y)**	**Sandwich layers (X+Y)**
1	450 ± 22	425 ± 21
2	430 ± 18	398 ± 12
3	408 ± 19	375 ± 17
4	380 ± 20	345 ± 14
5	4100 ± 36	3700 ± 72
6	3900 ± 39	3450 ± 32
7	3500 ± 32	3321 ± 28
8	650 ± 12	620 ± 9
9	625 ± 18	589 ± 11

It is visible that by using the 3D spacer as the interlining significantly improves the breathability of the car seat. But overall there is a significant decrease in air permeability when interlining (Layer Y).

In the car seat cover materials, the air permeability and water vapor resistance show very similar trend and performance, and the effect of the interlining materials can be easily predicted.

5. Conclusion

It can be concluded from our research that highly permeable top layers alone cannot improve the overall breathability of the car seat. The problem zone for the breathability will always be the PU-foam and the lamination. The focus should be to use a breathable layer with improvement to the lamination and the PU-foam for better permeability. The car seat comfort should be evaluated considering overall car seat, not just the top layer. There was a significant 50% decrease in breathability due to lamination.

In this research different car seat materials are compared amongst which the 3D spacer fabric shows a great improvement for the car seat thermal comfort. Using 3D spacer fabric can reduce the number of layers of car seat cover, as higher numbers of layers negatively affect the thermal comfort of the car seat. The high thickness variety of 3D spacer fabrics gives the opportunity to use them as car seat covers as well as cushion part of the car seat.

Acknowledgment

This work was supported by the Ministry of Education, Youth and Sports in the Czech Republic under the “Inter Excellence – Action programme” within the framework of project ‘‘Micro-struCtural imaging as a Tool for modelinG fibrOus materiALS (μ-CT GOALS)” (registration number LTAUSA18135). This work was also supported by the Ministry of Education, Youth and Sports of the Czech Republic and the European Union – European Structural and Investment Funds in the frames of Operational Programme Research, Development and Education – project Hybrid Materials for Hierarchical Structures (HyHi, Reg. No. CZ.02.1.01/0.0/0.0/16_019/0000843).

References

[1] Bartels, V. T. Physiologically optimized car seats. In *Textile Advances in Automobile Industry*; Woodhead Publishing. 2008; pp.150–170. ISBN: 9781845693312

[2] Umbach, K. H. Physiologischer Sitzkomfort im Kfz. *Kettenwirk-Praxis*, 2000, 34, 34–40.

[3] Umbach, K. H. Parameters for the physiological comfort on car seats. *38th International Man-Made Fibres Congress*, Dornbirn, Austria. 1999.

[4] Sreenivasan, S.; Nachane, R. P.; Patel, G. S.; Chidambareswaran, P. K.; Patil, N. B. Parameters related to clothing comfort – diffusive moisture transport evaluation. *Indian J. Fibre Text. Res.*, 1991, 16, 189–194.

[5] Mazari, F. B.; Chotebor, M.; Naeem, J.; Mazari, A.; Havelka, A. Effect of perforated polyurethane foam on moisture permeability for car seat comfort. *Fibres Text. East. Eur*., 2016, 26 (6), 14–18. DOI: 10.5604/12303666.1221752.

[6] Wendl, M. C. Fundamentals of heat transfer theory and applications. Class Notes for ME 371, Department of Mechanical Engineering and School of Medicine Washington University, Available online: https://www.scribd.com/document/40466365/ht (accessed on 10 December, 2020).

[7] Holcombe, B. V.; Hoschke, B. N. Dry heat transfer characteristics of underwear fabrics. *Text. Res. J*., 1983, 53, 368–374.

[8] Das, B.; Das, A.; Kothari, V. K.; Fanguiero, R.; Araújo, M. Moisture transmission through textiles Part I: Processes involved in moisture transmission and the factors at play. *AUTEX Res. J.*, 2007, 7 (2), 100–110.

[9] Mazari, F. B.; Mazari, A.; Havelka, A.; Glombikova, V. Novel portable device to analyze the moisture permeability of car seat. *Ind. Textila*, 2018, 69 (3), 183–189. DOI: 10.35530/IT.069.03.1455.

COMMUNICATIONS IN
DEVELOPMENT AND ASSEMBLING OF TEXTILE PRODUCTS

Development workflow for virtual design of clothing for pregnant women

Katarzyna Cieśla[1,*], Iwona Frydrych[1], Sybille Krzywinski[2], Yordan Kyosev[2]

[1] *Faculty of Material Technologies and Textile Design, Institute of Architecture of Textiles, Lodz University of Technology, Lodz, Poland*
[2] *Faculty of Mechanical Science and Engineering, Institute of Textile Machinery and High Performance Material Technology, Dresden University of Technology, Dresden, Germany*
**E-mail address:* katarzynaciesla7@gmail.com

INFO

CDAPT, ISSN 2701-939X
Peer reviewed article
2020, Vol. 1, No. 2, pp. 148-159
DOI 10.25367/cdatp.2020.1.p148-159
Received: 30 June 2020
Accepted: 13 December 2020
Available online: 13 December 2020

Keywords
Blender software,
garment 3D fitting,
Lectra ModarisV8R2,
maternity wear,
pregnancy,
pregnant body model

ABSTRACT

This study presents a workflow for the development of pregnant women's maternity dresses. It starts with the review of the main changes and requirements of the pregnant women. Using Blender, a special overlay is created, which can be added to the normal body and used for modelling of the different stages of the pregnancy. The pattern is created by Lectra ModarisV8R2 with connection to grading table. The 3D simulation is performed with Lectra 3D Fit for simulation and visualization. The result of the application of the workflow is a collection of pregnancy dresses in 4 sizes and tailored to each stage of pregnancy.

1 Introduction

Pregnancy is a time in a woman's life that requires special care and attention. Women are very sensitive at this time and overwhelmed by the new situation. The situation is so unique that the lifestyle can be completely transformed in order to provide the best possible conditions for the child. The changes in a woman's body are happening without her control, so that her attitude and well-being can change rapidly. The changes in the figure are so large that it is necessary to change the wardrobe, but the "new figure" does not exclude the possibility of looking good. Unfortunately, the range of maternity clothes on the market is mainly focused on clothes for typical figures.

While 3D CAD software are becoming more readily available in the apparel industry, it is important to continue to explore the possible and practical uses of these technologies in apparel discipline. Advantages of these programs are fast decision making, shortened development time and less physical samples reduced to one prototype. 3D CAD is able to replace design in different sizes and add physical properties of fabrics.

2 Changes during pregnancy

Medical literature and apparel field are good sources of information on body changes during the pregnancy. There are five changes during this period: of the body silhouette, size, posture, weight and psychological state. In several studies, the trimesters are used as single periods of pregnancy:

- first trimester – from conception to 12th week,
- second trimester – from the 13th week to the 28th week,
- third trimester – from the 28th week until the birth of the baby.

The first external physical changes appear at about month four, which is in the second trimester. All of these physical changes involve special care of comfort, fit and size in developing maternity garments [1].

2.1 Body silhouette changes

The period of pregnancy is related to rapid changes in the body size over a relatively short period of time. Every woman experiences this. External physical changes are most prominently seen in the bust and abdomen. They appear throughout the last two trimesters of pregnancy. For the purpose of studying the clothing, the last two trimesters are most important. The women at that time need clothing which accommodates these changes [1].

2.2 Body measurement changes

The changes are visible in the circumferences. Most women observe an increase from 20 to 26 centimeters around the waist. Abdominal extension varies because of the position of the fetus [1]. Some pregnant women carry their babies low and others carry their babies high. Sometimes the abdomen may seem to be pushed forward or hidden in their bodies [2].

Breasts also expand in size with an average of 5-8 cm circumference from the bust point at the fullest part of the bust [1].

Specific studies show that the waist, chest hip and high hip change are the most significant ones in pregnant women’s body. The maximum value of chest circumference measurement is 125.23 cm, while the minimum value is 86.90 cm. There is a range of differences up to 38 cm and the maximum value is 1.44 times of the minimum. With regard to waist circumference, the maximum value was 120.85 cm, while the minimum value is 83.82 cm; the maximum value is 1.44 times of the minimum, which confirms that great changes also come to the waist. As to the high hip circumference (approx. 10 cm below waist), it is indicated that the maximum value of the measurement is 138.43 cm while the minimum value is 101.60 cm, which makes the difference up to 36 cm. Another data shows the maximum value of hip circumference measurement is 134.62 cm while the minimum value is 97.79 cm, giving a difference of 36 cm and a multiple of 1.38 times. These data prove particularly a huge variation of these areas during the pregnancy [3].

2.3 Posture changes

During the pregnancy, the body weight balance must remain maintained. Abdominal expansion disturbs it. Because of this, the spine is temporarily curved to keep the body balance. This changes the body posture tilting it backwards. It happens in the second and third trimesters of pregnancy [1]. Changes in the posture, center of gravity, and gait cause discomfort such as a lower back pain, pelvic girdle pain, fatigue, and general malaise [4].

2.4 Weight changes

During a 40-week of pregnancy, a woman gains about 13 kilograms [1].

2.5 Psychological changes

Psychologically, the pregnancy is defined as a balance between positive and negative feel. Feelings switch rapidly from joy and exhilaration to fear and loss. Maturation and adaptation processes are simultaneous. Women may react with uncontrollable laughter or tears during daily events. However, emotional fluctuations are a normal reaction during pregnancy [2]. It may seem like the pregnant women feel bad about their body during the pregnancy. Research shows that the most of them have specific attitude to their body size. It turns out that the increasing girth does not bother women. Only the pregnancy is an exception to the rule. This can be influenced by the positive attitude of the community on this issue today. Moreover, women who have at least one other child feel better about their bodies than the first-time mothers [2].

It is worth noting that up to 80 percent of women feel uncomfortable with physiological changes. These discomforts can vary in the strength, from very weak to strong. This may lead to reduced functional mobility and disabling conditions during and post pregnancy [4]. Sometimes other people seem to stare at or try to avoid pregnant women. Such situations can make pregnant women feel uncomfortable and excluded from society [2].

Nine months of pregnancy turns out to be a tough time. Women have to face many discomforts and prepare themselves for the role of mother. Despite all the disadvantages, every mother recognizes this time as unique, extraordinary and wonderful.

3 Maternity clothing

Clothing plays a significant role in establishing and maintaining self-assessment. Indirectly, the appropriate clothing can help to maintain or redefine the self-worth in a positive way [2].

Due to all physical changes, women have to replace their old clothes with new ones. As it turns out, it is not so easy to find clothes that are comfortable during the whole pregnancy. Clothes that will fit in the 4th month will not fit in the 9th month. As a result, women are not sure how to fit their wardrobe. According to Burggraf, the moment when clothes become too tight for the most women is between 4 and 5 months. It is time to find suitable maternity clothes [1]. It is worth mentioning that young women are not ashamed of their pregnant belly and are even proud of it. Spacious clothes hiding the belly are out of date. Modern women want to underline it, but in a subtle way.

Shopping for well-fitting garments can lead to frustration for pregnant consumers. Moreover, the changes during the pregnancy among women are strongly varying [1]. Nowadays, women have the possibility to buy garments in the maternity size. Most literature recommends buying the maternity clothing in the same size as before the pregnancy. However, larger size can provide more comfort for some women [2].

The market for maternity clothes represents a very small part of the overall clothing market. Clothes for pregnant women can be bought mainly in specialty and department stores which assortment is not as varied in style and profitable as in other stores [2]. Women’s quality and fashion requirements are the same during pregnancy as before the pregnancy. They want well-fitting apparel made of natural fibers [2].

3.1 Design

Consumers decide to buy clothes if they are properly fitted, so pregnant clothes design should focus on this. *“However, research on everyday maternity clothing is scarce and there are no studies on maternity wear focusing on body shape changes during pregnancy”* [1].

It is also important not to focus only on the size and shape. Design aspect should also include lifestyle and multidimensional comfort (thermo-physiological comfort, sensory comfort, comfort during the movement, and psychological comfort) [4].

Studies show that most women *“prefer minimalistic and stylish garments, as well as practical rather than decorative and embellished garments. Maternity wear should look like non-maternity, but still be extremely functional for pregnancy”* [4].

Nowadays, we need also reconsideration of maternity clothing design, because the number of obese pregnant women has increased over the last decades. They represent as much as 25% of all pregnancies [4].

3.2 You are what you wear

What we wear has power over our mood and others. Psychologists see a strong relation between clothing and mood. There is proof that we should wear not how we feel but how we want to feel. Even if we feel bad, the clothes we associate with happiness will be a good choice. We must be aware that the clothes we choose are sending a message also to us. It can make us feel powerful, in control or wealthy. So, if you are well-dressed, you are going to feel better about yourself [5].

4 Observation

Nine months is a small part of life. For pregnant women this period is so intense and unique that it stays in their memories for many years. Every woman more or less wants to go through this. New challenges and duties lead to transformation and prepare a woman to be a mother. Mental, physical and physiological discomforts are increasing and are tiring for them. Various thoughts and feelings appear constantly. This puts a woman in a poor mental condition.

Something that best defines a pregnant woman is a new figure. The silhouette of future mums changes dramatically. Apart from a constantly growing belly, the waist disappears, breasts grow and hips widen. The body weight increases by several kilograms. This is usually problematic for women, but becomes more and more often acceptable. Changes in the figure have an impact on physical symptoms. Increasing the body weight causes strain on the joints and a displacement of the center of gravity. The body is overloaded, which causes permanent pain.

New dimensions of figure also require new clothes. Wardrobe for pregnant women should meet the expectations of future mothers, ensuring aesthetic and functional comfort. There are few manufacturers of this type of clothing, which determines the small variety on the market. There is also very little research focusing on the clothing for pregnant women. Undoubtedly, this part needs a fresh look and improvement.

A pregnant woman during nine months of pregnancy encounters many dilemmas and difficulties. Normal, everyday issues during this time may turn out to be problematic. It is very important to reduce stress at this particular time and provide physical and mental comfort. Taking care of herself, avoiding worries, a woman has a positive influence on her own health and that of her baby.

5 Purpose

Taking into consideration the mental and physical condition of pregnant women and the ‘power’ of clothes, the goal of this study was to develop a dress in which they can feel better. The dress should make them feel attractive and elegant. Another idea was to create a garment that is universal and up-to-date throughout the whole pregnancy period. Thanks to that, the product ensures psychological and functional comfort.

6 Modelling of the pregnant body geometry

The body of the pregnant woman changes it geometry. For the modification of the body, the Blender software is used. This is a computer graphics software used for visual effects, arts, motion graphics, and interactive 3D applications. Using Blender, a 3D model can be created from scratch, sculpt, rig, texture, animate and render it to still or movie formats [6]. Blender can export to a variety of industry standard formats, including the .STL format and .OBJ format [7], so that it can be used in the clothing CAD software.

6.1 Body avatars

Starting point of our work were woman body avatars based on the SizeGERMANY portal [8] in sizes from 38 to 50. The SizeGERMANY portal presents the detailed results of German serial measurement. Within this project, serial measurements were carried out on 13,362 men, women and children between the ages of 6 and 87. From this, updated body dimension statistics, size tables and market share tables were developed and new findings for technical ergonomics were collected. Measurements were taken using the latest 3D body scanner technology [8]. The figures were the groundwork for creating a pregnancy figure (Fig. 1).

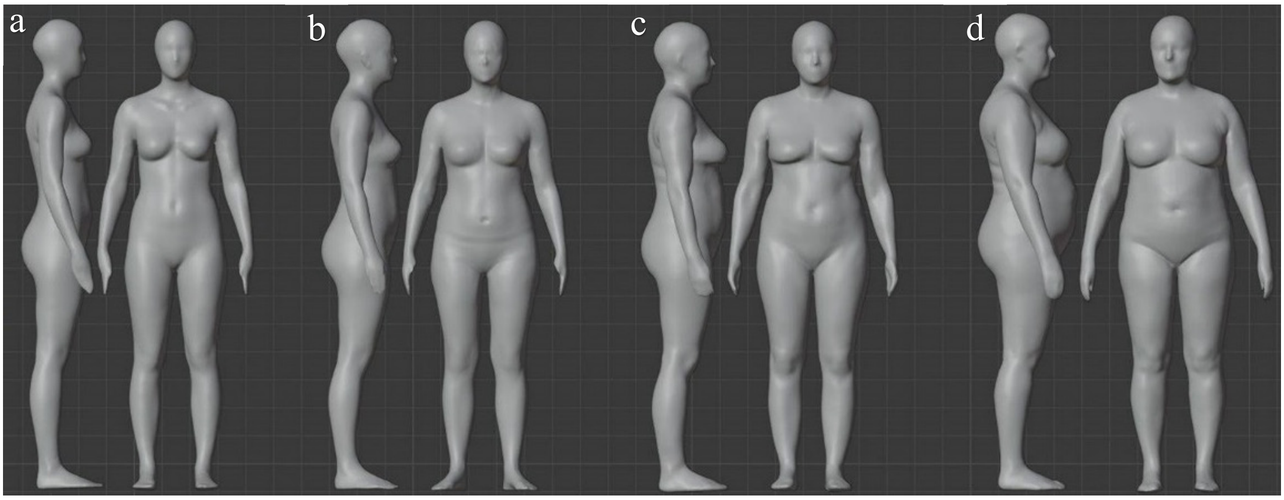

Fig. 1 Body avatars, side and front views: (a) size 38; (b) size 42; (c) size 46; (d) size 50 [8]

6.2 Pregnant body avatar

The source of the pregnant 3D model was a 3D Mag website [9], which contains 3D objects from scans and CAD software, normally used for 3D printing. This model was combined with the normal 3D models for the creation of the pregnant body (Fig. 2). Before that happened, several modifications on the body were done using Blender.

6.3 Simplifying pregnant torso

The removal of arms, breasts, back and legs made it easier to fit the figures later on (Fig. 3). This simplification is allowing the creation of something like an overlay that could fit into any figure. The most important body part is left, i.e. the abdomen and part of chest, to make it easier to orientate the whole piece. The removal of arms, breasts, back and legs made it easier to fit the figures later on. The breast size and shape was changed at a later research stage due to the complexity according to the dimensions in measurement tables [3].

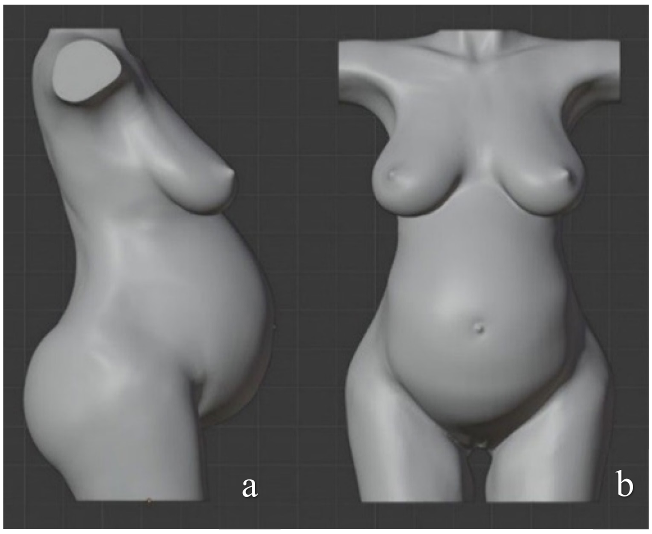

Fig. 2 Pregnant body avatar – 9 months of pregnancy:(a) side view; (b) front view [9]

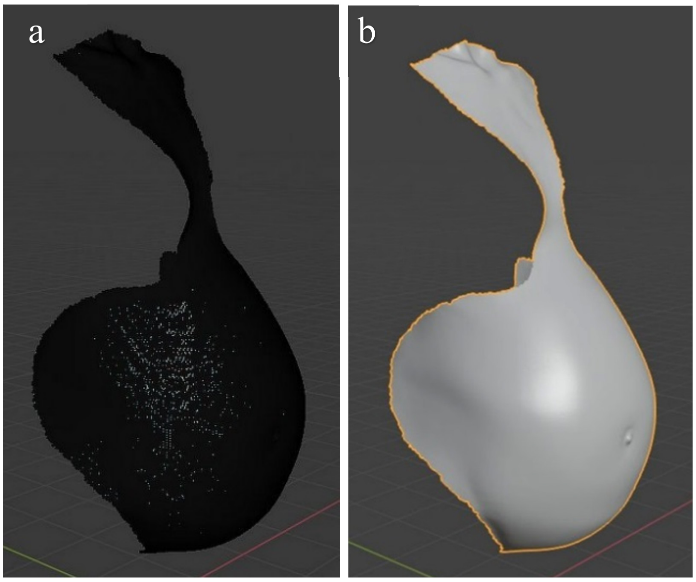

Fig. 3 (a) View in Edit Mode; (b) view in Object Mode.

6.4 Union

The next step was to merge the modified torso with the figure into one object. The abdomen has been permanently connected which is shown by the illumination around the silhouette which includes the abdomen (Fig. 4).

6.5 Results

The results of work in Blender are the figures of pregnant women in 4 sizes and in 3 different stages, as shown in Fig. 5:

- First stage – standard silhouette
- Second stage – half the maximum circumference of the pregnant abdomen
- Third stage – maximum abdominal circumference according to the table dimensions [3]

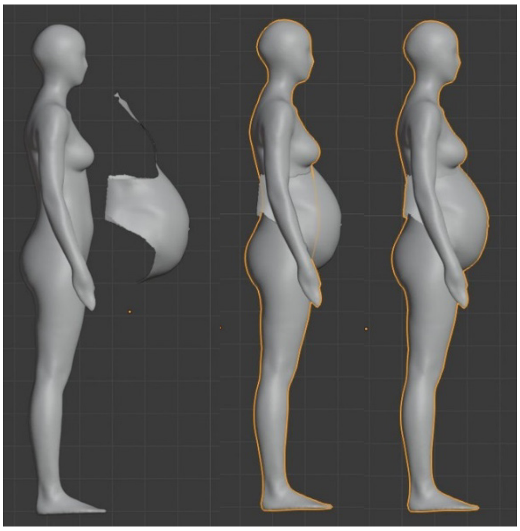

Fig. 4 Three stages of union

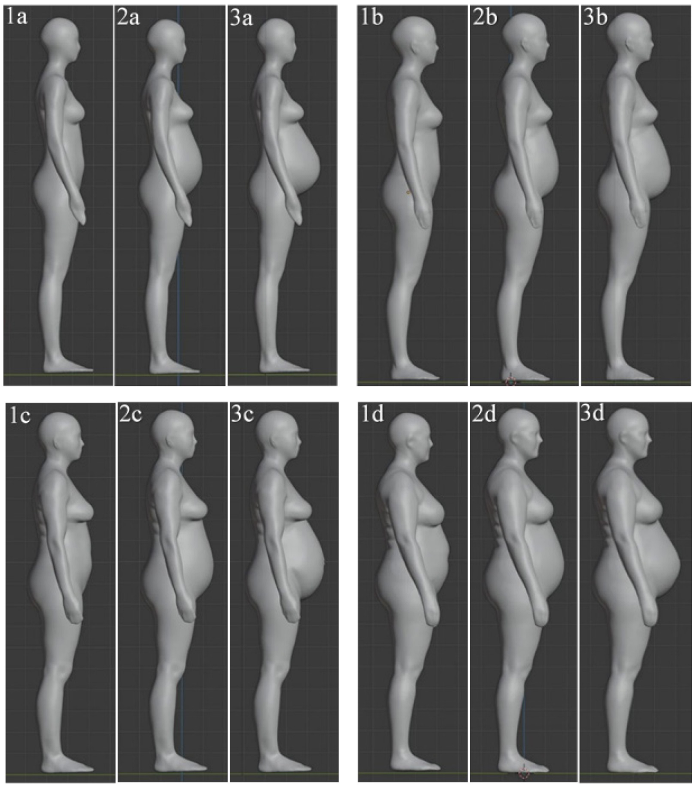

Fig. 5 Three stages of pregnancy: (a) size 38; (b) size 42; (c) size 46; (d) size 50

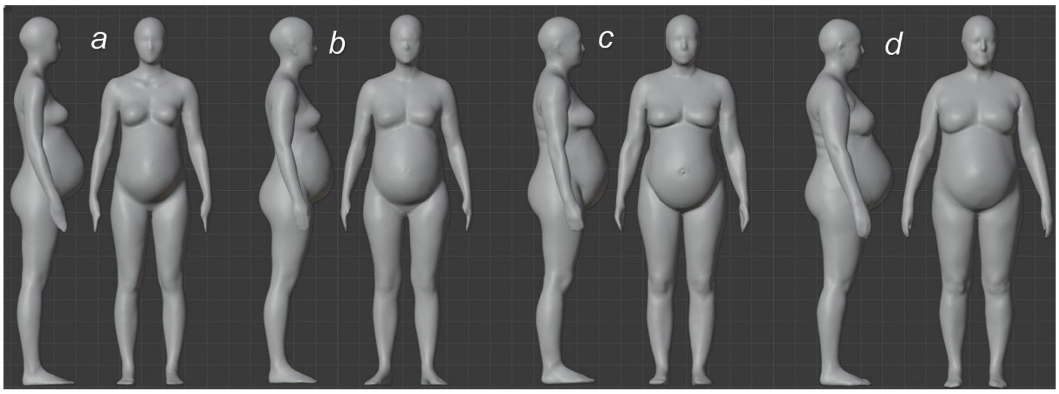

Fig. 6 Pregnant body, side and front view: (a) size 38; (b) size 42; (c) size 46; (d) size 50

7 Clothing Development with Lectra Modaris

Lectra Modaris, Grafis, Assyst and Clo3D are the most used tools in the pattern production. For the current purpose, Lectra Modaris was used. The software is used for creating patterns in 2D for all garment types – lingerie, suits, men's and women's pants, children's wear, swimwear, uniforms, and work clothing. Additionally, the software has a digitalization and gradation option. All options are possible by using appropriate tools [10]. In this section, the setting up of the dress for the Virtual Dressing in Lectra 3D is described.

7.1 Creation of Model Identification Sheet with size range and sheets for pattern construction

The planned project is illustrated in the technical sketch (Fig. 7a and 7b). The project consists of two parts: a dress and a bolero. The model identification sheet was created (Fig. 7c), and a construction sheet was selected (Fig. 7d).

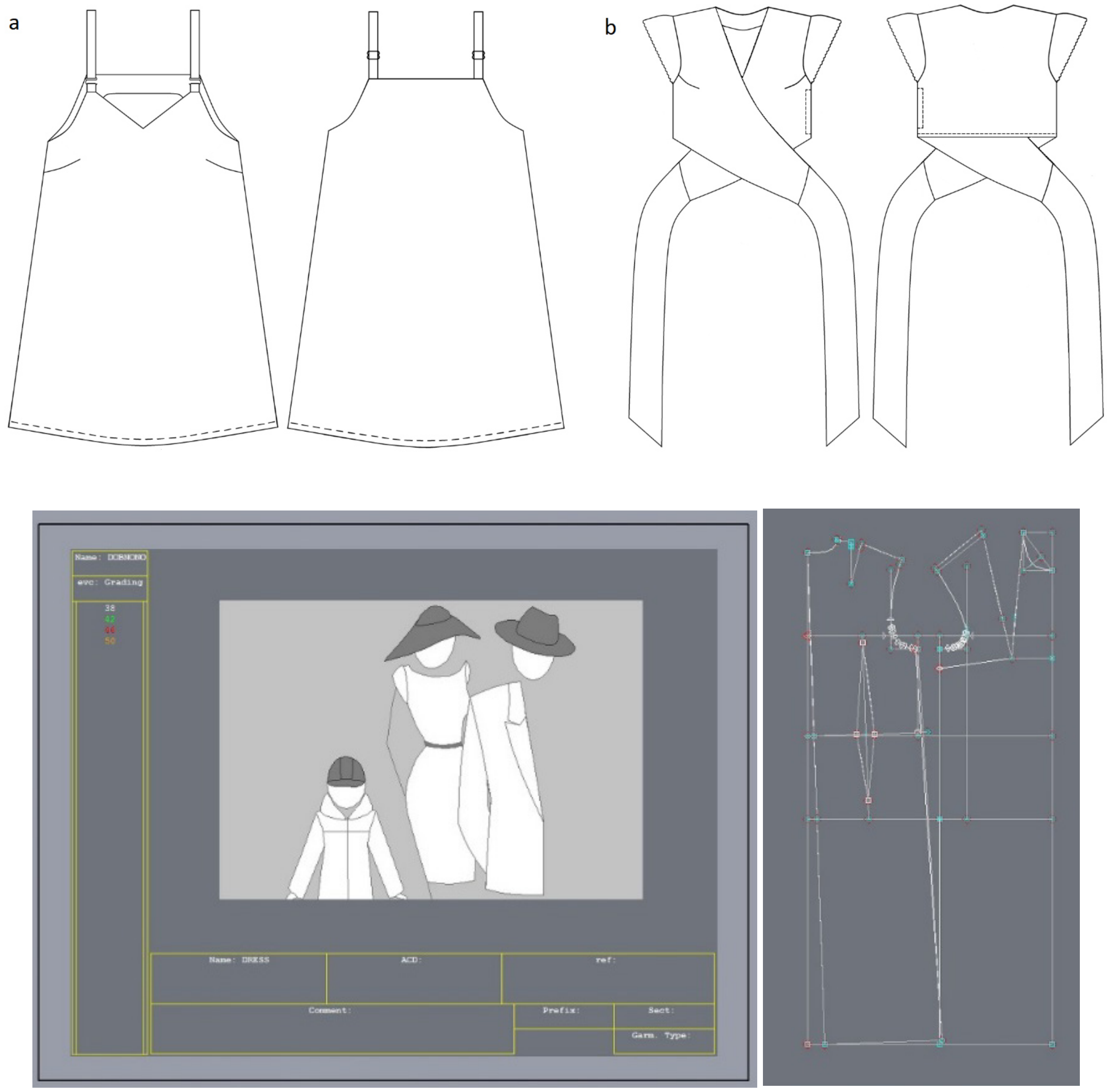

c d

Fig. 7 Technical sketch of the project (a) front and back view of the dress (b) front and back view of the bolero (c) Model identification sheet; (d) construction sheet

7.2 Transform the shape outline into patterns

The main modifications were made in the abdomen and bust area. To cover the abdomen, the patterns were extended at the waist and hip (Fig 8). The dress has shoulder straps. Additionally, a bolero covers the bust and is tied at the back. The bolero stripes are long enough to allow the user to adjust to the bust circumference. There are also elastic seams under the bust to ensure a better fit. The dimensions of the dress were adjusted to the figure at 9 months of pregnancy. The dress type ensures that it looks good on a figure with a small belly and a figure without a belly.

7.3 Grading

After the development of the pattern, these have to be graded, and for this task the key points have to be recorded as grade points. Each point was connected to its reference in a table, which enlarges or reduces the pattern automatically according to the predetermined direction. The values that were added were determined by the size table for pregnant women [3].

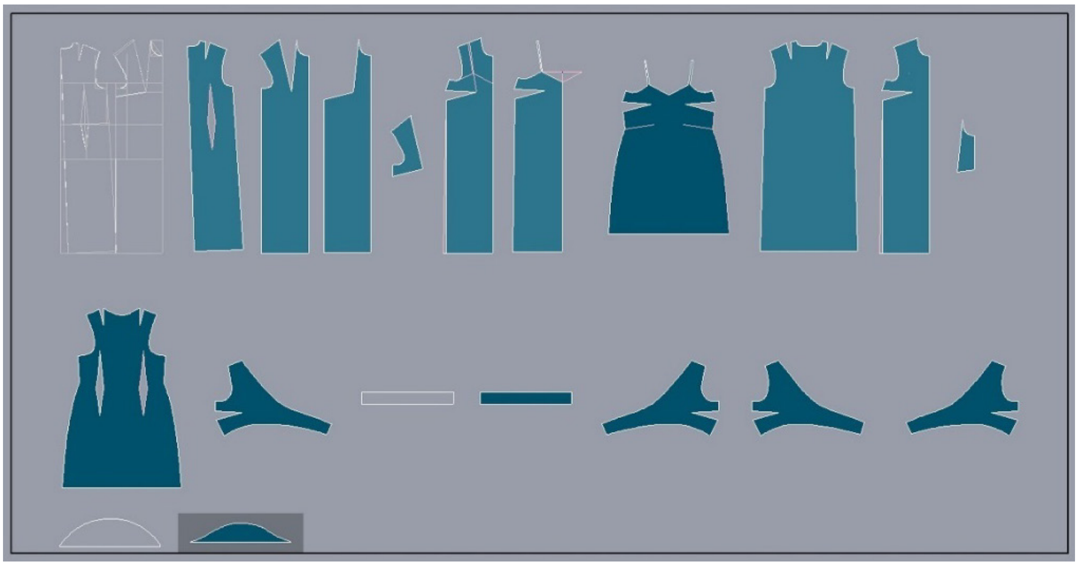

Fig. 8 All patterns in Lectra

7.4 Creation of variants for the normal and pregnant and figure

Based on the grading points, variants of normal and pregnant figure were created (Fig. 9). They differ only in the length of the bolero under the bust.

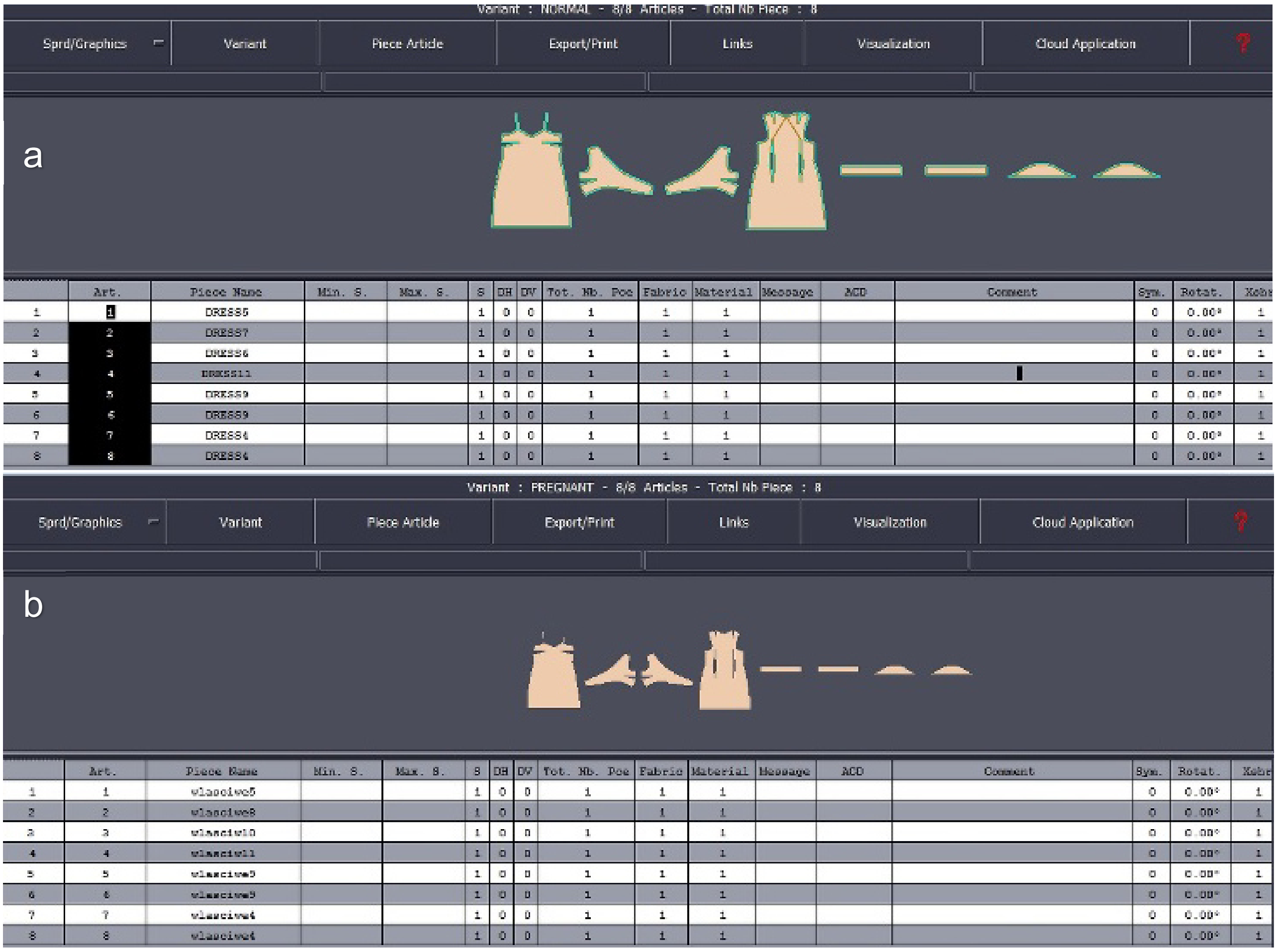

Fig. 9 (a) Variant for normal figure; and (b) variant for pregnant figure

8 Fit simulation with Modaris 3D Fit

Modaris 3D Fit enables to simulate and visualize models in 3D on a virtual mannequin, including the colors, motifs, and fabrics originally created in 2D. With Modaris 3D Fit, the look and fit of the garment can be verified, and its style. Virtual 3D prototyping ensures the quality of garment and its look and fit in all graded sizes and reduces the number of physical prototypes necessary to finalize a model [11]. An appropriate tool in the software Lectra 3D helps to sew together virtual patterns into final garment simulations. Lectra 3D allows visualizing the garment (Fig. 10). This gives the opportunity to take a closer look at the garment from all sides and see if any improvements are necessary. Thanks to this, it was possible to see how the dress fits on each figure and easily to assess if the product meets our expectations.

Fig. 10 Maternity dress in three stages of pregnancy: (a) size 38; (b) size 42; (c) size 46; (d) size 50

The style of the dress is minimalistic in order not to put additional weight on the body. The project has design solutions such as wrapped bolero and elastic seams for a better adaptation of the dress to the changing figure. The fabric used is thin and delicate, which will provide sensory comfort. The form of the dress is loose-fitting in order not to limit the movement. The dress is suitable for a casual use and elegant outing as well.

9 Material selection of maternity dress

Nowadays, the profile of pregnant women is fashionable and modern. They lead a high-quality life and pay attention to every single detail. This highlights how significant the pregnancy is and how excited women are about it.

Health and safety at this time are extremely important. Garments for pregnant women are also worth considering in this context. It is worthwhile selecting environmentally friendly materials and designing in the green natural way. Good examples would be organic cotton, soybean protein, silk and other materials, which have no additives and no pollution. Natural fibers are compatible with ecological environment and thanks to that do not harm the human body. In addition, these materials have the function of anti-inflammation, anti-bacterial and protection against radiation. A basic and good choice is cotton. It is soft and feels comfortable even if the user has sensitive skin [12]. An important problem today is the radiation of electromagnetic fields, which can have a large impact on fetus development. As a result, there is research focused on the development of radiation-resistant fabrics. The material protecting the fetus against radiation is based on metal fibers containing 30 % of them. A good example is also silver fiber fabric, which has anti-bacterial and skin-protection properties. Silk has great properties as well. Natural silk is able to smooth the skin, nourish body and heart and reduce stress for a better sleep. Mixing silk with silver fibers in appropriate proportion leads to fabrics with a soft touch and light texture. These fabrics are safe to put on and can be key part of garments during pregnancy [12].

10 Conclusions

Pregnant women are not a wide social group, but deserve an attention in their clothing. Their needs are strictly defined. There is only a lack of understanding and methods for the development of clothing for them. This work presents a development workflow, including all required steps during the development. This include modification of the human body geometry by meshing processing software Blender, modification of the pattern construction and its connection to a reference table for grading, creation of the different pattern and 3D fit simulation with Lectra 3D Fit. This workflow speeds up the development of collections for pregnant women and will help to fill the gap in the clothing market.

References

[1] Sohn, M. H. A pattern adaptation for body changes during pregnancy: a single case study. Master thesis, University of Minnesota, November 2009.

[2] Manley, J. M. Self-worth, body cathexis, and satisfaction with available selection for those who wear different-size maternity clothing. Dissertation thesis, Virginia Polytechnic Institute and State University, May 1991. Available online: LD5655.V856_1991.M365.pdf.

[3] ASTM D7197 - 13, Standard table of body measurements for misses maternity sizes two to twenty-two (2-22), ASTM International. DOI: 10.1520/D7197-13.

[4] Quintero Rodriguez, C.; Anisimova, A.; Ryan, S.; Troynikov, O. Critical design aspects of maternity support-garments and its contemporary perspective. *KnE Engineering*, 2017, 2 (1), 91-97. DOI: 10.18502/keg.v2i2.600.

[5] LearnVest. What your clothes say about you. Forbes, April 3, 2012. Available online: https://www.forbes.com/sites/learnvest/2012/04/03/what-your-clothes-say-about-you/ (accessed on February 17, 2020).

[6] Blender 2.82 Reference Manual – Blender Manual. Available online: https://docs.blender.org/manual/en/latest/# (accessed on February 27, 2020).

[7] Blender (software), Wikipedia, February 05, 2020 Available online: https://en.wikipedia.org/w/index.php?title=Blender_(software)&oldid=939251869 (accessed on February 14, 2020).

[8] SizeGERMANY – Startseite. Available online: https://portal.sizegermany.de/SizeGermany/pages/home.seam (accessed on February 19, 2020).

[9] Pregnant woman torso free 3d model – download stl file. Available online: http://3dmag.org/en/market/item/3951/ (accessed on February 19, 2020).

[10] Stott, M. Pattern cutting for clothing using CAD: how to use Lectra Modaris pattern cutting software. Oxford: Woodhead Publ, 2012.

[11] Lectra Systems. Available online: https://www.sciencedirect.com/topics/engineering/lectra-systems (accessed on February 18, 2020).

[12] Shang, Y., Hu, X. Ergonomic maternity dress design. *Procedia Manufacturing*, 2015, 3, 187–191. DOI: 10.1016/j.promfg.2015.07.127.

CDATP

COMMUNICATIONS IN
DEVELOPMENT AND ASSEMBLING OF TEXTILE PRODUCTS

Efficient virtual garment fit evaluation infrastructure based on synthetic avatar target customer groups for MtM application

Michael Ernst[1], Antje Christophersen[1], Monika Böhm[1], Ulrich Botzenhardt[2]

[1] Hochschule Niederrhein - University of Applied Sciences, Virtual Lab, Mönchengladbach, Germany, michael.ernst@hs-niederrhein.de, antje.christophersen@hs-niederrhein.de, monika.boehm@hs-niederrhein.de
[2] Avalution GmbH, Kaiserslautern, Germany, ulrich.botzenhardt@avalution.de

INFO

CDAPT, ISSN 2701-939X
Peer reviewed article
2020, Vol. 1, No. 2, pp. 160-169
DOI 10.25367/cdatp.2020.1.p160-169
Received: 30 June 2020
Accepted: 13 December 2020
Available online: 22 December 2020

ABSTRACT

Customization becomes more and more popular and influences the product development process in apparel industry. In addition to individualized products, the fit of garments is very important for the customization. Numerous tools are used to take the right measurements, to transport individual posture information and to implement these data correctly into a product pattern based on a predefined construction system. Unfortunately, in most cases the mass customization process takes place without a fitting session. Usually fit and design will be checked in the last process step, when the product is already manufactured. Virtual product development is a powerful tool to change this process getting an early fit and design check. By using a test population representing the target group, it is possible to check the sizing and to screen the fit of a product on individual bodies and postures in a short time. In a joint project between the Virtual Lab of Niederrhein University of Applied Sciences and Avalution GmbH, a practical approach for the implementation of a fitting session to a mass customization product development process was developed. The entire process has a three-level structure: First, the avatar population is built up using garment specific body measurements. Connected to a 3D simulation program, an automatic process of determining the made-to-measure (MtM) values, carrying out the MtM grading and the fitting on the selected avatar are initiated. In a special application, the digital try-ons are finally output as images in different physical aspects for evaluation.

Keywords

Mass customization,
test population,
target group,
sizing and fit,
fit control,
3D simulation,
virtual product development

1 Introduction

The shape of the human body is individual. A wide range of body types and dimensions can be observed. Pattern systems that aim for a good fit, even more MtM systems that promise a good individual fit for a really wide range of potential customers are critical, but in any case, expensive to evaluate.

This typically leads to two extreme situations during operation. Conservatively speaking, some systems remain completely unchanged during operation (never change a running system) and therefore potentially have a suboptimal success on the market. Other systems are constantly changed during production operation, with a correspondingly high risk that these changes are only focused on the last short-term adjustments. Although obviously introduced with the best intentions, these changes can have undesirable negative side effects or even destabilize the entire system.

In order to prevent such a situation, it is therefore essential to validate and optimize such complex systems prior to commissioning. If changes are required and the system is already productive, it is important to have a tool that somehow broadens the perspective, shows side effects of changes and thus helps to avoid deteriorating the overall performance of the system.

It is therefore essential to have a simulation system available that reduces these risks by virtually validating the system or its behavior on a variety of body types [1,2] (given by so-called "avatar test populations"), specifically designed for a single target group or covering a wide range of customers, in order to improve size sets in the apparel industry.

2 Technological Approach

The fit is the most critical part of a successful "made to measure" process in the garment industry [1].

Frequently, the individual fit is determined by means of a second grading, the so-called MtM grading. MtM grading means an additional grading process based on the standard grading. First the reference size is assigned, then the MtM grading is used.

The structure of the MtM grading is very complex, because every customer has different values and especially different combinations of body measurements.

The iMtM process developed in this project is based on the use of 3D technologies and thus offers considerable advantages over the established 2D MtM process. An avatar population representing the MtM customers, garment simulations for fit control and last but not least the automation within these processes characterise the strength of the 3D technologies and thus the advantages of the iMtM process.

An overview of the technological approach of the so-called iMtM process is shown in figure 1. The iMtM process chain starts with the generation of avatar test populations, which are connected to a garment simulation system via an innovative batch simulator, resulting in a viewer that offers a new approach to fit assessment. The fit is the most critical part of a successful "tailor-made" process in the garment industry [1].

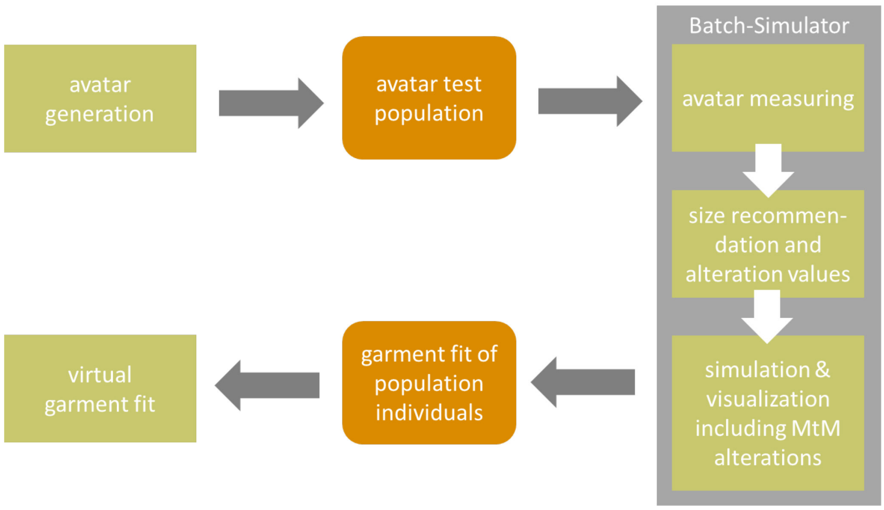

Figure 1 Overall process chain

2.1 Definition and synthesis of the target group

The technology presented in this paper is primarily based on the so-called AvatarStudio technology. This technology currently drives the avatar generator “AvatarTool” in Vidya [3]. In the “Vidya” implementation, it enables the creation of 3D avatars using typical standard body dimensions. The technology “3D-Side” is based on a principal component analysis (PCA) approach using all 3D scan material (>>10k scans) collected within the measurement series Size Germany [4]. It goes beyond the aim of this paper to present the working principles of PCA and its theory in detail, but it is important to understand that PCA acts in a certain way like a learning method, causing extreme data compression [5]. This means that AvatarStudio uses the most important aspects of the 3D shapes, and thus has “learned” the most important aspects of what human geometry looks like. In this particular use case, 100 main components are used [6,7,8]. Since each major component has about 500k 3D vectors [9,10], this gives us the possibility to use a relatively compact representation of the most important aspects of the 3D data observed in the serial measurement. The data structure used is about 0.5 GB for each gender. This means that it can be kept completely in the computer memory during runtime, resulting in a very fast and interactive mechanism of avatar generation (~20 ms per avatar generation).

Another positive side effect of the compression aspect is that the anonymity of the output can always be guaranteed, which is very important nowadays. Using PCA technology, the output range is not necessarily limited to the observed shapes, which fills the “holes” between the observations and also allows meaningful output to regions outside the observation range, e.g. for more extreme body types [11,12].

Of course, the PCA is only the basic component of the AvatarStudio technology. The technology also uses other (statistical and mathematical) approaches to calculate the precise linear combination of eigenvalues to produce a specific, valid and accurate avatar output. Fig. 2 shows avatars for DOB 40 and HAKA 106 size, defined on 22 typical measurements of an industry size chart.

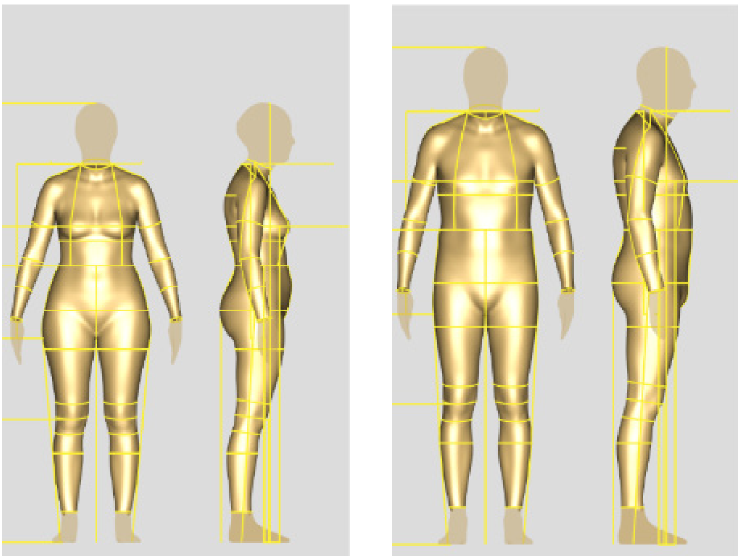

Figure 2 Female and male avatar based on 22 measurements

Avatar Concept

The design of the specific MtM avatar control dimensions, or more precisely the selection of the so-called features or feature vectors (generic term for the sum of parameters defining an avatar) is deliberately based on typical design rules as in mechanical or civil engineering (technical drawings).

Accordingly, perimeter measurements are provided with a height component. The specific portion of each such segment can be configured more precisely through its width and depth. Equipped with all these input parameters, a wide range of body types and morphological aspects can be expressed and systematically investigated (Fig. 3).

Fig. 4 shows two avatars generated from exactly the same body dimensions (HAKA 106S), with the morphological variation of triangle and inverted triangle.

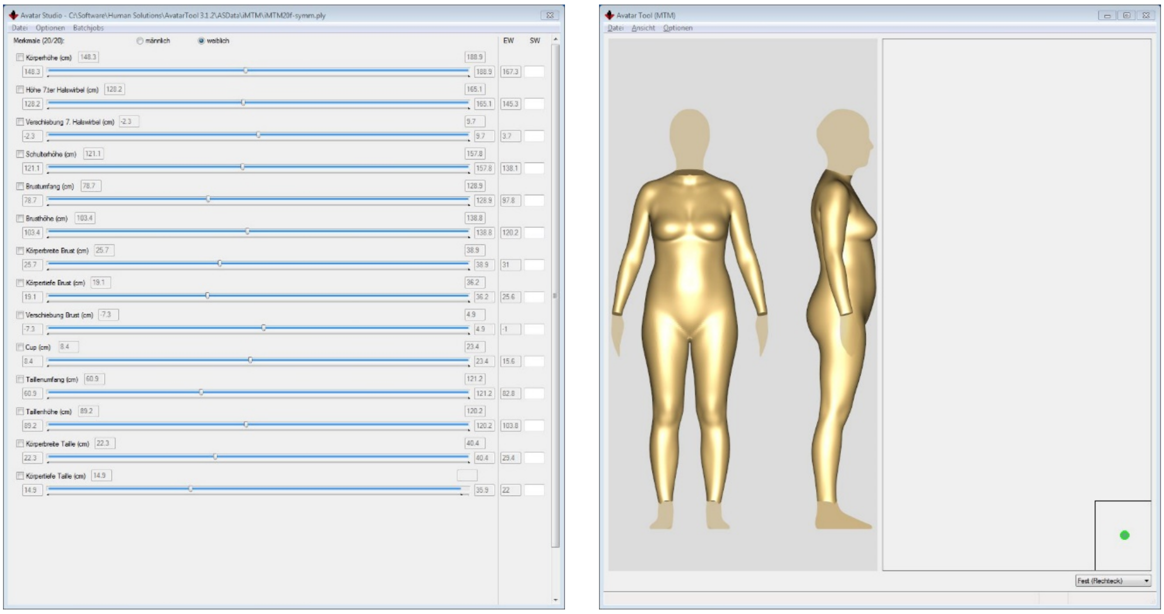

Figure 3 AvatarTool

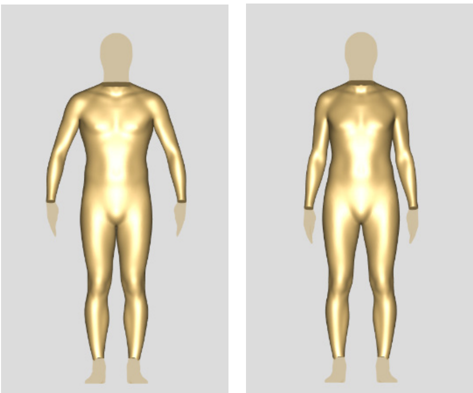

Figure 4 Male avatars with same body measurements but different morphological shape

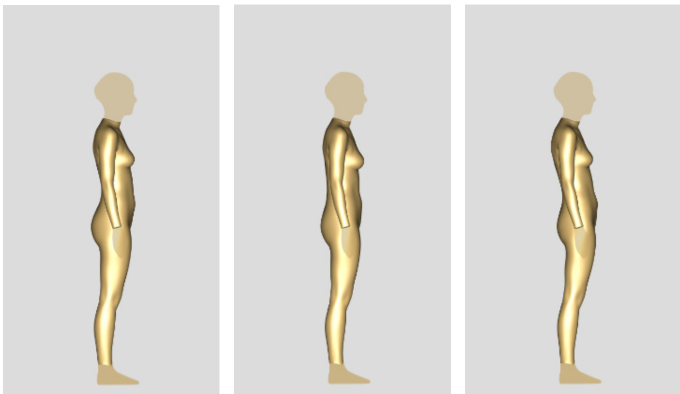

Figure 5 Female avatars vary in shape and posture

In addition to that, special features had been introduced that control typical postural aspects to e.g. examine to which extend a specific body (or body size) given by its measurements may still vary in its shape and posture (Fig. 5), and to what extend this affects the fit.

2.2 Automatic evaluation of MtM values based on an avatar test population

Using garment simulation on avatar test populations provides an opportunity to validate the MtM grading process and, by visualizing the simulation results, enable the user to approve size, fit and design.

Automatic creation of an avatar test population with automatic measurement creation and output for MtM

From an architectural point of view, the system consists of 3 major components:

1. the avatar test population definition system (AvatarTool)
2. a batch executing system including (BatchSimulator)
   - avatar measuring

- size recommendation and calculation of alteration values
- a garment simulation (Vidya) system in combination with a CAD system including MtM functionality

3. result viewing and simulation comparison system (SimulationViewer)

2.3 Research methodology

Investigations were carried out with various MtM products of classical women's and men's clothing as well as workwear. All products have been fitted and evaluated on the avatar test population with 3D garment simulation applications – Vidya, V-Stitcher – regarding realistic material simulation following the research methodology shown in Fig. 6.

Figure 6 Research methodology

2.4 Target group

The target group for MtM garments is related to the target group of the defined standard sizes. The aim is to dress customers with bodies and shapes different from the standard sizes.

Definition of target group

The target group investigated comprises female and male avatars split into three groups, depending on the predefined MtM modifications:

- Level 1: Length modifications
- Level 2: Length and girth modifications + distribution of girth modifications
- Level 3: Posture modifications

All test avatars based on statistically verified bodies and therefore extreme body data are excluded and not part of the survey. Figure 7 shows a selection of the target group.

Size recommendation

The selection of the product-related reference size is based on chest, waist and hip circumference for outerwear, and only waist and hip circumference for lower body garments. For this purpose the measurements are evaluated with different priorities.

Calculation of alteration values

Alteration values are calculated by the difference of individual measurements to the values in the size chart.

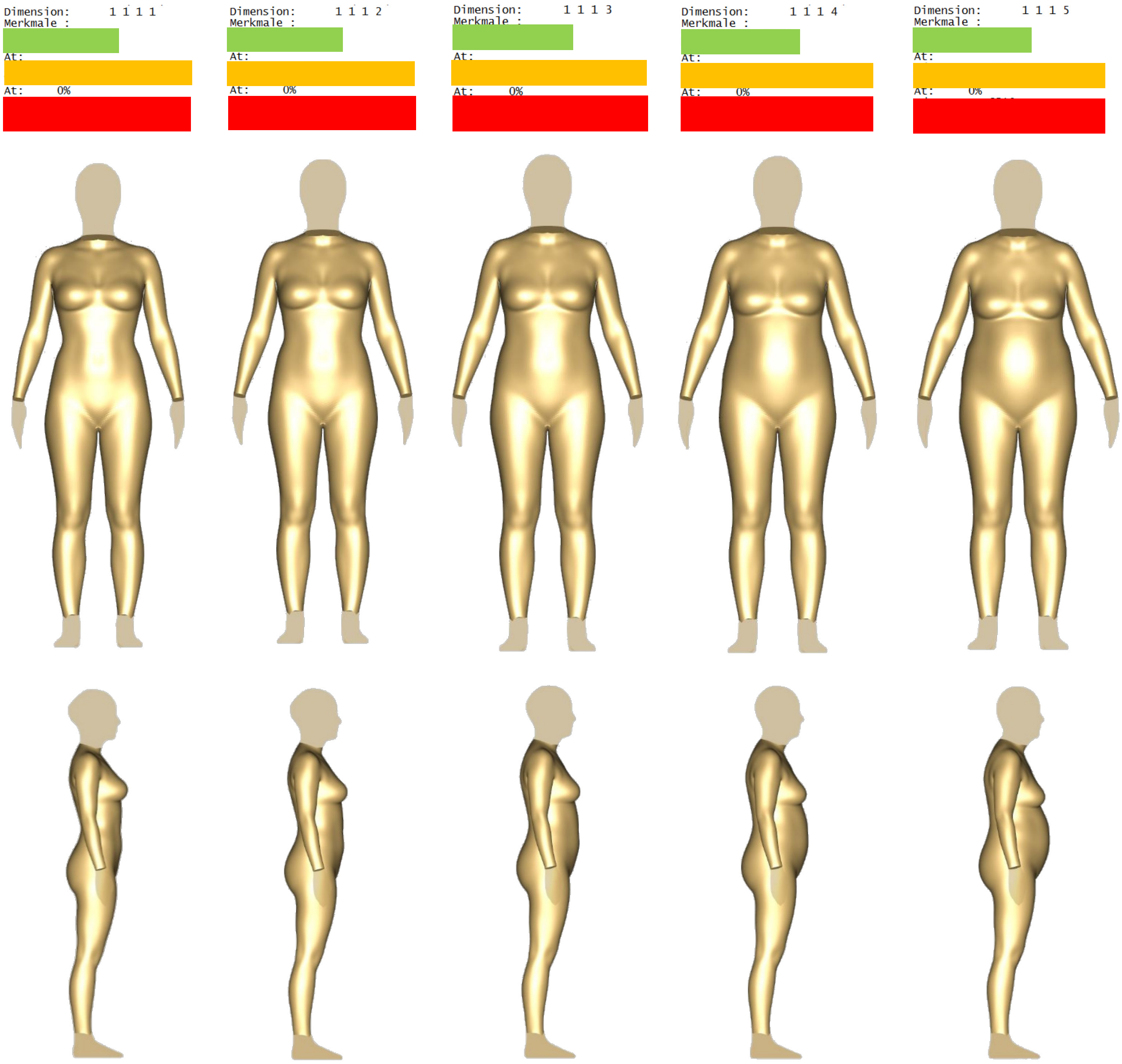

Figure 7 Target group with same body height and hip girth but different waist girths

Divided into four areas – length modifications, girth modifications, distribution of girth measurements and posture – rules are developed to transfer the modifications directly to the MtM grading process. The overview below shows the different rules for each area.

- Length modifications: difference of individual and standard body measurement
- Girth modifications: difference of individual and standard body measurement, with standard distribution based on the selected construction system
- Distribution of girth measurements: the distribution is measured on the individual body and the difference to the standard distribution is used for the MtM rule
- Posture: comparison of different body measurements, e.g. for a hollow back comparison of neck to waist center back with neck to waist over bust

Product group

Representative for the investigated products – classic products of skirts, blouses, shirts and trousers as well as workwear products –, the results of a blouse and a smock overall are shown below.

- **CAD pattern:** The product development as well as the standard and MtM grading is done for all products with the 2D CAD system Cad.Assyst. A second test with the 2D CAD system Grafis has shown that the process can be transferred to each other 2D CAD system.
- **Basic pattern:** Both patterns – blouse and smock overall – based on the iSize body measurement chart for women from size 32 to 60.
- **MtM Grading**: Based on the reference size, the predefined MtM-values will be automatically calculated and directly imported to the CAD System.

2.5 3D Simulation

3D simulations are used to evaluate the fit at an early stage – before the start of a manufacturing process. Virtual stitching is performed with the Vidya and V-Stitcher 3D CAD systems to ensure that a virtual fit is not dependent on a specific 3D CAD system.

MtM fitting

The MtM fit will be checked for the avatar test population and different products using a batch mode of the 3D simulation system Vidya. The output of different simulation pictures for each single simulation offers the possibility to verify the MtM fit.

Fit evaluation

Figure 8 gives a review about the fit evaluation based on virtual try-ons. Different simulation views like body-distance, elongation, and elasticity give detailed information about the fitting.

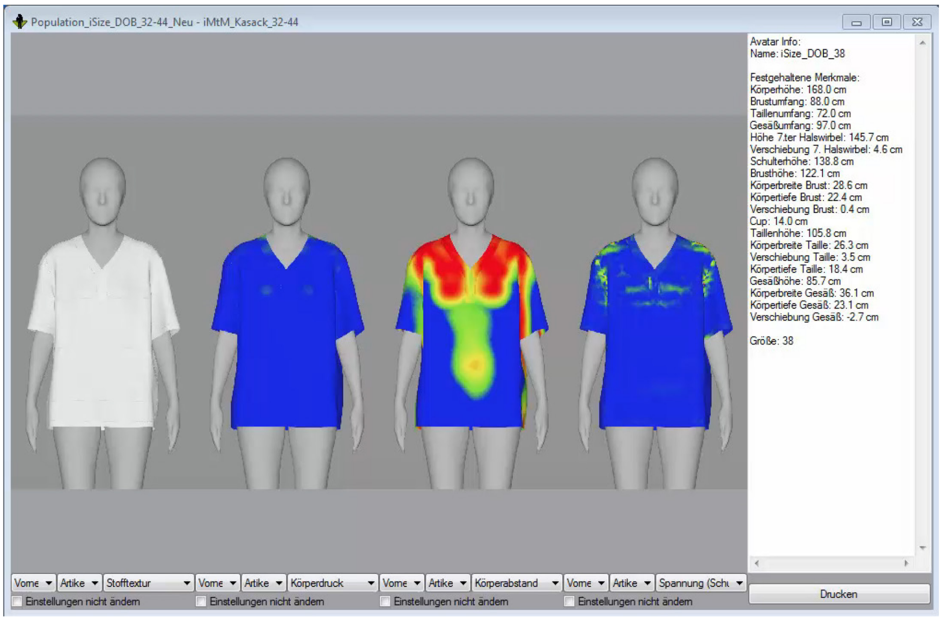

Figure 8 Simulation Viewer – simulation results for fit control

3 Results

The following results (Figs. 9, 10) are just a few samples from tests conducted with a large Avatar test population of both men and women and the resulting adjustments. They are divided into four sections: the generation of the avatar test population, the validation of the measurements of the avatar test population obtained with a special software application, the approach of implementing posture and shape parameters into the MtM pattern design, and the 3D fit studies for accelerated preliminary fit testing within the MtM process.

Figure 9 IMtM design evaluation

	Reference size	MtM grading	Body distance
hip – 15 cm			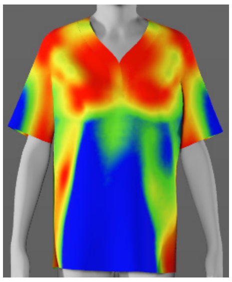

hip + 8 cm			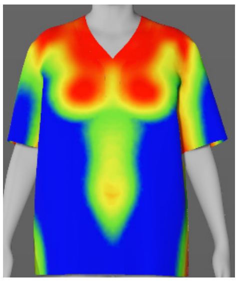
hip + 15 cm			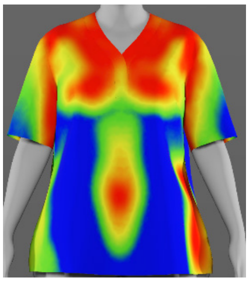

Figure 10 IMtM fit evaluation

4 Future Works

This work presents new software solutions with an interface to the simulation software Vidya. As Avalution and Assyst belong to the Human Solutions Group, the development of an interface to their own software has proven to be useful. Alternative developments with different 3D-software are conceivable and can be subject of separate investigation.

5 Conclusion

The findings of this paper have demonstrated the importance and usefulness of examining MtM classification at an early stage of the product development process. The automatic creation of avatar test populations and the batch mode for the 3D simulations are very helpful tools to make the virtual try-ons fast and available for the MtM validation process. Knowing that not all individual topics can be covered by the MtM process, a realistic avatar test population can be visualized for industrial applications, and the extraction of measurements provides multiple MtM information. The algorithm for evaluating the size recommendation is very flexible and can be specified for individual purposes.

The next step to complete the whole process aims to simplify the fit validation step by providing an automated and objective evaluation system for the apparel industry.

Acknowledgment

This work was performed within the cooperative Project ZIM ZF4102205CJ and the authors would like to thank to BMWi -AIF Projekt GmbH for the financial support of this investigation.

References

[1] Ernst, M.; Detering-Koll, U. Posture Dependency of 3D-Body Scanning Data for a Virtual Product Development Process. In *Proc. of 5th International Conference on 3D Body Scanning Technologies*, Lugano, Switzerland, 21-22 October 2014.

[2] Löffler-Wirth, H. Body typing of the adult population of Leipzig. Application forum Human Solutions. Kaiserslautern, Germany, 21 April 2016.

[3] Vidya, Assyst. Available online: https://www.assyst.de/de/produkte/3d-vidya/index.html (accessed on February 19, 2020)

[4] SizeGERMANY – Startseite'. Available online: https://portal.sizegermany.de/SizeGermany/pages/home.seam (accessed on February 19, 2020).

[5] Fischer, T.; Artschwager, A.; Pfleiderer, K.; Rissiek, A.; Mandalka, M.; Seidl, A.; Trieb, R. Automatic morphological classification with Case-Based Reasoning. 7th International Conference on 3D Body Scanning Technologies. Lugano, Switzerland, 30 Nov. – 1 Dec. 2016.

[6] Ernst, M.; Detering-Koll, U. Investigation on Body shaping Structures Using Body Scanning Technology and 3D Simulation Tools. In *Proc. of 3nd International Conference on 3D Body Scanning Technologies*, Lugano, Switzerland, 16-17 October 2012.

[7] Ernst, M. Next generation of product development – obtaining 3D buy-in, building capability and generating a fruitful roadmap. PI Conference Berlin, Germany, 5-6 October 2016.

[8] Ernst, M.; Böhm, M.; Detering-Koll, U. Rapid body scanning technology for a virtual mass customization process in garment industry. In *Proc. of 7th International Conference on 3D Body Scanning Technologies*, Lugano, Switzerland, 30 Nov. – 1 Dec. 2016.

[9] Allen, B.; Curless, B.; Popovic, Z. The space of human body shapes: reconstruction and parameterization from range scans. In *Proc. of SIGGRAPH '03 ACM SIGGRAPH 2003 Papers*, 587-594, San Diego, California: ACM New York.

[10] Blanz, V.; Vetter, T. A morphable model for the synthesis of 3D faces. In *Proceedings of ACM SIGGRAPH 99*, 187–194, 1999.

[11] Praun, E.; Sweldens, W.; Schröder, P. Consistent mesh parameterizations. In *Proceedings of ACM SIGGRAPH 2001*, 179–184. New York: ACM Press/ACMSIGGRAPH.

[12] Turk, M.; Pentland, A. Eigenfaces for recognition. *Journal of Cognitive Neuroscience*, 1991, 3 (1), 71-86. DOI: 10.1162/jocn.1991.3.1.71.

COMMUNICATIONS IN
DEVELOPMENT AND ASSEMBLING OF TEXTILE PRODUCTS

Suitability of common single circuit boards for sensing and actuating in smart textiles

Guido Ehrmann[1], **Andrea Ehrmann**[2,*]

[1] *Virtual Institute of Applied Research on Advanced Materials (VIARAM)*
[2] *Bielefeld University of Applied Sciences, Faculty of Engineering and Mathematics, Bielefeld, Germany*
*Corresponding author *E-mail address:* andrea.ehrmann@fh-bielefeld.de

INFO

CDAPT, ISSN 2701-939X
Peer reviewed article
2020, Vol. 1, No. 2, pp. 170-179
DOI 10.25367/cdatp.2020.1.p170-179
Received: 04 December 2020
Accepted: 22 December 2020
Available online: 22 December 2020

ABSTRACT

Single-board computers and microcontrollers such as Raspberry Pi or Arduino are nowadays used in a broad range of applications. Their relatively low power consumption and low price, compact dimensions and relative ease to program them make them suitable for diverse areas of measuring and controlling various parameters. In the textile area, however, such single-board computers are still less often used than in other projects, in spite of their aforementioned advantages in comparison to other solutions. Here we give an overview of the differences between single-board computers and single-board microcontrollers in general, compare different versions and give examples which projects are reported in the scientific literature, in design or in the maker scene, enabling researchers, designers and makers to decide which future projects necessitate which single circuit boards.

Keywords
Microcontroller,
Single-board computer,
Single circuit board
Arduino,
RaspberryPi,
Smart textiles,
Smart clothes

1 Introduction

Smart textiles can be defined in different ways. The “smartness” can be based on inherent material properties, e.g. in case of thermochromics or photochromic materials, changing their color due to temperature or photo-irradiation [1,2]. Smart functions can also be implemented by integration of optical fibers [3], phase change materials [4], or the like. Most smart textiles, however, nowadays include electronics for a broad range of applications, from medical garments sensing body functions [5] to new design opportunities [6].

Typically, smart textiles contain the following components, implemented by textile or textile-integrated parts: sensors and actuators, internal and external communication, a power source and a data processor

[7]. Many research groups investigate and develop textile sensors and actuators [8-10], think about textile batteries or solar cells [11-13], textile circuits [14,15] and textile-based antennae [16,17], resulting in an increasing number of publications from year to year (Fig. 1).

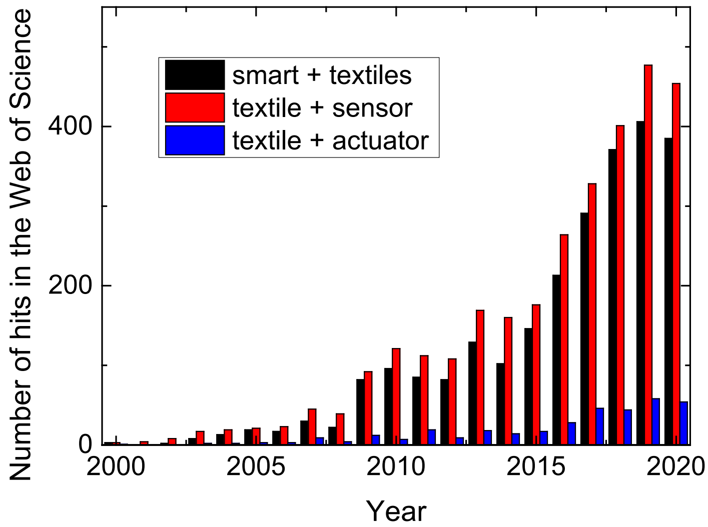

Fig. 1 Numbers of hits for different search phrases in the Web of Science (data accessed on December 5, 2020).

While the integration of diverse electronic elements into textile fabrics, e.g. in the form of automated connection of LEDs with textiles circuits by specialized embroidery machines [18], has already entered the commercial sector, not much research is visible yet in the area of data processing. Obviously, it is not possible to prepare textile-based computers simply due to miniaturization issues. While single textile transistors are investigated for diverse purposes [19-21], reducing their sizes to dimensions which would enable very basic computation on reasonable overall dimensions cannot be imagined at the recent state of technology. Thus, for many smart textile applications, it is necessary to include specialized or more general microcontrollers or single-board computers into the textile fabrics or garments.

Here we give an overview of recent single circuit boards, i.e. single-board computers (SBCs) and single-board microcontrollers (SBMs), with their advantages and disadvantages, and show recent projects implemented with such single circuit boards, to enable researchers, designers and makers to choose the ideal boards for future projects.

2 Recent SBCs and SBMs

Here we concentrate on the most often used SBCs and SBMs, the Raspberry Pi and the Arduino family, which are not necessarily aiming at integration into textile fabrics, and investigate their suitability for combinations with smart textile projects. It should be mentioned that there are several more specialized microcomputers and micro-computers available which may be better suitable for special textile projects; however, the here described SBCs and SBMs are quite often used by makers as well as for lab automation and thus well-known by different groups of people, making them especially suitable in interdisciplinary projects in which, e.g., textile designers or medical engineers work together with electronic specialists.

For a first impression, Fig. 2 shows some of these SBCs and SBMs. Here, the dimensional differences between different boards are already visible, even without showing the LilyPad board or other special textile-related boards. It should be mentioned that there are not only large dimensional differences between SBCs and SBMs, but also inside each family.

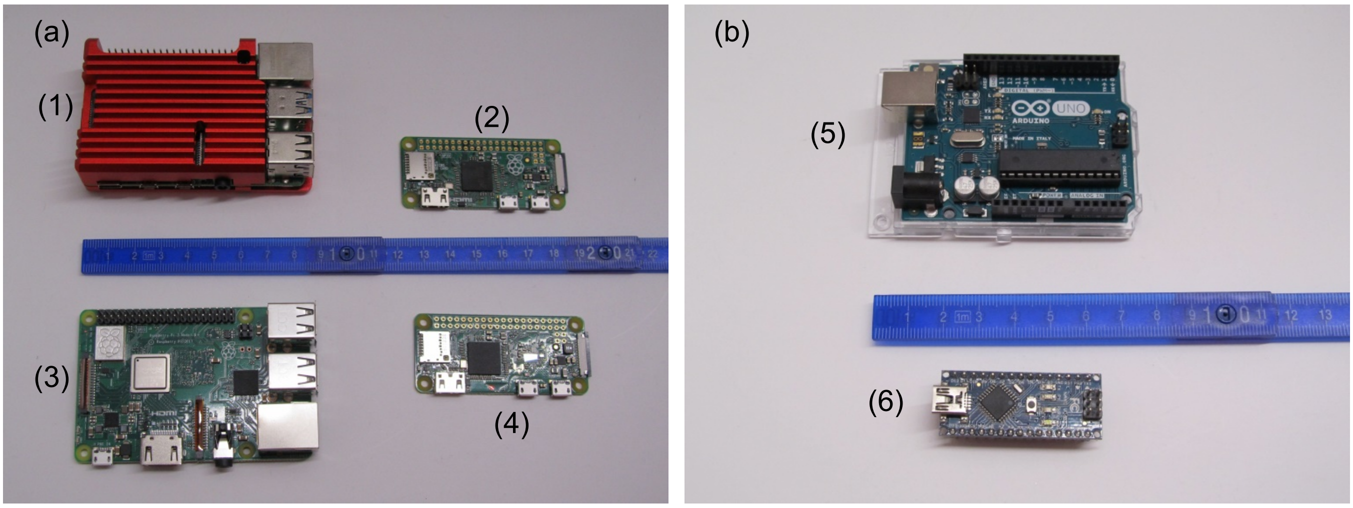

Fig. 2 (a) Different Raspberry Pi (1: Raspberry Pi 4B with passive cooler (red); 2: Raspberry Pi Zero; 3: Raspberry Pi 3B+; 4: Raspberry Pi Zero W) and (b) Arduino boards (5: Arduino UNO; 6: Arduino Nano).

Table 1 gives an overview of typical features of some chosen Raspberry Pi versions; Table 2 correspondingly shows parameters of some chosen Arduinos. It must be mentioned that both tables contain different parameters since some of them are only suitable for SBCs or SBMs – the latter, e.g., do not have cores since they are no full computers but microcontrollers.

Table 1. Technological parameters of some Raspberry Pi computers. From [22].

Board	**Raspberry Pi 4B**	**Raspberry Pi 3B+**	**Rasp. Pi Zero W**	**Rasp. Pi Zero**
Price [23]	€ 38-78	€ 37	€ 11.00	€ 5.50
SOC	BCM2711	BCM2837B0	BCM2835	BCM2835
Cores	4	4	1	1
Core Type	Cortex-A72	Cortex-A53	ARM1176JZF-S	ARM1176JZF-S
CPU Clock	1.5 GHz	1.4 GHz	1 GHz	1 GHz
RAM	1-8 GB LPDDR4	1 GB DDR2	512 MB	512 MB
USB 3.0	2	none	none	none
USB 2.0	2	4	none	none
micro OTG	none	none	1	1
Video	2x micro HDMI	HDMI	mini HDMI	mini HDMI
Analog Audio	3.5 mm jack	3.5 mm jack	none	none
SPI	yes	yes	yes	yes
I^2C	yes	yes	yes	yes
GPIO	40 pins	40 pins	40 pins	40 pins
Storage	microSD	microSD	microSD	microSD
WiFi	802.11 b/g/n/ac	802.11 b/g/n/ac	802.11n	none
Bluetooth	5.0	4.2, BLE	4.1	none
Size	85.6 x 56.5 x 11 mm^3	85.6 x 56.5 x 17 mm^3	65 x 30 x 5 mm^3	65 x 30 x 5 mm^3
Weight	46 g	45 g	9 g	9 g
Power	1.25 A @ 5 V	1.13 A @ 5 V	180 mA @ 5 V	160 mA @ 5 V

Power Connector	USB-C	microUSB or GPIO	microUSB or GPIO	microUSB or GPIO

Generally, Raspberry Pi models are full computers, usually with 1-4 cores, up to 8 GB RAM, typically working with a Linux operating system, e.g. Raspberry Pi OS. As Table 1 shows, many features of “common” computers are included, such as video and often also analog audio output, WiFi, USB ports etc. This broad functionality, however, results in relatively large systems, usually with the largest dimension being 65 mm or 85.6 mm, respectively.

This shows already that these fully functional microcomputers may be more suitable for “larger” projects in a doubled sense – they can perform more complicated tasks, but necessitate also more space than the Arduinos, some of which are exemplarily described in Table 2. Other Arduino IDE-based microcontrollers are available, e.g., from LilyPad (round boards with sewable connections), espressif (the well-known microcontroller ESP8266 with integrated WiFi), etc.

Table 2. Technological parameters of some Arduino microcontrollers. From [24,25].

Board	Arduino Uno	Arduino Nano	Arduino Micro	Ard. Nano 33 BLE	Digispark Mini
Price (official)	€ 20,00	€ 20,00	€ 18,00	€ 17,50	€ 5,00
Controller	ATmega328P	ATmega328	ATmega32U4	nRF52840	ATtiny85
Operating Voltage	5V	5V	5V	3.3V	5V
Input Voltage	6-20V	6-20V	6-9V	4.5-21V	7-35V
Input Voltage (recommended)	7-12V	7-12V	7-9V		
Power Consumption		19 mA	20 mA	< 20 mA	
I/O Pins Digital	14	22	20	14	6
I/O Pins Digital PWM shared	6	6	7	14	3
I/O Pins Digital PWM	none	none	none	none	none
I/O Pins Analog	6	8	12	8	4
UART	yes	yes	yes	yes	no
SPI	yes	yes	yes	yes	yes
I^2C	yes	yes	yes	yes	yes
Current per I/O Pin (DC)	20 mA	40 mA	20 mA	15 mA	
Current per 3.3V Pin (DC)	50 mA		50 mA		
Flash Memory	32 KB	32 KB	32 KB	1 MB	8 KB
SRAM	2 KB	2 KB	2.5 KB	256 KB	0.5 KB
EEPROM	1 KB	1 KB	1 KB	none	0,5 KB
Clock Speed	16 MHz	16 MHz	16 MHz	64 MHz	20 MHz
Length	68.6 mm	45 mm	48 mm	45 mm	26 mm
Width	53.4 mm	18 mm	18 mm	18 mm	12 mm
Weight	25 g	7 g	13 g	5 g	2 g
Connector	USB 2.0 Type B	Mini-B USB	Micro USB	Micro USB	USB 2.0 A

Battery	no	no	no	no	no
Programming via	Arduino IDE	Arduino IDE	Arduino IDE	Arduino IDE	Arduino IDE
Special Features				BLE, Bluetooth	

These microcontrollers can only execute compiled C-code and are no stand-alone computers. They are available in smaller dimensions, down to lateral dimensions of 26 mm x 12 mm for the examples shown here and with a minimum mass of only 2 g. However, the ATmega328P has already similar dimensions and even a higher mass than the smaller Raspberry Pi versions.

Another important factor, comparing both families of single circuit boards, is the power consumption. In both tables, only the power consumption of the board alone is given; each sensor or actor necessitates additional power. While the smallest Raspberry Pi needs a power of 160 mA @ 5 V, Arduino microcontrollers typically use 20 mA @ 3.3-5 V, allowing for using such a system for much longer times than a Raspberry Pi with the same battery or power-pack.

It must be mentioned, however, that in many cases the additional sensors and actuators need much more power than the boards themselves, often levelling out this difference to a certain amount. Driving, e.g., 20 LEDs with a typical power consumption of 20 mA @ 2 V with one of these systems consumes the same power as a pure Raspberry Pi Zero with the aforementioned 160 mA @ 5 V. As visible from Table 2, such relatively high powers cannot be taken from one of the I/O pins (with a maximum of 15-40 mA), but the I/O pin can control a relay-based circuit enabling switching higher currents and/or voltages.

Comparing the different Arduino SBMs, several differences become visible, not only related to dimensions and mass, but also to the amount of digital and analog I/O pins, the flash memory and SRAM, and the clock speed, clearly showing that for each project, the right Arduino or Raspberry Pi has to be chosen.

For a first decision whether an SBC or an SBM is best suited for a planned project, there are different rules of thumb and more sophisticated comparisons available:

- Arduino boards are easier to use for people with low programming experience [26].
- The IDE (integrated development environment) of the Arduino family is platform independent (i.e. usable in Windows, Linux and macOS) [26].
- Several libraries can be included into the IDE of Arduinos, supporting single sensors / actuators or complete sensor / actuator families.
- For many more sophisticated applications, Arduinos need so-called shields which let dimensions, mass and costs increase [26].
- Most Raspberry Pi models contain Ethernet, WiFi or both, while amongst the common Arduinos, only a few, like the Nano 33 BLE, contains Bluetooth LE (BLE).
- Generally, an Arduino can be used for simple, repeated tasks, while a Raspberry Pi is better suited for more sophisticated applications [26]. Both systems can be combined to profit from their respective advantages [27].
- And as a rule of thumb: Projects which can be explained by maximum one “and” can be performed by an Arduino; projects whose descriptions need more than two “and” should be performed on a Raspberry Pi [28].

Especially for applications in smart textiles, where important features are low power consumption, usability for basic electronics and simple circuits, microcontrollers from the Arduino family are often better suited than Raspberry Pi computers [29]. The next section will introduce several sample projects, making these differences clearer.

3 Sample projects

In spite of the large amount of research on smart textiles (Fig. 1), scientific literature on using SBCs or SBMs in such research is scarce. Most recently, Lin *et al.* gave an overview of the learning outcomes of students in maker-based assessments. They found that amongst the large number of maker platforms, the aforementioned LilyPad Arduino combined with electronic textiles was most popular for measuring STEM-related learning outcomes [30]. Serrano-Pérez describes a project with early-year students which should be motivated for learning physics by programming an Arduino Uno for controlling LEDs in garments [31].

An Arduino Uno was also used by Anbalagan *et al.* for data transmission by a textile antenna in a wearable system [32]. The Arduino, however, was not integrated into the textile material since the development of the textile antenna was the main purpose of this study. Similarly, Oldfrey *et al.* did not investigate the integration of the not exactly specified Arduino used in their study into a textile environment, but used it only for calibration purposes [33], as visible in Fig. 3. Nuramdhani *et al.* also used an Arduino Uno as a not-integrated part to investigate a textile energy storage device [34], while Li *et al.* applied an Arduino ATmega2560 for data collection and visualization of a step pressure sensing and position mapping system, based on textile pressure sensor mats [35]. Frequency-based measurements in smart textiles were also applied by an Arduino Uno placed next to the textile fabric under investigation [36].

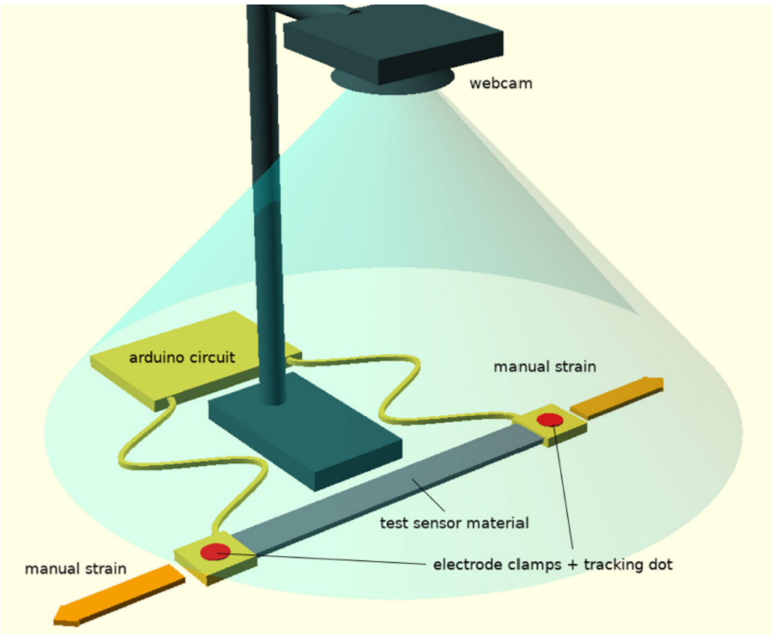

Fig. 3 Experimental setup applying an Arduino-based circuit for resistance measurements during stretching textile strain sensors. From [33], originally published under a CC-BY license.

Raad *et al.*, on the other hand, integrated a LilyPad Arduino into a smart glove which was used to monitor hand joint movements of patients suffering from rheumatoid arthritis, enabling observing the effort of medication or recommended movements [37]. A LilyPad Arduino was also integrated into a sensor sock measuring plantar pressure and acceleration signals, allowing for taking data necessary for postural and gait analysis [38]. An Arduino Nano, positioned at the forearm by an arm band, was coupled with a smart glove used to collect data of the movement of volleyball players during the service [39].

It must be mentioned that even a sophisticated task like measuring an ECG signal was tested by an Arduino-based device. Here, however, Ankhili *et al.* found that in comparison with a portable medical device, the low-cost Arduino-based solution showed higher distortions of cardiac waveforms and higher noise in case of high-resistant electrodes, suggesting that amplifiers with high input impedance are necessary to compensate the high contact impedance of typical textile electrodes [40].

Such complicated applications are the only ones which were found in the scientific literature as examples for using a Raspberry Pi. Bystricky *et al.* applied a module Medlab EG05000, connected to a Raspberry

Pi, for ECG measurements. The measured data were stored and sent to a mobile device. Using this specific module, they measured reliable ECG signals with embroidered electrodes [41].

Similarly, Pina *et al.* combined a Raspberry Pi B+ with a custom-made circuit for measuring EMG data of different muscles with a sampling rate of 1 kHz and a resolution of 24 bit. With this electronic equipment, gel-based and textile electrodes showed highly similar EMG signals. However, the authors mention that Python as programming language used on the Raspberry Pi B+ with 700 MHz ARM11 CPU may not be suitable for real-life applications due to the observed CPU workload [42].

In these cases, however, the Raspberry Pi was not reported to be integrated into the textile fabrics or garments. This is mostly done with the Arduino Nano or an Arduino LilyPad which is especially designed for integration in textile fabrics [43-45], while neither ESP8266 nor Digispark Mini were found in combination with textile fabrics in the scientific literature. Even the Wattuino Nanite85, based on an ATtiny85 microcontroller and with ~ 10 mm x 17.5 mm area much smaller than the LilyPad [46], is not reported for scientific applications in textile fabrics.

In the field of smart textiles, however, scientists are not the only ones investigating new solutions for well-known problems or also testing and extending the technological limits of new functionalities. Already in 2015, a complete issue of the magazine “Make” dealt with Wearables, suggesting several design-related projects including electroluminescent wires and foils, controlled by diverse specialized microcontrollers, mostly round and sewable for improved integration into textile fabrics [47]. Diameters of the boards shown there are between 14 mm and 50 mm, i.e. often larger than Arduino Nano or Digispark Mini. The mostly round shape, however, enables wearing these boards unhidden on the outer side of smart clothes, using them as additional design elements, as shown in Fig. 4 [48,49].

Fig. 4 (a) Safety vest for children, applying an Arduino LilyPad, from [48], originally published under a CC-BY-NC-ND license; (b) wireless smart glove, from [49], originally published under a CC-BY license.

In the designer and maker scenes, a broad range of highly creative projects exist, mostly based on SBMs. Such projects can be found, e.g., directly on the Arduino website [50] and the sites of more specialized textile-related boards [51,52], but also on maker sites like Instructables [53] or Kobakant [54].

While many of these projects are design- or fun-related and thus their products are often not fully reliable, they can nevertheless offer new and unusual solutions for scientific problems, e.g. related to monitoring vital sensors and other health and safety related issues. Thus they can not only be used by beginners to start coding and start working with typical “smart” materials, especially combining textiles with electronics, but also support researchers by adding creative ideas and new perspectives to old problems.

Besides, especially in research related to tight fitting smart clothes, researchers should go beyond the typical textile-specific boards like LilyPad and the boards used in other areas, such as Arduino Nano, and test the even smaller boards, such as Digispark Mini or Wattuino Nanite85, which may be sufficient for several projects, have smaller dimensions and sometimes also lower power consumption than the more often applied SBMs. Finally, the possibility should be taken into account to develop a project on a common Arduino microcontroller, where it can easily be modified, and shift the final software to a pure microcontroller with only the necessary in- and outputs connected, in this way reducing the dimensions as far as possible for a certain project.

4 Conclusions

This brief overview of typical single-board computers (e.g. Raspberry Pi) and single-board microcontrollers (e.g. Arduino) shows large differences not only between SBCs and SBMs, but also within the respective families, the latter especially in terms of dimensions, masses and functionalities. The literature survey shows only scarce utilization of SBCs in smart textile projects, while for smart textiles including SBMs, often boards specialized for such textile applications were used. It is striking that many more projects dealing with SBMs are found in the design area and maker scene than in the scientific literature. Besides, it must be mentioned that some of the smallest and thus often well-suited SBMs are nearly never used, indicating a gap between the available electronic solutions and the knowledge about them which should be closed to enable a more inconspicuous integration of electronics in smart textiles.

References

[1] Staffová, M.; Kucera, F.; Tochácek, J.; Dzik, P.; Ondreás, F.; Jancár, J. Insight into color change of reversible thermochromic systems and their incorporation into textile coating. *J. Appl. Polymer Sci.*, 2021, 138 (4), 49724. DOI: 10.1002/app.49724.

[2] Periyasami, A. P.; Vikova, M.; Vik, M. A review of photochromism in textiles and its measurement. *Textile Progress*, 2017, 49 (2), 53-136. DOI: 10.1080/00405167.2017.1305833.

[3] Issatayeva, A.; Beisenova, A.; Tosi, D.; Molardi, C. Fiber-optic based smart textiles for real-time monitoring of breathing rate. *Sensors*, 2020, 20 (12), 3408. DOI: 10.3390/s20123408.

[4] Tang, S. L. P.; Stylios, G. K. An overview of smart technologies for clothing design and engineering. *Int. J. Clothing Sci. Technol.*, 2006, 18 (2), 108-128. DOI: 10.1108/09556220610645766.

[5] Trummer, S.; Ehrmann, A.; Büsgen, A. Development of underwear with integrated 12 channel ECG for men and women. *AUTEX Res. J.*, 2017, 17 (4), 344-349. DOI: 10.1515/aut-2017-0008.

[6] Fafenrot, S.; Silbermann, P.; Grimmelsmann, N.; Assig, J.; Ehrmann, A. Integration of solar cells and other electronic components into clothes. Kyosev, Y.; Mahltig, B.; Schwarz-Pfeiffer, A. (eds.) *Narrow and Smart Textiles*, 2017, 229-239. Springer, Cham. DOI: 10.1007/978-3-319-69050-6_20.

[7] Schwarz, A.; van Langenhove, L.; Guermonprez, P.; Deguillemont, D. A roadmap on smart textiles. *Textile Progress*, 2010, 42 (2), 99-180. DOI: 10.1080/00405160903465220.

[8] Catrysse, M.; Puers, R.; Hertleer, C.; van Langenhove, L.; van Egmond, H.; Matthys, D. Towards the integration of textile sensors in a wireless monitoring suit. *Sens. Act. A Phys.*, 2004, 114 (2-3), 302-311. DOI: 10.1016/j.sna.2003.10.071.

[9] Langereis, G. R.; Bouwstra, S.; Chen, W. Sensors, actuators and computing systems for smart textiles for protection. In: Chapman, R. A. (Ed.) *Smart textiles for protection*, 2013, 190-213. Woodhead Publishing Series in Textiles. DOI: 10.1533/9780857097620.1.190.

[10] Kaynak, A.; Zolfagharian, A. Functional polymers in sensors and actuators: fabrication and analysis. *Polymers*, 2020, 12(7), 1569. DOI: 10.3390/polym12071569.

[11] Jost, K.; Dion, G.; Gogotsi, Y. Textile energy storage in perspective. *J. Mater. Chem. A*, 2014, 2, 10776-10787. DOI: 10.1039/C4TA00203B.

[12] Heo, J. S.; Eom, J.; Kim, Y.-H.; Park, S. K. Recent progress of textile-based wearable electronics: a comprehensive review of materials, devices, and applications. *Small*, 2018, 14 (3), 1703034. DOI: 10.1002/smll.201703034.

[13] Ehrmann, A.; Blachowicz, T. Recent coating materials for textile-based solar cells. *AIMS Mater. Sci.*, 2019, 6 (2), 234-251. DOI: 10.3934/matersci.2019.2.234.

[14] Bonderover, E.; Wagner, S. A woven inverter circuit for e-textile applications. *IEEE Electron Device Letters*, 2004, 25 (5), 295-297. DOI: 10.1109/LED.2004.826537.

[15] Ojuroye, O.; Torah, R.; Beeby, S. Modified PDMS packaging of sensory e-textile circuit microsystems for improved robustness with washing. *Microsystems Technologies*, 2019.
[16] Kiourti, A.; Lee, C.; Volakis, J. L. Fabrication of textile antennas and circuits with 0.1 mm precision. *IEEE Antennas and Wireless Propagation Letters*, 2015, 15, 151-153. DOI: 10.1109/LAWP.2015.2435257
[17] Del-Rio-Ruiz, R.; Lopez-arde, J.-M.; Legarda, J. Planar textile off-body communication antennas: a survey. *Electronics*, 2019, 8 (6), 714. DOI: 10.3390/electronics8060714.
[18] Schwarz-Pfeiffer, A.; Obermann, M.; Weber, M. O.; Ehrmann, A. Smarten up garments through knitting. *IOP Conf. Series Mater Sci. Eng.*, 2016, 141, 012008. DOI: 10.1088/1757-899X/141/1/012008.
[19] Coppedè, N.; Giannetto, M.; Villani, M.; Lucchini, V.; Battista, E.; Careri, M.; Zappettini, A. Ion selective textile organic electrochemical transistor for wearable sweat monitoring. *Organic Electronics*, 2020, 78, 105579. DOI: 10.1016/j.orgel.2019.105579.
[20] Kim, S. J.; Kim, H. J.; Ahn, J. T.; Hwang, D. K.; Ju, H. S.; Park, M.-C.; Yang, H. C.; Kim, S. H.; Jang, H. W.; Lim, J. A. A new architecture for fibrous organic transistors based on a double-stranded assembly of electrode microfibers for electronic textile applications. *Adv. Mater.*, 2019, 31 (23), 1900564.
[21] Owyeung, R. E.; Terse-Thakoor, Tr.; Nejad, H. R.; Panzer, M. J.; Sonkusale, S. R. Highly flexible transistor threads for all-thread based integrated circuits and multiplexed diagnostics. *ACS Appl. Mater. Interfaces*, 2019, 11 (34), 31096-31104. DOI: 10.1021/acsami.9b09522.
[22] RaspberryPI models comparison. Available online: https://socialcompare.com/en/comparison/raspberrypi-models-comparison (accessed on December 5, 2020).
[23] BerryBase, The Maker Shop. By Sertronics GmbH, Berlin, Germany. Available online: https://www.berrybase.de/ (accessed on December 5, 2020).
[24] Arduino Products. Available online: https://www.arduino.cc/en/Main/Products (accessed on December 5, 2020).
[25] Joy-it Digispark Mikrocontroller. Available online: https://joy-it.net/de/products/ARD-Digispark (accessed on December 5, 2020).
[26] Arduino vs. Raspberry Pi: Mikrocontroller und Einplatinencomputer im Vergleich. Available online: https://www.ionos.de/digitalguide/server/knowhow/arduino-vs-raspberry-pi/ (accessed on December 5, 2020).
[27] Strobel, C. Arduino vs. Raspberry Pi: Wo liegt der Unterschied? Techtag 12/08/2016. Available online: https://www.techtag.de/it-und-hightech/arduino-vs-raspberry-pi-wo-liegt-der-unterschied/ (accessed on December 5, 2020).
[28] Di Justo, P. Raspberry Pi or Arduino Uno? One Simple Rule to Choose the Right Board. *Make*, Dec. 4, 2015. Available online: https://makezine.com/2015/12/04/admittedly-simplistic-guide-raspberry-pi-vs-arduino/ (accessed on December 5, 2020).
[29] Pounder, L. Raspberry Pi vs Arduino: Which board is best? Tom's Hardware, July 10, 2020. Available online: https://www.tomshardware.com/features/raspberry-pi-vs-arduino (accessed December 5, 2020).
[30] Lin, Q.; Yin, Y.; Tang, X. D.; Hadad, R.; Zhai, X. M. Assessing learning in technology-rich maker activities: A systematic review of empirical research. *Computers & Education*, 2020, 157, 103944. DOI: 10.1016/j.compedu.2020.103944.
[31] Serrano-Perez, E. Arduino-based low-cost electronic textiles to introduce electric circuits and programming. *Revista Cubana de Fisica*, 2019, 36 (2), 110-113.
[32] Anbalgan, A.; Sundarsingh, E. F.; Ramalingam, V. S. Design and experimental evaluation of a novel on-body textile antenna for unicast applications. *Microwave and Optical Technology Letters*, 2020, 62 (2), 789-799. DOI: 10.1002/mop.32075.
[33] Oldfrey, B.; Jackson, R.; Smitham, P.; Miodownik, M. A deep learning approach to non-linearity in wearable stretch sensors. *Frontiers in Robotics and AI*, 2019, 6, 27. DOI: 10.3389/frobt.2019.00027.
[34] Nuramdhani, I.; Jose M.; Samyn, P.; Adriaensens, P.; Malengier, B.; Deferme, W.; de Mey, G.; van Langenhove, L. Charge-discharge characteristics of textile energy storage devices having different PEDOT:PSS ratios and conductive yarns configuration. *Polymers*, 2019, 11, 345. DOI: 10.3390/polym11020345.
[35] Li, E.; Lin, X. Y.; Seet, B.-C.; Joseph, F.; Neville, J. Low profile and low cost textile smart mat for step pressure sensing and position mapping. *IEEE Instrumentation and Measurement Technology Conference*, 2019, 1564-1568. DOI: 10.1109/I2MTC.2019.8826892.
[36] Mikkonen, J.; Townsend, R. Frequency-Based Design of Smart Textiles. *Proceedings of the 2019 CHI conference on human factors in computing systems ACM*, 2019, 294. DOI: 10.1145/3290605.3300524.
[37] Raad, M.; Deriche, M.; Bin Hafeedh, A.; Almasawa, H.; Bin Jofan, K.; Alsakkaf, H.; Bahumran, A.; Salem, M. An IOT based wearable smart glove for remote monitoring of rheumatoid arthritis patients. *Biosignals: Proceedings of the 12th International Joint Conference on Biomedical Engineering Systems and Technologies, Vol 4: Biosignals*, 2019, 224-228.
[38] D'addio, G.; Evangelista, S.; Donisi, L.; Biancardi, A.; Andreozzi, E.; Pagano, G.; Arpaia, P.; Cesarelli, M. Development of a prototype e-textile sock. *IEEE Engineering in Medicine and Biology Society Conference Proceedings*, 2019, 1749-1752. DOI: 10.1109/EMBC.2019.8856739.
[39] Di Tore, P. A.; Raiola, G. Powerglove: Genesis of a wearable technology aimed at studying volleyball service. *Journal of Human Sport and Exercise*, 2019, 14, S77-S83. DOI: 10.14198/jhse.2019.14.Proc1.09.

[40] Ankhili, A.; Tao, X. Y.; Cochrane, C.; Koncar, V.; Coulon, D.; Tarlet, J.-M. Comparative study on conductive knitted fabric electrodes for long-term electrocardiography monitoring: silver-plated and PEDOT:PSS coated fabrics. *Sensors*, 2018, 18, 3890. DOI: 10.3390/s18113890.
[41] Bystricky, T.; Moravcova, D.; Kaspar, P.; Soukup, R.; Hamacek, A. A Comparison of embroidered and woven textile electrodes for continuous measurement of ECG. *39th International Spring Seminar on Electronics Technology ISSE*, 2016, 7-11. DOI: 10.1109/ISSE.2016.7562871.
[42] Pina, D. S.; Fernandes, A. A.; Jorge, R. N.; Mendes, J. G. Development of a Portable System for Online EMG Monitoring. *Proceedings of 2015 3rd Experiment at International Conference (Exp At'15)*, 2015, 13-16. DOI: 10.1109/EXPAT.2015.7463206.
[43] Caya, M. V. C.; Casaje, J. S.; Catapang, G. B.; Dandan, R. A. V.; Sinsangan, N. B. Warning system for firefighters using e-textile. *Proceedings of 2018 3rd International Conference on Computer and Communication Systems (ICCCS)*, 2018, 362-366. DOI: 10.1109/CCOMS.2018.8463320.
[44] Litts, B. K.; Kafai, Y. B.; Lui, D.; Walker, J.; Widman, S. Understanding high school students' reading, remixing, and writing codeable circuits for electronic textiles. *Proceedings of the 2017 ACM SIGCSE Technical Symposium on Computer Science Education (SIGCSE'17)*, 2017, 381-386. DOI: 10.1145/3017680.3017740.
[45] Fields, D. A.; Lui, D.; Kafai, Y. B. Teaching computational thinking with electronic textiles: high school teachers' contextualizing strategies in exploring computer science. *Proceedings of International Conference on Computational Thinking Education*, 2017, 67-72.
[46] Wattuino Nanite 85. Available online: https://shop.watterott.com/Wattuino-Nanite-85-ATtiny85-mit-USB-Bootloader (accessed on December 5, 2020).
[47] Make: Magazin 4/2015, Maker Media GmbH, Hannover, Germany.
[48] Jutila, M.; Rivas, H.; Karhula, P.; Pantsar-Syväniemi, S. Implementation of a wearable sensor vest for the safety and well-being of children. *Proc. Computer Sci.*, 2014, 32, 888-893. DOI: 10.1016/j.procs.2014.05.507.
[49] Chuang, W.-C.; Hwang, W.-J.; Tai, T.-M.; Huang, D.-R.; Jhang, Y.-J. Continuous finger gesture recognition based on flex sensors. *Sensors*, 2019, 19 (18), 3986. DOI: 10.3390/s19183986.
[50] Wearable projects. Available online: https://create.arduino.cc/projecthub/projects/tags/wearables?page=1 (accessed on December 5, 2020).
[51] Make Archives – Wearic. Available online: https://www.wearic.com/make/ (accessed online on December 5, 2020).
[52] E-Textiles / Tutorials – learn.sparkfun.com. Available online: https://learn.sparkfun.com/tutorials/tags/e-textiles?page=all (accessed online on December 5, 2020).
[53] Instructables circuits: Make your own e-textile Arduino board. Available online: https://www.instructables.com/Make-Your-Own-E-Textile-Arduino-Board/ (accessed online on December 5, 2020).
[54] How to get what you want. Available online: https://www.kobakant.at/DIY/?cat=179 (accessed online on December 5, 2020).

COMMUNICATIONS IN
DEVELOPMENT AND ASSEMBLING OF TEXTILE PRODUCTS

CDATP

Estimation of spatial distribution and symmetry of textile materials using numerical classification

Jacek Grzybowski[1] and Tomasz Błachowicz[2,*]

[1] *Faculty of Automatic Control, Electronics and Computer Science, Silesian University of Technology, Akademicka 16, 44-100 Gliwice, Poland*
[2] *Institute of Physics – Center for Science and Education, Silesian University of Technology, S. Konarskiego 22 B, 44-100 Gliwice, Poland*
*Corresponding author *E-mail address:* tomasz.blachowicz@polsl.pl

INFO

CDAPT, ISSN 2701-939X
Peer reviewed article
2020, Vol. 1, No. 2, pp. 180-185
DOI 10.25367/cdatp.2020.1.p180-185
Received: 18 December 2020
Accepted: 24 December 2020
Available online: 25 December 2020

Keywords
Lacunarity,
Succolarity,
Structural analysis,
Knitted fabrics,
Microscopic images

ABSTRACT

Numerical classification of textile materials, here aramid, viscose, and PAN/WV, is proposed using lacunarity analysis of monochromatic digital representations of optical microscopic images. The method is sensitive to the spatial distribution of fibers and, equivalently, to the empty spaces between them. This means that lacunarity is able to quantitatively express a given level of spatial in-plane symmetries of single-face fabrics.

1 Introduction

Structural analysis using image processing approaches is an important tool for quantitative characterization of textile materials, i.e., regularity, periodicity, yarns quality and fibers structure symmetry. Such testing methods can be implemented in computer programs based on different mathematical algorithms, such as simple pixel counting, random walks on digital photographs [1], fractal dimension calculations [2,3], and other less known characteristics such as succolarity [4] and lacunarity [5,6]. Statistical analysis of images and/or structural samples can be carried out by many different methods, like for example, diffusion with hopping [7-9] and deterministic chaos [10-11].

While fractal dimension measures self-similarity of patterns and is directly related to the material structure or its spatial regularity, the lacunarity senses additionally empty spaces between areas filled with material and correspondingly the associated material spatial distribution. However, what is especially important for the analysis presented here, the properly calculated lacunarity parameter is insensitive to spatial directional properties – i. e. isotropy vs. anisotropy – what can be tested by analysis of rotated photographs of samples. We explain the reasons for that property in the next section.

In this paper we report first results of lacunarity calculations for three textile samples weft-knitted from aramid, viscose, and polyacrylonitrile (PAN)/wool, providing a quantitative estimation of the materials' spatial distribution and the spatial in-plane symmetry of single-jersey fabrics [6]. Before, we shortly introduce the notion of lacunarity, and finally provide some conclusions.

2 Notion of lacunarity

Calculation of lacunarity is based on repeated pixel counting performed on monochromatic photographs. A picture under investigation is covered with squares of a defined side length a (Fig. 1). Firstly, a square is drawn in the upper left position, then it is moved horizontally step by step, from left to right, with a step width smaller than or equal to the square side length, for example half of it, followed by the next row, etc. [12]. The overlap of boxes is the same in horizontal and vertical directions.

The number of material (black) pixels, here representing textile material, is counted at each square position – the obtained result is called a box-mass. Next, the squares and box-masses are classified in the form of a probability distribution $P(a, p)$. The distribution tells us how many squares $N_p(a)$ of side length a contain p black pixels, thus $P(a, p) = N_p(a)/N(a)$, where $N(a)$ is total number of squares covering the whole image. The experiment is repeated for a wide range of side lengths a, usually ranging from 0.1 to 1.0 of one of the photograph edge lengths.

For the obtained probability distribution, we can calculate two quantities: the weighted average value of box-masses $\sum_p p \cdot P(a, p)$, and the weighted average of squared box-masses $\sum_p p^2 \cdot P(a, p)$. Finally, the lacunarity is defined as

$$L(a) = \sum_p p^2 \cdot P(a, p) / \left(\sum_p p \cdot P(a, p)\right)^2. \qquad (1)$$

This quantity is proportional to the ratio of the standard deviation of the probability distribution to the mean value of the box-mass. In other words, it measures the ratio of the uncertainty of spatial material distribution – in this way it is sensitive to empty space regions located between material-covered areas – to the mean value of material distribution in single face fabrics. Since the procedure is repeated for a range of covering box sizes, it is then possible to prepare the $L = L(a)$ dependence, usually in the form of a double-logarithmic figure.

An especially important property of the proposed method is its insensitivity to the image orientation. Thus, the comparative test can be carried out with a given image orientation and with an image rotated in-plane by 90 degrees. Such a procedure enables finding the parameter of lacunarity which characterizes textile patterns. In the next paragraph we present results of both lacunarity and special tests with rotated samples.

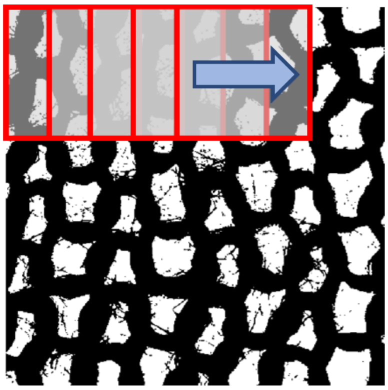

Fig. 1 Graphical presentation of the local collection of the material pixel density using horizontally moved square regions. The number of black pixels collected at a given position represents the box-mass for the corresponding position.

3 Samples

Single face fabrics were produced on a flat knitting machine CMS 302TC by Stoll, gauge E8, using the following yarns: aramid (550 dtex), viscose (2 x 330 dtex), and blended fibers with 70 % polyacrylonitrile (PAN) and 30 % new wool (WV). Photographic images were captured using the digital optical microscope VHX-600D (Keyence) and a nominal magnification of 20 x. The pictures, before calculations, were then transformed into 1-bit, monochromatic maps in the png format using arbitrary free graphics software. Each analyzed region has the size of 5000 x 5000 pixels. Fig. 2 presents samples in the original orientation (left panels) as well as in the 90° rotated form (right panels).

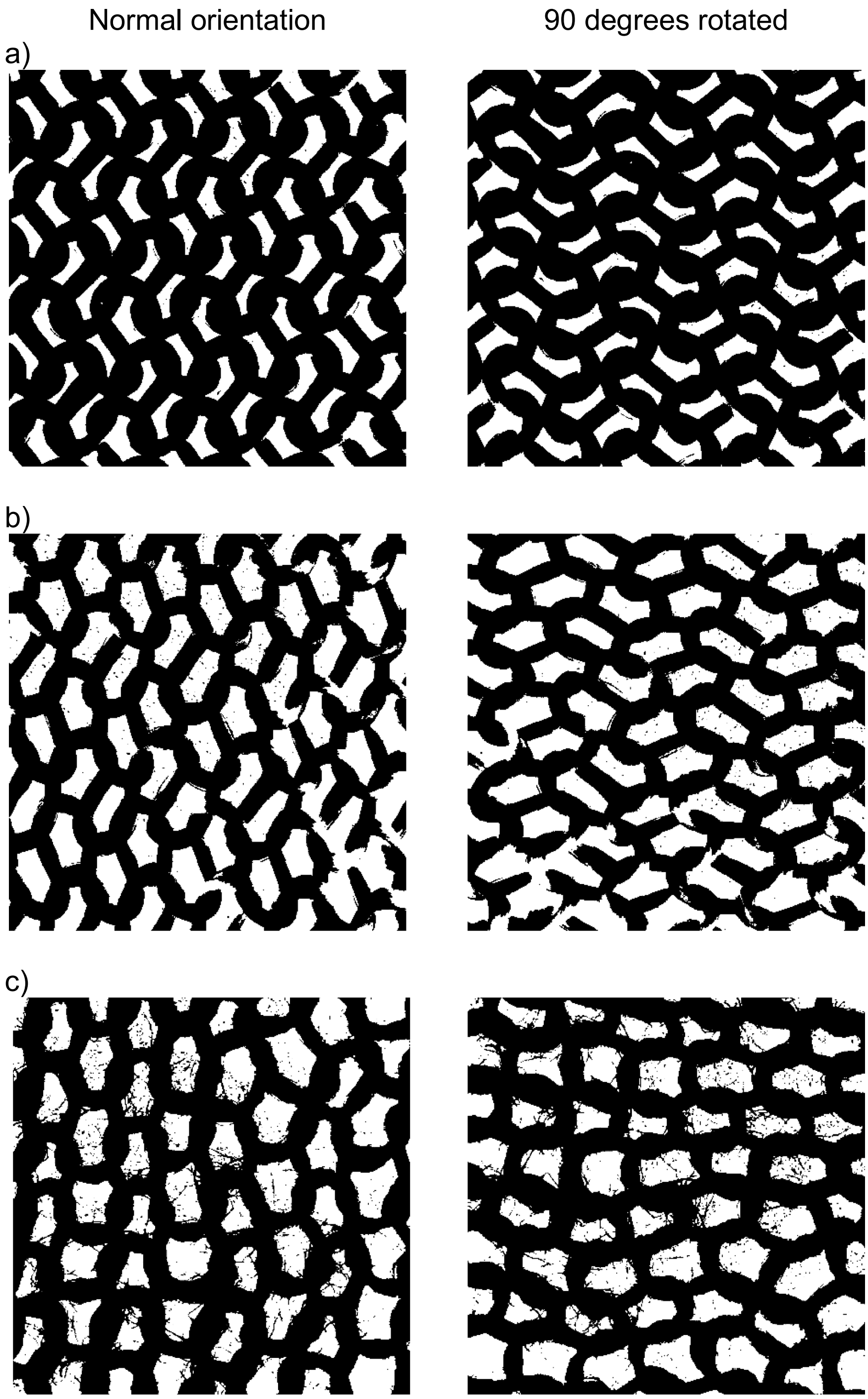

Fig. 2. Three types of samples in original orientation (left panel) and 90° rotated orientation (right panel): (a) aramid, (b) viscose, and (c) PAN/WV.

4 Results of Calculations

The visual inspection of the photographs in Fig. 2 might provide some intuitive estimation of the spatial distribution and symmetry of fibers. This is, however, a very inadequate approach of rather weak technological importance.

In Fig. 3, the calculated lacunarity, for the original images, is depicted for different sensing squares as defined above, providing an unambiguous method of dividing the analyzed structures into two classes: aramid and viscose belongs to the same group of lower lacunarity, while the PAN/WV is unequivocally different. In other words, a lower lacunarity is clearly visible in the range of $\mathrm{a} > 800$, meaning denser material with less empty regions. It should be mentioned, however, that the slopes of all curves are “concave down”, as typical for images with high lacunarity [13,14], due to the large open pores between the yarns in all cases.

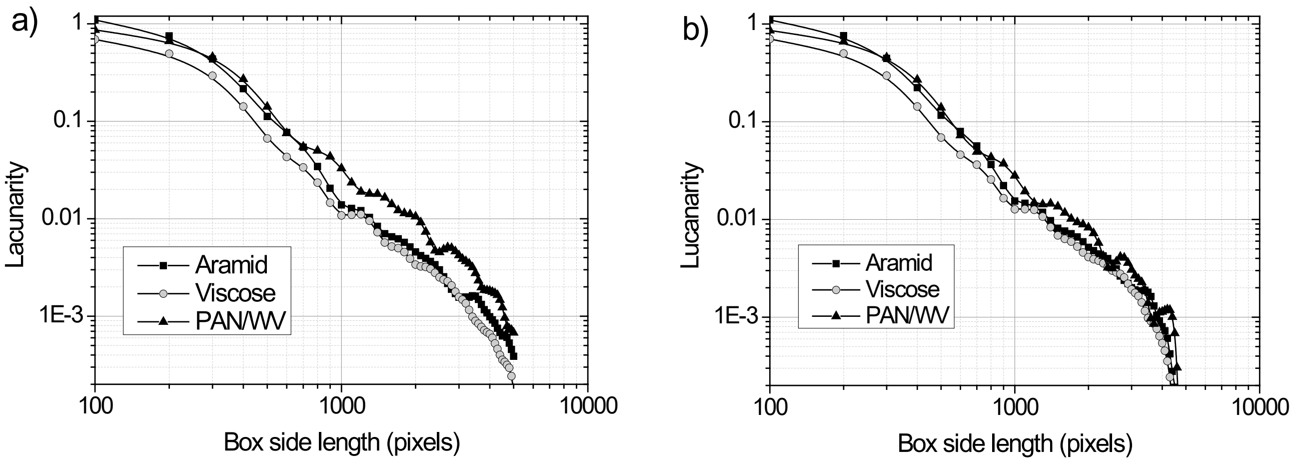

Fig. 3. Lacunarity of investigated samples as a function of the moving square-side length a for nonoverlapping testing boxes (a), and for 50 % overlapping boxes (b). The maximum value of a equals 5000, i.e. the length of the analyzed photographs.

Rotation symmetry analysis proves quantitative results which cannot be directly checked by the human eye (Fig. 4). The lacunarity is calculated as the absolute, stable average value of normal and rotated positions. From the linear scale point of view, for $\mathrm{a} < 750$, the results are numerically unstable, providing some inside into the nature of the pattern; however, with relatively small deviations between both rotational directions (< 1 %) which can in most practical cases be ignored.

For the presented samples, lacunarity can be read out with an even higher accuracy above a threshold value of $a > 750$. Thus for example, for $a = 800$ the lacunarity read out from Fig. 3a equals 0.034 for aramid, 0.024 for viscose, and 0.050 for PAN/WV, i.e. values differing significantly more than the maximum deviations visible in Fig. 4.

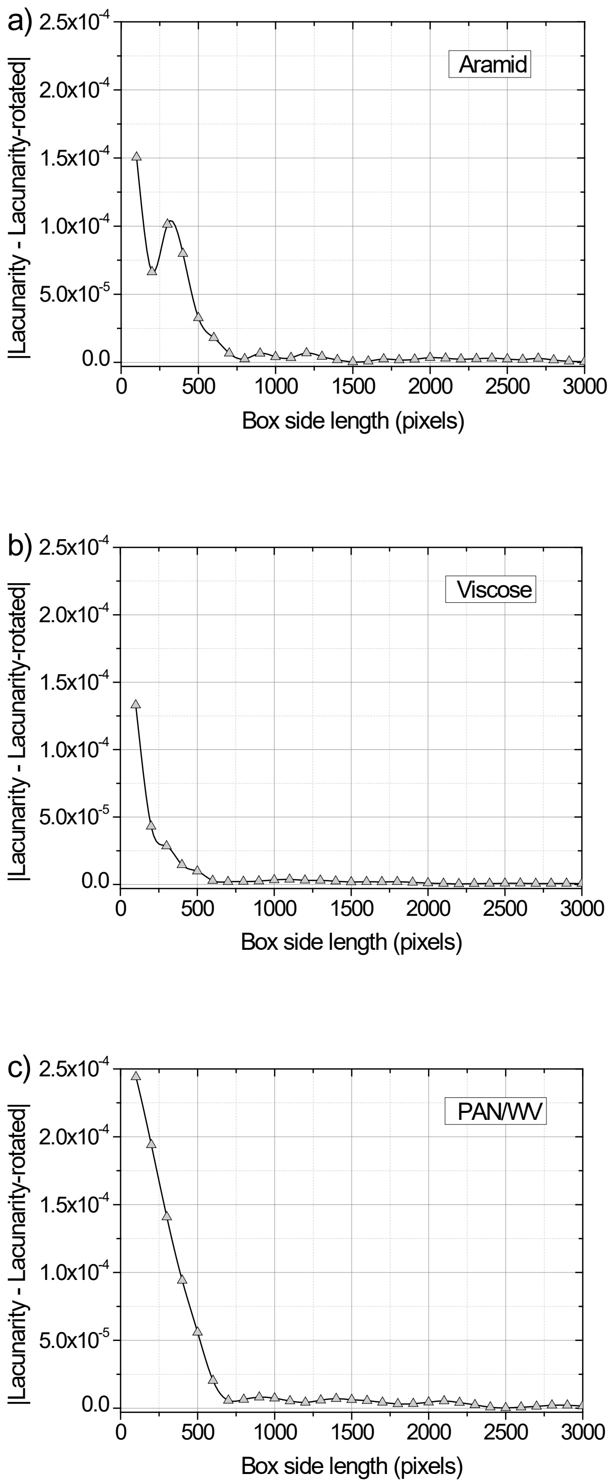

Fig. 4. Lacunarity of tested materials as a function of the moving square side-length α with a linear scale. The maximum value of α equals 5000, i. e. the edge length of the analyzed photographs: (a) aramid, (b) viscose, and (c) PAN/WV.

5 Conclusions

Lacunarity analysis, less commonly known as a tool for textile material characterization – in comparison to standardized methods – appears to be a very useful tool for the quantitative classification of the spatial symmetry and the degree of material filling of textiles, while it is angle-independent within the accuracy of numerical treatment. This new classification method should support the existing tests. Comparing three different materials, we were able to classify their regularity and their cover factors. The quantitative analysis performed with aramid, viscose and PAN/WV revealed that the latter exhibited the highest value of lacunarity.

Future research efforts will try to correlate this type of analysis with other physical parameters and technological methods used in the textile industry. Also, the aim of authors is to elaborate a lacunarity database for a wide range of textile samples and offer in this way a new adequate method of quantitative classification.

References

[1] Blachowicz, T.; Ehrmann, A.; Domino, K. Statistical analysis of digital images of periodic fibrous structures using generalized Hurst exponent distributions. *Physica A* 2016, 452, 167-177. DOI: 10.1016/j.physa.2016.02.013.

[2] Mandelbrot, B. and van Ness, J. W. Fractional Brownian motions, fractional noises and applications. *SIAM Rev*. 1968, 10, 422-437.

[3] Blachowicz, T.; Cwikiel, K.; Binkowski, M.; Zghidi, H. Analysis of the three-dimensional TGS crystal spatial inhomogeneity of the fractal structure, *Chaos Solitons Fractals* 2015, 75, 185–190. DOI: 10.1016/j.chaos.2015.02.023.

[4] de Melo, R. H. C., Conci, A. How succolarity could be used as another fractal measure in image analysis, *Telecommun. Sys.* 2013, 52, 1643-1655. DOI: 10.1007/s11235-011-9657-3.

[5] Plotnik, R. E.; Gardner, R. H.; Hargrove, W. W.; Prestegaard, K.; Perlmutter, M. Lacunarity analysis: A general technique for the analysis for spatial patterns. *Phys. Rev. E* 1996, 53, 5461-5468. DOI: 10.1103/PhysRevE.53.5461.

[6] Reiss, M. A.; Lemmerer, B.; Hansmeier, A.; Ahammer, H. Tug-of-war lacunarity – A novel approach for estimating lacunarity. *Chaos* 2016, 26, 113102. DOI: 10.1063/1.4966539.

[7] Gonzalez-Vazquez, J. P.; Anta, J. A.; Bisquert, J. Random walk numerical simulation for hopping transport at finite carrier concentrations: diffusion coefficient and transport energy concept. *Phys. Chem. Chem. Phys.* 2009, 11, 10359–10367. DOI: 10.1039/B912935A.

[8] Montes-Saralegui, M.; Nikoubashman, A.; Kahl, G. Hopping and diffusion of ultrasoft particles in cluster crystals in the explicit presence of a solvent. *J. Phys.: Condens. Matter* 2013, 25, 195101. DOI: 10.1088/0953-8984/25/19/195101.

[9] Yang, Ji-H.; Park, Ji-S.; Kang, J.; Wei, Su-H. First-principles multiple-barrier diffusion theory: The case study of interstitial diffusion in CdTe, *Phys. Rev.* 2015, B91, 075202. DOI: 10.1103/PhysRevB.91.075202.

[10] Grassberger, P. Chaos and diffusion in deterministic cellular automata. *Physica D* 1984, 10, 52–58. DOI: 10.1016/0167-2789(84)90248-3.

[11] Gaspard, P.; Klages, R. Chaotic and fractal properties of deterministic diffusion–reaction processes. *Chaos* 1998, 8, 409–423. DOI: 10.1063/1.166323.

[12] Suzuki, Y.; Sukigara, S. Mechanical and tactile properties of plain knitted fabrics produced from rayon vortex yarns. *Text. Res. J.* 2013, 83, 740-751. DOI: 10.1177/0040517512467132.

[13] Luo, L.; Lin, H. Lacunarity and fractal analyses of soil macropores and preferential transport using micro-X-ray computed tomography. *Vadose Zone Journal* 2009, 8, 233–241. DOI: 10.2136/vzj2008.0010.

[14] Kilic, K. I.; Abiyev, R. H. Exploiting the synergy between fractal dimension and lacunarity for improved texture recognition. *Signal Processing* 2011, 91, 2332-2344. DOI: 10.1016/j.sigpro.2011.04.018.